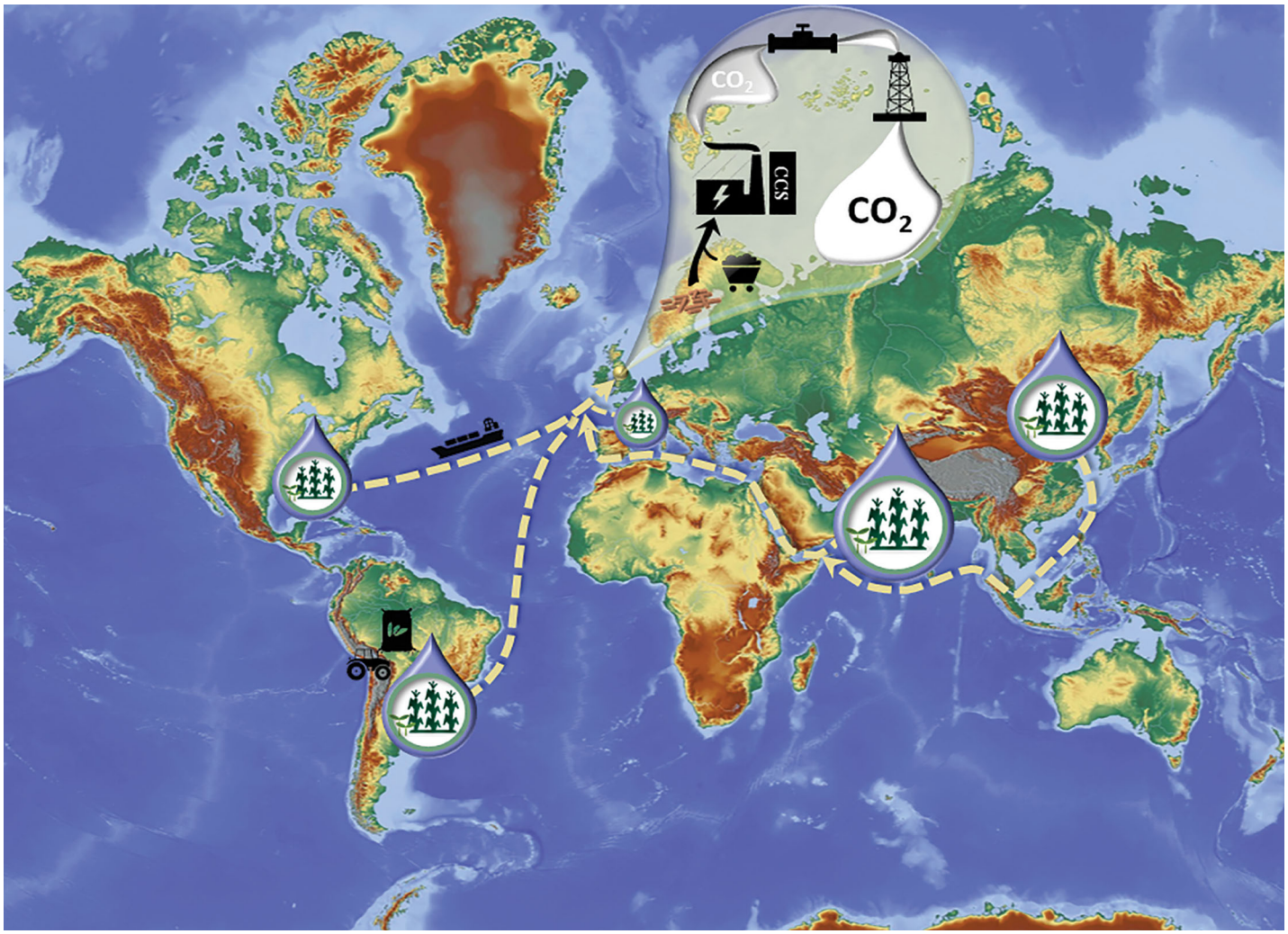

Showcasing research by Mathilde Fajardy and Niall Mac Dowell, Imperial College London

Can BECCS deliver sustainable and resource efficient negative emissions?

In meeting our climate goals, bioenergy with carbon capture and storage (BECCS) has been identified as a vital, yet controversial, negative emissions technology. Our whole-system analysis investigates the controversy around BECCS by answering two key questions: a) Under which conditions is BECCS a carbon negative and resource efficient technology? and, b) From a temporal perspective, how much CO_2 can be removed over the lifetime of a BECCS project?

As featured in:

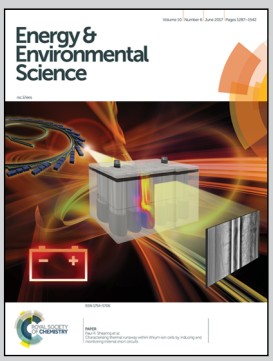

See Mathilde Fajardy and Niall Mac Dowell, *Energy Environ. Sci.*, 2017, **10**, 1389.

ROYAL SOCIETY OF CHEMISTRY

rsc.li/ees

Registered charity number: 207890

Energy & Environmental Science

PAPER

View Article Online
View Journal | View Issue

Cite this: *Energy Environ. Sci.*, 2017, **10**, 1389

Can BECCS deliver sustainable and resource efficient negative emissions?

Mathilde Fajardy[ab] and Niall Mac Dowell *[ab]

Negative emissions technologies (NETs) in general and bioenergy with CO_2 capture and storage (BECCS) in particular are commonly regarded as vital yet controversial to meeting our climate goals. In this contribution we present a whole-systems analysis of the BECCS value chain associated with cultivation, harvesting, transport and conversion in dedicated biomass power stations in conjunction with CCS, of a range of biomass resources – both dedicated energy crops (miscanthus, switchgrass, short rotation coppice willow), and agricultural residues (wheat straw). We explicitly consider the implications of sourcing the biomass from different regions, climates and land types. The water, carbon and energy footprints of each value chain were calculated, and their impact on the overall system water, carbon and power efficiencies was evaluated. An extensive literature review was performed and a statistical analysis of the available data is presented. In order to describe the dynamic greenhouse gas balance of such a system, a yearly accounting of the emissions was performed over the lifetime of a BECCS facility, and the carbon "breakeven time" and lifetime net CO_2 removal from the atmosphere were determined. The effects of direct and indirect land use change were included, and were found to be a key determinant of the viability of a BECCS project. Overall we conclude that, depending on the conditions of its deployment, BECCS could lead to both carbon positive and negative results. The total quantity of CO_2 removed from the atmosphere over the project lifetime and the carbon breakeven time were observed to be highly case specific. This has profound implications for the policy frameworks required to incentivise and regulate the widespread deployment of BECCS technology. The results of a sensitivity analysis on the model combined with the investigation of alternate supply chain scenarios elucidated key levers to improve the sustainability of BECCS: (1) measuring and limiting the impacts of direct and indirect land use change, (2) using carbon neutral power and organic fertilizer, (3) minimising biomass transport, and prioritising sea over road transport, (4) maximising the use of carbon negative fuels, and (5) exploiting alternative biomass processing options, *e.g.*, natural drying or torrefaction. A key conclusion is that, regardless of the biomass and region studied, the sustainability of BECCS relies heavily on intelligent management of the supply chain.

Received 17th February 2017,
Accepted 6th April 2017

DOI: 10.1039/c7ee00465f

rsc.li/ees

Broader context

Negative emissions technologies, in general, and bioenergy with carbon capture and storage (BECCS), in particular, are fundamental to achieving the 1.5 °C goal as articulated by the 2015 Paris COP agreement. However, as a technology BECCS remains dogged by controversy arising from the competition for arable land and fresh water, in addition to questions concerning its ability to actually remove CO_2 from the atmosphere. In this contribution, we present a whole-systems assessment of BECCS, explicitly accounting for the cultivation, harvesting, transport and conversion of biomass and the subsequent sequestration of the arising CO_2. Owing to CO_2 emissions associated with the initial land use change and these subsequent emissions, BECCS projects incur an initial and ongoing carbon debt. Thus, the viability of BECCS as a negative emissions technology option depends entirely on the choices made throughout the supply chain. Moreover, owing to the uncertainty primarily associated with land use change, "one size fits all" regulation may be particularly challenging. In particular, the carbon breakeven time and the lifetime net CO_2 removal from the atmosphere tend to be case-specific. Key policy challenges will likely include (a) how carbon negative should the BECCS project be in order to warrant support and (b) how should a BECCS plant which has not yet started to remove CO_2 from the atmosphere be supported?

1 Introduction

1.1 BECCS and negative emissions

Bioenergy with carbon capture and storage is the combination of two well-known technologies for climate change mitigation.

[a] *Centre for Environmental Policy, Imperial College London, Exhibition Road, London, SW7 1NA, UK. E-mail: niall@imperial.ac.uk; Tel: +44 (0)20 7594 9298*
[b] *Centre for Process Systems Engineering, Imperial College London, Exhibition Road, London, SW7 2AZ, UK*

Carbon capture and sequestration (CCS) as a means to mitigate CO_2 emissions arising from the power and industrial sectors has been widely investigated in the literature,[1–3] and the use of biomass as an energy source is ubiquitous throughout human history. Their combination was first identified as a negative emission technology (NET) by Williams *et al.* for the production of hydrogen,[4] and by Herzog for power generation[5] in 1996. However, the combination of bio-energy and carbon capture and storage was not referred to as "BECS" or "BECCS" until 2003 when Kraxner *et al.* first coined the term.[6] A core element of the utility of BECCS is its potential to remove CO_2 from the atmosphere,[6–14] and in so doing permit the offsetting, or mitigation, of otherwise hard to reach point sources such as transport or sources which are remote from the CO_2 transport and storage infrastructure.[15] In the context of meeting ambitious climate change mitigation scenarios, BECCS plays an increasingly important role in the outputs of integrated assessment models (IAMs),[16,17] both as an offset technology and as a means to address any overshoot in emissions.

However, despite its potential advantages, BECCS is not without controversy. Land competition for food production,[18] as well as CO_2 emissions associated with biomass cultivation, harvesting and processing[19] cast doubt on the general ability of a BECCS facility to actually result in a net removal of CO_2 from the atmosphere. It is recognised[20] that a detailed assessment of the water, land and carbon intensity of the biomass supply chain and conversion technology is vital to quantitatively addressing the uncertainty in this area, identifying key points for improvement and thus facilitating the large scale deployment of BECCS.

1.2 BECCS technical challenges

One category of challenges BECCS faces relates to conversion and CO_2 capture technologies. In a post-combustion capture system, steam is taken out of the steam cycle to regenerate the solvent. This imposes a first energy penalty on the system, on the order of 20% with conventional technologies at 90% capture, or 9% in efficiency points[21] with conventional solvents (*i.e.*, alkanolamines). Using state-of-the-art solvents could bring the heat requirement to values as low as 2.3 GJ $t_{CO_2}^{-1}$,[22,23] or even 2 GJ $t_{CO_2}^{-1}$ in the case of biphasic solvents.[24] Bui *et al.* investigated the impact of solvent heat duty on the system efficiency and carbon intensity, and showed that using advanced solvents combined with heat recovery from the boiler exhaust gases could reduce the efficiency penalty associated with solvent regeneration to zero.[25]

This efficiency penalty is further increased by the use of a potentially lower quality fuel – biomass – in complement or supplement to coal. While the average higher heating value (HHV) of bituminous coal is approximately 27 MJ t_{MW}^{-1} at 11% moisture and 64% carbon content,[26] raw biomass with a higher moisture content – up to 50% with woody biomass[27] – and a lower carbon content – around 48% dry mass – tends to exhibit an HHV around 18–20 MJ t_{DM}^{-1}.[28–33] In addition to the efficiency loss at the boiler, the physical properties of biomass will increase the costs associated with fuel storage, handling and size reduction. In the case of high moisture biomass, drying will automatically represent a substantial energy cost. Furthermore, as shown in Williams *et al.*,[34] biomass grindability is significantly lower than that of coal, resulting in a grinding energy cost up to four to five times higher on a mass basis. On an HHV basis, grinding energy cost can be up to seven times higher for biomass relative to coal, with an energy requirement of 20 kW h MW h_{HHV}^{-1} in the case of wood pellets, against 3 kW h MW h_{HHV}^{-1} in the case of coal. In addition to a reduction in efficiency associated with increased fuel processing costs, another concern is associated with transitioning from dedicated coal to dedicated biomass combustion and the resulting impact on the boiler technology. Experimental studies[35] and recent reports from Drax power station, which converted two 660 MW units to dedicated biomass in 2014,[36] demonstrate that large scale biomass firing is feasible with no major change, provided a modern boiler technology is used. Utility-scale biomass-fired power plants are inherently more costly than their coal-fired counterparts, primarily as a result of the more costly fuel handling and storage infrastructure. In addition to the capital cost, the ongoing operating cost associated with providing a nitrogen-rich atmosphere for the biomass is also an important consideration. Moreover, an improved understanding of the impact of ash formation and slagging behaviour on boiler efficiency and maintenance[37,38] costs is also necessary.

However, Mac Dowell and Fajardy showed that BECCS facilities that are less efficient at converting biomass to electricity could remove more CO_2 at a lower cost than their more efficient counterparts.[39] This paradoxical observation has important implications for the way in which CDR technologies will be integrated with the broader energy system.

1.3 BECCS and the water concern

Agriculture and power generation are highly water intense, accounting for 70%[40] and 15%[41] of the world's total water consumption. Thus the sustainability of BECCS warrants close scrutiny.[42] According to the Food and Agriculture Organization,[40] 1.2 billion people already live in absolute water scarcity, and this number could be further increased by the additional 1.6 billion who are currently facing water shortage. As agriculture is responsible for up to 90% of water consumption in the Asia-Pacific region,[43] the combination of population growth and climate change has the potential to further exacerbate this situation.[44,45] The shift towards the sustainable use of water in farming relies heavily on region-specific guidelines regarding crop irrigation need. One of the main principle methodologies in common use is the blue, green and grey water footprint model developed by Hoesktra *et al.*[46] Based partly on the crop evapotranspiration model developed by Allen *et al.*,[47] this methodology enables the quantification of the water requirements of a given crop, based on the climate conditions (green water), ground and surface water local availability (blue water) and pollution (grey water).[48] This methodology has been used to reliably determine the water footprint of a range of agricultural products,[49,50] including cellulosic biomass[51] and biofuels.[52] The water footprint of bioelectricity

was also investigated,[53] but did not include the power plant water requirement. Further, several studies have focused on quantifying water use in the power generation sector.[41,54,55] Wu *et al.* developed a modeling framework to evaluate the blue water footprint as a function of cooling technologies, power plant type, and fuel, and included solid biomass as one of its case studies. Biomass upstream water requirement was however assumed to be met by rainfall, and biomass grey water footprint was not considered.[54] In order to evaluate the BECCS overall water cost, both evaluations – biomass production and water requirement for power generation – need to be integrated within the same framework.

1.4 Biomass production energy cost

Before being combusted, biomass needs to be grown, harvested, processed (dried, densified for transport, *etc.*) and transported to the power plant. This results in a substantial energy cost, which will further decrease the net power generation efficiency of a given BECCS project, on a whole-systems basis. Many studies adopt a life cycle assessment (LCA) approach to determine biomass embodied energy (EE) – direct and indirect energy use to produce a ton of biomass – or biomass energy ratio (ER) – EE over the fuel heating value. Bioenergy production has extended its potential feedstock from conventional cereal and oil crops, to cellulosic biomass, with both dedicated production and agriculture residue collection such as wheat straw.[56–59] Among dedicated energy crops, perennial grasses and short rotation coppice have been extensively investigated. Both perennial grasses, miscanthus[60–78] and switchgrass[9,30,57,61,66,67,79–92] have been studied and compared at the farming, processing or conversion level. Woody biomass such as short rotation willow has also been widely investigated for temperate climates.[15,58,67,69,93–99] Studies based on transparent model with clearly outlined system boundaries, such as the Farm Energy Analysis tool (FEAT[67]), the Biomass Emissions and Counterfactual (BEAC[99]) and the Greenhouse Gases, Regulated Emissions, and Energy Use in Transportation (GREET[54]) Model do exist. However, some studies only focus on a portion of the supply chain – adopting either a farm gate[67,69,96] or a power plant gate[57,65,100] perspective – and only a few include irrigation[76,87] and drying.[57,65,94] Both processes could represent significant contributions in the biomass supply energy cost, and were included in this analysis. The extensive literature on the subject results in a high variability in EE and ER values for a wide range of biomass. A detailed and transparent model of the entire BECCS value chain, including biomass conversion, with clear boundaries and assumptions, is required for the reliable evaluation of BECCS.

1.5 Accounting for direct and indirect GHG emissions

In addition to a high energy cost, the biomass supply chain may result in a substantial amount of direct and indirect GHG emissions. This represents the main challenge to BECCS' ability to deliver net CO_2 removal. A first issue often raised involves biomass sourcing and transportation related emissions. There are several biogeophysical and geopolitical constraints to consider: all geological storage sites do not coincide with available land for biomass production, or locations of thermal power plants. The deployment of BECCS at the scale envisioned by IAM solutions will likely require a multi-national biomass supply chain, with stakeholders based in different regions acting to provide a reliable supply of sustainably sourced biomass. In 2015, over 70% of UK Drax power plant biomass supply was imported from North America, incurring a carbon cost of 36 g_{CO_2} MJ^{-1} of electricity produced.[36] The UK Bioenergy Strategy published in 2012[101] provides a precise GHG emissions accounting methodology, which includes the direct and indirect emissions resulting from land conversion, *i.e.*, converting a certain type of land – cropland, grassland, forest – to a biomass crop. This is referred to as direct land use change, and as defined by Fargione *et al.*,[102] encompasses the direct emissions released during the initial plant combustion and eventual decomposition of roots and leaves, the carbon converted into charcoal, and the carbon incorporated into merchantable forestry products (considered to have a half-life of 30 years). Land conversion factors are a strong function of the land type converted, and are reported to be in the range 0–70 kg_{CO_2} ha^{-1} for marginal land,[102] 350–120 t_{CO_2} ha^{-1} for forest[102,103] or even up to 3450 t_{CO_2} ha^{-1} for wetland.[102] However, some studies[42,104,105] argue that this accounting method cannot be complete without taking into account the indirect effects of altering a land economic function (*e.g.*, agriculture, grazing) by converting part of it for biomass production. Models evaluating those effects do exist, but their level of specificity limits their applicability to a case-to-case basis.[103,106–108] Plevin *et al.* evaluated indirect emission factors to range from 10 to 340 $g_{CO_2\text{-eq}}$ MJ^{-1} of liquid biofuel, with a strong sensitivity to socio-economic activity and time horizon within a specific region.

This dependence on time also raises the question of dynamic accounting of carbon emissions. Some studies indicate that on a transient basis, the "carbon debt" initiated by land conversion to biomass production cannot offset CO_2 savings from displacing coal, or only over a period of time that is greater than the power plant lifetime.[109,110] This is referred to as "carbon payback time", or carbon breakeven time, and can be understood as the amount of time required for a system to reach carbon neutrality. In those studies however, biofuels pay back this initial carbon debt by offsetting fossil fuel related emissions, and carbon breakeven time thus has to be calculated relatively to a given fossil fuel. In the BECCS case, because it physically captures carbon from the atmosphere, we define it as the time required for a BECCS power plant to pay back this initial debt by biomass combustion and carbon storage.

The aforementioned uncertainties result in BECCS' net CO_2 removal which varies greatly on both a spatial and temporal basis. As a result, input data uncertainty needs to be captured in BECCS CO_2 balance for the assessment to be meaningful.

The purpose of this contribution is to present a spatially and temporally explicit, whole-systems assessment of the BECCS supply chain, accounting for the cultivation, harvesting, processing, transport, and conversion of biomass and the subsequent sequestration of the arising CO_2. We evaluate each distinct

BECCS system on the basis of energy, carbon, water, and land-use intensity, using the net removal of CO_2 from the atmosphere as a determining key performance indicator. The rest of the paper is structured as follows. Section 2 provides an overview of the approach adopted in this analysis, in particular presenting a detailed analysis of the uncertainty associated with the published data required to characterise the biomass supply chain. Section 3 quantifies and qualifies the different contributions to the water, energy and land intensities of the integrated BECCS system, and the resulting impact on the overall system thermo- and hydrodynamic efficiencies, in addition to the carbon intensity and carbon efficiency. Finally, Section 4 focuses on the dynamic accounting of GHG emissions over the system lifetime, on its sensitivities, and concludes with some perspectives on the implications for the potential of BECCS to result in the net removal of CO_2 from the atmosphere.

2 Model overview

In order to meet the objectives of the study, four sub-models were developed and integrated: biomass cultivation, processing, transport to a UK-based power plant, and conversion in a 500 MW thermal power plant combined with CCS. For each sub-model, energy, GHG (CO_2 and N_2O) and water balances were carried out. Biomass can be supplied to the power plant in various forms, such as bales, chips, pellets or briquettes.[111] Each biomass conditioning process involves different processing stages and moisture requirements, resulting in a different supply chain energy cost. As the optimal moisture content for biomass combustion is around 10–15 wt%,[112,113] drying of biomass is generally required. Biomass pelleting also requires a feedstock at around 10 wt% moisture.[65] For this analysis, a pellet supply chain including biomass production, processing (chopping, drying, grinding, pelleting), pellet transport and further treatment (pellet grinding) at the power plant was chosen as a base case. A comparison with alternative supply chains is left for future work. In order to compare different feedstock, four representative types of biomass were selected: miscanthus and switchgrass, short rotation coppice (SRC) willow, and wheat straw. Thus, this range allows us to evaluate perennial grasses, woody biomass, and agricultural residues. To capture the spatial dependence of this model (biomass productivity, climate, road and sea transport distance to the UK), five regions of the world, associated with distinct climates, were considered: sub-tropical south-west Brazil, continental temperate central China, temperate western Europe, semi-arid northern India and subtropical southern USA. Finally four land types were considered (cropland, grassland, forest, marginal cropland) to capture effects of direct and indirect land use changes.

The evaluation of the thermo- and hydrodynamic efficiencies and carbon intensity of a 500 MW BECCS power plant was carried out in the conversion model. Different cooling technologies (once-through, wet cooling tower), CO_2 capture rates (60–90%) and co-firing proportions (0–100%) were considered in the model. Biomass physical properties and supply chain footprints previously evaluated were included in the model to evaluate how BECCS performed with each feedstock. BECCS efficiency to convert biologically stored CO_2 into geologically stored CO_2 was also determined. Finally, in order to capture BECCS CO_2 removal time efficiency, this model included an evaluation of the cumulative emissions and carbon breakeven time of a hectare of land used in such a system over 50 years. The different interactions between these sub-models are outlined in Fig. 1.

2.1 Data collection and curation

As is evident from the foregoing description, this model requires a significant amount of input data. Thus, a key activity was the collection and statistical analysis of these data. The model input parameters are of several types:

- Energy data: all indirect energy data – chemicals, seeds and fuels embodied energy – and direct energy data – fuel LHV, energy for irrigation, transport fuel efficiency and drying system characteristics.
- Carbon data: all indirect emission data – carbon footprint of chemicals, seeds and fuels – and direct emission data – fuel and transport emission factors, N_2O model emission factors, gas global warming potential and land conversion factors.
- Crop data: the physical properties of each biomass type – composition, Cp, HHV – as well as farming data – yields over lifetime and in different regions, moisture content, lifetime and harvest rotation cycle, crop coefficients and calendar, chemical input rates, fuel efficiencies and processing energy requirements of in-field operations.
- Climate data: precipitations, altitude, longitude, sunshine hours, wind speed, average low and high temperatures and relative humidity for each region.
- Land type for direct and indirect land use change evaluation.

Some input parameters have a great impact on all aspects of the supply chain. Yield for example is a key parameter. As all supply chain inputs during the growth stage are on a per hectare basis (land use effects, chemicals input, in-field operations), biomass productivity (or yield) in dry tons per hectare will directly impact the extent of these contributions per dry ton or GJ of biomass delivered at the power plant. Another example is biomass moisture content. It directly impacts not only drying energy requirements, but also all of the processing and transport stages whose energy requirements depend on the incoming wet biomass mass flow, and are finally converted into MJ per dry ton.

The values for these parameters are reported over a wide range in the literature. Miscanthus in Europe for example has been widely investigated, and productivity as low as 4 t_{DM} ha^{-1} [75] and as high as 60 t_{DM} ha^{-1} [77] have been reported. To capture this uncertainty in the model, a database gathering the 150 input parameters, and their value according to different sources, was developed. 50 input parameters were selected on the basis of their impact on the model, number of sources

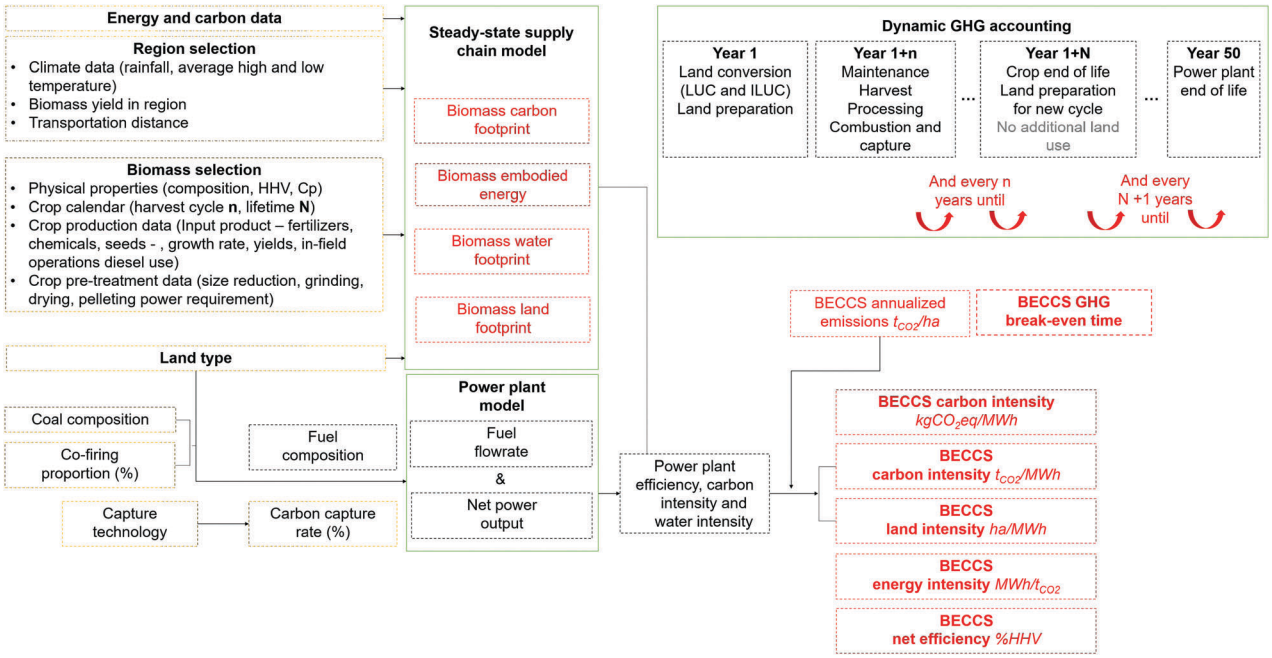

Fig. 1 Biomass water, carbon, energy and land footprints were calculated using energy and carbon data, region specific data, biomass data and land data. The power plant calculations were carried out in IECM.[26] BECCS hydro, energy and carbon efficiencies were calculated by combining the supply chain and the power plant model. The temporal carbon efficiency of BECCS was evaluated with a dynamic GHG balance over 50 years.

and scatter. Normalized data series length and scatter of these parameters are presented in Fig. 2.

As can be observed in Fig. 2, it is important to acknowledge the level of variability in some of the input data, *e.g.* the embodied energy and carbon footprint of chemicals, land conversion emission factors, and yield values. This uncertainty associated with key input parameters can clearly lead to a wide range of model outcomes. In order to evaluate the uncertainty in these outcomes, the model was evaluated with the lower bound and upper bound of the selected parameters. If the data series contained more than five sources, and in order to avoid unlikely data (very extreme yield value for example), the lower bounds and upper bounds chosen were the 95% confidence interval bounds. To use the example of miscanthus productivity in Europe, the range 15.6–22.1 was used instead of the 4–60 found in the literature. For parameters with less than five sources, minimum and maximum values were taken as the uncertainty bounds. Tables 17–19 in Appendix C gather the average value and range of uncertainty of each input parameter of the model.

2.2 System boundaries for agriculture residues

For agricultural residues, it is assumed that straw is a by-product of wheat production. Whilst there are a variety of approaches to attribute the energy use and GHG emissions associated with the production of a crop, to agricultural residues,[114–116] we have decided to assume that land conversion and farming contributions were not attributed to the residue. Straw LCA starts at its collection from the field and ends at the power plant boiler. However, as straw would have normally been left on the field to provide the crop with nutrients, additional fertilizers need to be applied to compensate for its removal. This has been included in the analysis following the work of Parajuli *et al.*, where it was assumed that 30%, 100% and 100% of straw nitrogen, phosphorus and potassium content, respectively, was available to the field.[56] Given the composition of wheat straw, extra NPK fertilizer input was then determined and included in the model.

From this perspective, water consumption during wheat growth was not included in the evaluation of the water intensity of a wheat straw-based BECCS facility. However, wheat water footprint is presented in this analysis to compare the water footprint of energy dedicated crops with that of conventional crops such as wheat.

2.3 The question of marginal land

One of the input parameters of the model is land type. In order to include the potential effect of direct and indirect land use changes, a number of different land types were considered: grassland, cropland, marginal cropland, forests and wetland or peatland. In the debate on bioenergy land competition with food,[117] the potential mobilisation of marginal land for bioenergy production has been investigated.[68] Land classification usually differentiates forests, cropland, grassland, protected land, inland water and shores, urban land, and miscellaneous.[118] Marginal lands are defined by low productivity lands unsuitable for agriculture. However, many studies have studied the potential of biomass production on marginal land,[119–121] resulting in different conclusions as to biomass resilience to land type. In this analysis, biomass yield and land type were considered as independent variables. Considering the embedded range of uncertainties in yield values considered for each biomass, with data obtained on

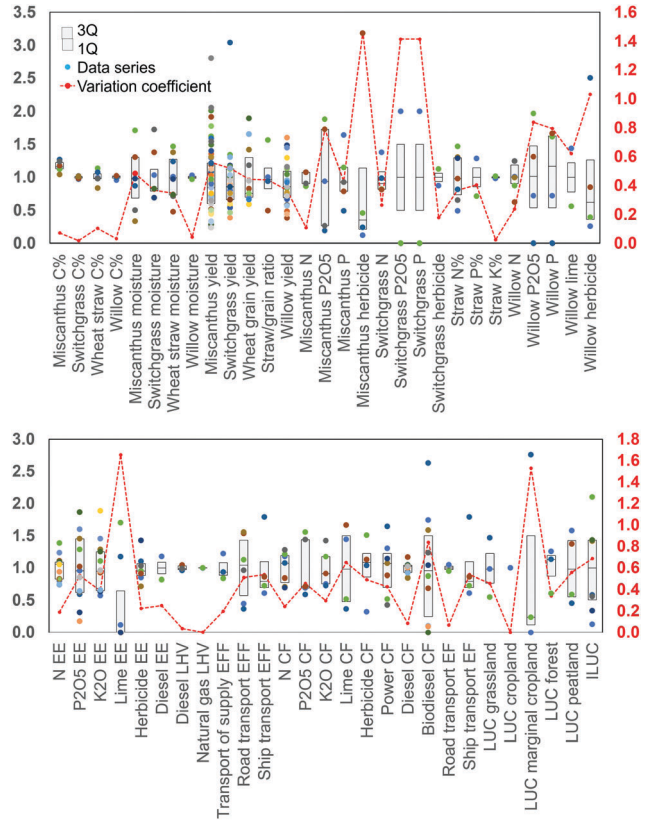

Fig. 2 This figure presents the length and scatter of biomass (top) and GHG and energy (bottom) normalized data series of the 50 parameters selected for the model uncertainty evaluation. Biomass data include biomass carbon content, moisture content at harvest, and the application rate of fertilizers and chemicals. GHG and energy data include fertilizers, chemicals and fuel EE and CF, fuel LHV, transport fuel efficiency and emission factors, and LUC and ILUC conversion factors for different land types. Each circle in a data series corresponds to a value collected from the literature. Furnished series (miscanthus yield) as opposed to scarce series (lime application rate), as well as scattered series (P_2O_5 application rate for miscanthus), as opposed to unscattered series (straw potassium content) can be observed through the number and disposition of the circles relative to the first and third quartiles. The variation coefficient is a last indication of scatter, with values over 1.5 for uncertain data such as LUC for marginal cropland or lime EE.

both suitable land crops[122] and marginal lands,[121] it was considered that this range already captured yield potential variability with land type.

3 The water–energy–carbon nexus of BECCS

A water, energy and GHG balance was carried out on each selected biomass supplied from each selected region. As no data were found on willow growth in regions other than North America and Europe, the study of willow was limited to these regions.

3.1 BECCS water intensity

3.1.1 Biomass water footprint. We begin with an evaluation of the water footprint evaluation of each crop grown in each region – or more accurately in each climate. Fig. 22 in Appendix B gives an overview of the water footprint model used for this analysis. The water footprint of a crop in a given region can be interpreted as the summation of three contributions: the green, blue and grey water. In our model, green water footprint was calculated as the amount of effective rainfall, R_{EF}, available in a given region of the world. When expressed in $m^3\ ha^{-1}$ this value is only a function of the region (climate) considered. The climate data required are the average monthly precipitation in mm per month. Table 1 presents the representative regions and specific cities for which reported data were gathered for use in the model. For clarity, we are not suggesting that biomass will be cultivated in Sao Paulo, rather, measured climate data were available for this specific location, and hence these data were used in our model.

Table 1 Regions and climates selected in the model

Country/region	City	Climate
Brazil	Sao-Paulo	Subtropical summer rainfalls
China	Zhengzhou	Subcontinental temperate
Europe (Netherlands)	Eindhoven	Oceanic temperate
India	Amritsar	Semi-arid
The USA	Orlando (Florida)	Subtropical summer rainfalls

Precipitation was then collected from the FAO-clim database,[123] based on weather stations located in the aforementioned cities. Data were retrieved for a period of ten years. In the FAO guidelines to compute crop evapotranspiration,[47] water run-off has to be considered in the determination of the available water from rainfall. The FAO developed tool CROPWAT 8.0[124] enables the calculation of effective precipitation in a given region, based on empirical linear correlations established on a specific soil type. CROPWAT default soil composition was used since soil type was not considered as an input parameter in the analysis. A 10 year average of monthly precipitation data was implemented in CROPWAT 8.0 to get the monthly effective precipitation in mm ha^{-1}. The green water was then determined for a given crop in $m^3\ t_{DM}{}^{-1}$ of biomass using the crop annual dry mass yield in $t_{DM}\ ha^{-1}$.

$$\mathrm{GnWF} = \frac{R_{EF}}{Y_{1,dry}} \quad (1)$$

The blue water is the amount of fresh water required in addition to the green water to compensate for the crop evapotranspiration. In order to compute the blue water footprint, the crop theoretical water requirement for a given region is evaluated from the monthly reference evapotranspiration ET_0 and the crop growth coefficients for that region. ET_0 is by definition the evapotranspiration of a reference crop (grass) in the region, and only depends on the climate conditions (average low and high temperatures, relative humidity, sunshine hours, wind speed, latitude and altitude). CROPWAT also enables the calculation of the monthly ET_0 in mm per day using the Penman–Monteith equation detailed in Allen *et al.*[47] This standard evapotranspiration was then pondered by the crop growth rates: initial stage $K_{c_{ini}}$, mid-season stage $K_{c_{mid}}$ and late-season stage $K_{c_{end}}$.

The crop theoretical water requirement, CWR, in mm per month is calculated by the integration of the corrected evapotranspiration rate, over the length of each growth stages n_i (in days).

$$\mathrm{CWR} = \sum_{n_i} \mathrm{ET}_0 \times K_{c_i}, \quad \mathrm{i} = \mathrm{ini, mid, end} \qquad (2)$$

The blue water footprint is then calculated as the difference between CWR and R_{EF}, and expressed in $m^3\ t^{-1}$ biomass:

$$\mathrm{BWF} = \frac{\mathrm{CWR} - R_{\mathrm{EF}}}{Y_{1,\mathrm{dry}}} \qquad (3)$$

The last contribution accounts for water pollution resulting from farming. The main cause of water pollution is assumed to be nitrogen leaching from nitrogen-based fertilizer use.[48] Following the work of Mekonnen *et al.*, we calculate the amount of fresh water needed to dilute the concentration of water nitrates to its usual background level.[49] Grey water footprint is thus a direct function of nitrogen-based fertilizer application rate (in kg ha^{-1}), nitrogen leaching (assumed here to be 10%) and crop yield:

$$\mathrm{GyWF} = \frac{F_{\mathrm{N,leaching}} \times N}{0.01 \times Y_{1,\mathrm{dry}}} \qquad (4)$$

Fig. 3 shows the blue and grey water contributions in the growth of miscanthus, switchgrass, wheat, willow. The results are presented on a $m^3\ t_{DM}{}^{-1}$ harvested crop basis.

Given that the grey and blue water footprints represent the marginal amount of water required in addition to the green water (supplied by rainfall), these water footprints are presented in Fig. 3. Water requirements per hectare of energy dedicated crops were found to be higher on average than that of wheat: 834 mm ha^{-1} for miscanthus against 532 mm ha^{-1} for wheat. This is consistent with the BECCS water footprint analysis presented by Smith *et al.*,[42] and can be explained in the difference in crop calendars and coefficients. However, as pointed out by Smith *et al.*, this tendency changes when water footprints are expressed on a mass basis, due to the higher yield of energy dedicated crops as compared to that of conventional crops. Because of their low fertilizer input (impacts the grey water footprint) and relatively high yield, herbaceous biomass like miscanthus and switchgrass are thus found to be more sustainable water wise than conventional crops.

Among the energy dedicated crops, the water footprint of SRC willow was found to be slightly higher than that of switchgrass and miscanthus, which is mainly due to willow lower yield per hectare. However, the feasibility of irrigating and fertilizing SRC willow by waste water has been investigated in Sweden,[125,126] which could considerably lower both grey and blue water footprints.

Energy dedicated crops are also characterized by a wider uncertainty range, relative to conventional crops. The difference lies in the greater uncertainty in input data (fertilizer use and yield) for the latter crops, derived from local experiments or simulations, as opposed to wheat data extracted from national or regional scale database on actual fertilizer use[127] and yield.[128] Switchgrass crop coefficients for example were not available in the literature, and, as suggested by Yimam *et al.*,[129] coefficients of Sudan grasses,[47] the closest species in terms of growth, were used.

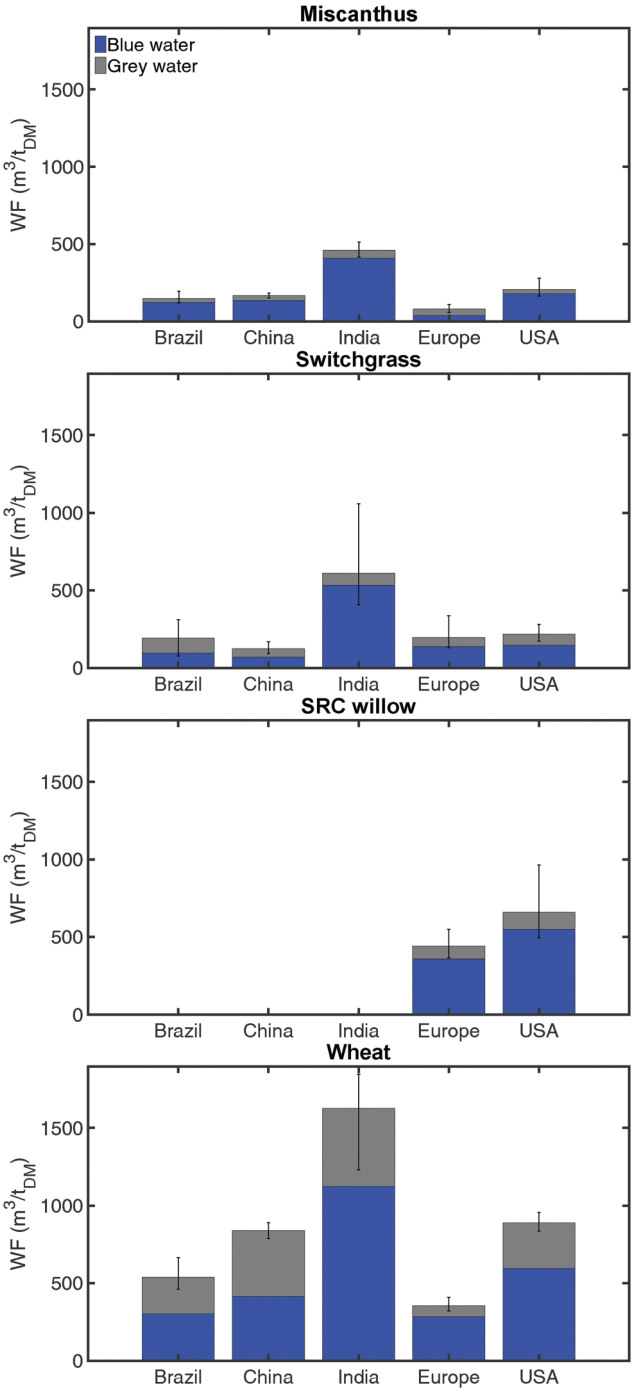

Fig. 3 Blue and grey water footprints of four crops in different regions. Yield and nitrogen inputs are key contributors to the blue and grey water footprints which explain the poor performance of wheat relative to perennial grasses, and to a smaller extent willow. Water footprints are highly dependent on the biomass type and regions, and all the more uncertain for energy dedicated crops.

The evaluation of the water footprint of agriculture products has been carried out in different studies,[49] and with a growing

Table 2 Water footprint model comparison with literature results

Crop, region[source]	Boundaries	Literature data	Model
Miscanthus, Netherlands[51]	CWR (m^3 t_{DM}^{-1})	334	175–248 (205)[a]
Miscanthus, Florida[90]	GnWF + BWF (m^3 t_{MW}^{-1})	330–495 (413)	289–373 (321)[b]
Switchgrass, Oklahoma[129]	CWR (mm $year^{-1}$)	521–786 (654)	414[c]–693[d]
Willow[69]	CWR (mm $year^{-1}$)	100–1790 (698)	628[c]–1034[d]
Wheat[50]	GnWF (m^3 t_{MW}^{-1})	1277	728[c]–1712[d]
Wheat[50]	BWF (m^3 t_{MW}^{-1})	342	255[c]–530[d]
Wheat[50]	GyWF (m^3 t_{MW}^{-1})	207	62[c]—262[d]

[a] Model lower bound–upper bound (average) results for Europe, Netherlands. [b] Model lower bound–upper bound (average) results for USA, Florida. [c] Model average result for Europe, Netherlands. [d] Model average result for USA, Florida.

interest in biomass production, studies now also focus on modeling or measuring water footprints of conventional and less-conventional biomass crops.[51,90,129] Studies however can differ in input data (climate conditions, yield, fertilizer use, fertilizer leaching), boundaries (crop theoretical requirement, green and blue water footprints, grey footprint), and complexity of the model (water stress correction, soil water capacity and type). Keeping in mind these differences, Table 2 compares model results with those in the literature. Overall results were found to be consistent with the sample of values selected from the literature.

3.1.2 BECCS net water use. A supercritical 500 MW coal-fired power plant (base efficiency of 38.9%$_{HHV}$) with post-combustion capture rate and a cooling tower was modelled in the Integrated Environment Control Model (IECM[26]). The capture system modelled is based on monoethanolamine solvent absorption which requires 3.6 GJ per tonne of CO_2 recovered. In the IECM modelling framework, the fuel flow rate, F_F, is adjusted to meet the 500 MW capacity depending on the fuel input conditions. The power plant net power output, NPO, in MW, and the water flowrate, F_W, in t_{H_2O} h^{-1}, are then calculated. It is important to differentiate between water withdrawal and water consumption. The water consumed is the fraction of the total water withdrawn from the cooling source which is not returned to the source after use. In this study, the power plant hydrodynamic efficiency is assessed by the water intensity, defined as the amount of fresh water consumed per MW h of electricity generated:

$$\mathrm{WI} = \frac{F_W}{\mathrm{NPO}} \quad (5)$$

IECM calculations for a coal fired power plant with a wet cooling tower and no CCS were compared to those in the literature. Table 3 presents both water withdrawal and consumption values, and IECM results for the base case were found to be consistent with those from the literature.

Table 3 Comparison of IECM water intensity calculations with the literature for a pulverized coal power plant with a wet cooling tower and no CCS

Source	Water withdrawal (m^3 MW h^{-1})	Water consumption (m^3 MW h^{-1})
IECM	2.4	1.5
Wu *et al.* (2011)[54]	1.7–4.5	1.5–3.9
IEAGHG (2013)[130]		1.2–1.9

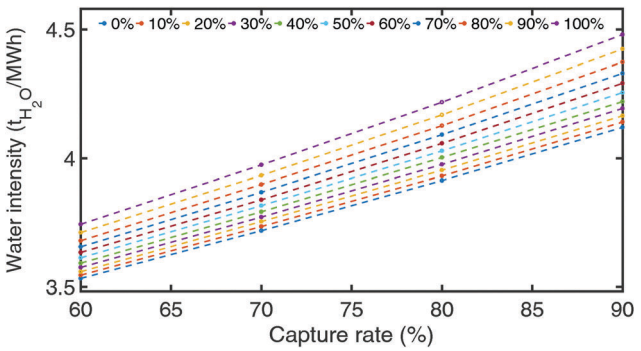

Fig. 4 500 MW supercritical coal – miscanthus pellet fired power plant water intensity as a function of capture and for different co-firing proportions. In a first instance, water consumption increases with capture rate, as steam is extracted from the steam cycle and used in the capture unit. To a smaller extent, water use increases with co-firing as a decrease in the fuel HHV increases the fuel flowrate required to generate the same amount of power.

In a second instance, it is interesting to see how the water intensity of a coal + CCS system changes as coal is substituted by biomass, and CCS capture rate increases. Fig. 4 shows the system water intensity evolution as a function of co-firing proportion and capture rate.

It is observed in Fig. 4 that co-firing and capture rate increases the water intensity, as such a system is likely to be less efficient, hence to burn more fuel per MW h of power generated, and therefore need more cooling water.

Given that the overall aim of this study is to evaluate BECCS performance across the entire supply chain, BECCS water intensity can also be calculated including the biomass water footprint WF_{WM} on a wet biomass basis:

$$\mathrm{WI_{SC}} = \frac{F_W + \mathrm{Cf} \times F_F \times \mathrm{WF_{WM}}}{\mathrm{NPO}} \quad (6)$$

Fig. 5 displays the water intensity of the power plant (in grey), and including the supply chain (in blue, yellow, red), within the biomass water footprint uncertainty range. Wheat straw water footprint was considered to be zero, since all water consumption during biomass growth was allocated to wheat production.

It can be observed that the water footprint of the biomass supply chain far outweighs that of the actual power plant. At 90% co-firing and 100% biomass firing, the water intensity

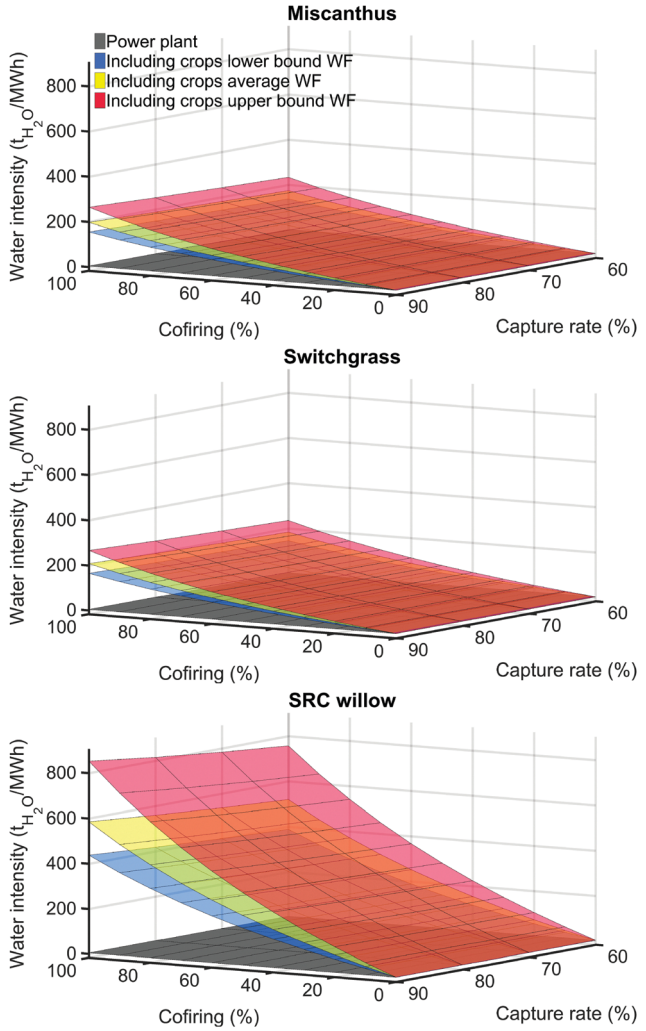

Fig. 5 500 MW supercritical coal – US miscanthus, switchgrass and willow pellet fired power plant water intensity as a function of capture rate and co-firing proportion, with and without a supply chain. Biomass water footprint impact on the power plant water intensity is two orders of magnitude greater than that of the power plant cooling requirement.

can be up to 150 times higher when including biomass production water cost in the case of willow. This highlights the importance of performing a whole-systems assessment of any given BECCS option in order to ensure its sustainability, and of including water footprint in this assessment.

3.2 BECCS energy intensity

3.2.1 Biomass production energy use. An energy balance was carried out across the entire BECCS supply chain. The following contributions were accounted for in the biomass supply embodied energy model:

- Farming indirect energy use which includes the embodied energy in different input (chemicals, seeds, fuel, power, fuel) used for crop establishment and maintenance,
- Farming direct energy (energy density) use which includes the use of fuel for product transportation and infield operations,
- Indirect (embodied energy) and direct energy use (energy density) of fuel or power input in biomass processing (size reduction, grinding, drying in rotary dryer, pelleting), transport and further pellet grinding at the power plant.

In order to compare the different contributions, each energy input was calculated per dry ton of pellet delivered to the power plant. This distinction between the embodied energy GJ t_{DM}^{-1} harvested and delivered is important since it accounts for dry and wet mass loss along the supply chain. The methodology of embodied energy evaluation is presented in Fig. 23 in Appendix B, with equations detailed in Appendix A. Similarly to the water footprint, comparing the embodied energy results with literature results is only possible when the boundaries and assumptions (yield, moisture, transportation distance, *etc.*) of the models are known. For a proper comparison, the model was evaluated under the closest conditions to those of the source. The analysis presented in Table 4 indicates that our results are in good agreement with the literature ones.

Fig. 6 shows the different energy contributions along the chain in GJ t_{DM}^{-1} pellets, with the overall uncertainty range.

As long-distance transportation was considered in some cases (Brazil, China, India and USA to the UK) it is observed that transport accounts for a substantial share of biomass embodied energy, up to 66% in the case of wheat straw imported from India. Road transport, in particular, is what drives the transport cost. With a diesel fuel efficiency of about 1.65 MJ (tons km)$^{-1}$ in road transport, and a heavy fuel oil (HFO) efficiency of 0.05 MJ (tons km)$^{-1}$, 1 km of road shipping costs about 30 km of sea shipping. Therefore, transporting national biomass a distance of 400 km by road requires as much energy as shipping biomass over 13 000 km. Taking the road distance between the farm to the harbour and the harbour to the power plant into consideration, an equivalent journey in energy cost could be for example transporting feedstock grown within 100 km of the American east coast to Drax power plant in the UK. This shows that global supply chains should be designed so as to minimise their reliance on road transport (ocean and rail being preferred), and that the development of low carbon (or carbon negative *via* BTL + CCS) transport fuels will be vital in ensuring the sustainability of BECCS. Focusing on road and ocean transport highlights the importance of coastal as opposed to inland regions for bioenergy production. However, this conclusion could be nuanced when exploring the combination of rail and barge transport as an alternative to road transport. This, as well as the impact of biomass storage, is left for future work. Willow stands out as unique in this study in that its embodied energy is primarily driven by drying. This is due to the fact that willow has a high average moisture content at harvest (52%), compared to 23% for miscanthus, 12% for switchgrass and 11% for wheat straw. The moisture target at the drying stage was set to 15% in this analysis, in order to meet the moisture requirement of 10% for the pelleting process, and assuming a 5% moisture loss during grinding. This explains the absence of drying requirement for both switchgrass and wheat straw. In another supply chain scenario (bale or chips), biomass could be dried at a higher moisture content. However transportation energy cost and boiler efficiency penalty in the

Table 4 Embodied energy model comparison with literature results

Crop, region[source]	Units	Results	Model
Miscanthus, average[67]	GJ t_{DM}^{-1}	0.52	0.31–1.02 (0.57)[a]
Miscanthus, Poland[69]	GJ t_{DM}^{-1}	0.77	0.32–1.03 (0.58)[b]
Miscanthus, Germany[76]	GJ t_{DM}^{-1}	1.25	0.86–2.00 (1.29)[c]
Miscanthus, Ireland[65]	GJ GJ_{HHV}^{-1}	0.28	0.08–0.14 (0.10)[d]
Switchgrass, US[87]	GJ t_{DM}^{-1}	1.5–1.9	0.7–1.8 (1.1)[e]
Switchgrass, US[79]	GJ t_{DM}^{-1}	0.2	0.4–1.4 (0.8)[f]
Switchgrass, US[67]	GJ t_{DM}^{-1}	1.1	0.4–1.4 (0.8)[f]
Willow, Sweden[131]	GJ t_{DM}^{-1}	0.86	1.5–2.6 (1.8)[g]
Willow, average[67]	GJ t_{DM}^{-1}	1.5	0.5–1.5 (0.9)[a]
Willow, Belgium[132]	GJ (ha year)$^{-1}$	3–16	6–12 (9)[a]
Wood pellets, Australia and Russia[94]	GJ t_{DM}^{-1}	1.13–7.5	3.7–8.0 (5.2)[h]
Willow, Poland[69]	GJ t_{DM}^{-1}	0.16	0.58–1.67 (1.01)[b]
Wood pellets[57]	MJ t_{H_2O}	4455	4563[i]
Wheat straw, New Zealand[133]	GJ GJ_e^{-1}	0.24	0.16–0.30 (0.22)[j]
Wheat straw, UK[97]	GJ GJ_e^{-1}	0.44	0.16–0.29 (0.22)[k]

[a] Model lower bound–upper bound (average) results for Europe, production only no irrigation. [b] Model lower bound–upper bound (average) results for Europe, production only no irrigation, 4k transport. [c] Model lower bound–upper bound (average) results for Europe, production (bale), 100k transport, chopping and milling for combustion. [d] Model lower bound–upper bound (average) results for Europe, production (bale) no irrigation, 100k transport, drying and pelleting. [e] Model lower bound–upper bound (average) results for the US, production (bale or chopped). [f] Model lower bound–upper bound (average) results for the US, production (bale) no irrigation. [g] Model lower bound–upper bound (average) results for Europe, production and 50k transport. [h] Model lower bound–upper bound (Europe–US) results, production, drying (50%), pelleting and transport. [i] Drying 45% to 15%. [j] Model lower bound–upper bound (average) results for the US, collection (bale), 90k transport grinding, combustion. [k] Model lower bound–upper bound (average) results for Europe, collection (bale), 40k transport grinding, combustion.

power plant would automatically be higher, which could potentially offset the energy saved at the drying stage. The embodied energy associated with the chemicals used also constitutes an important share contributing to above 10% of the overall embodied energy. This is due to the fact that willow is characterised by a relatively low yield for a high chemical input rate. Pellet grinding cost represents between 5 and 17% of the total production energy cost. Williams *et al.* showed that treatment on biomass pellets could reduce this cost by as much as a factor of four with steam-exploded pellets, and up to a factor of 25 with torrefied pellets.[34] The grinding cost of torrefied pellets would therefore be over five times lower than that of coal on a mass basis, and four times lower on an energy basis. Torrefaction was not included in this analysis, but the trade-off between torrefaction energy requirement and improved power plant performance with torrefied biomass is clearly an area which warrants further study. The relative magnitude of the uncertainty associated with the total embodied energy is observed to vary significantly between regions. For example, the calculated range for India is much greater than that for Europe. This observation is primarily driven by uncertainty in yield data. Yield data were widely available in Europe, which enabled the use of a 95% confidence interval as the uncertainty range, thus excluding extreme yield values. For India, yield values obtained from experiments in arid or semi-arid climates in other regions were used,[73,134,135] but these data were scarce and highly variable.

3.2.2 BECCS net chain efficiency. Using the power plant model presented previously, the power plant power generation efficiency η (in % HHV) can be calculated on the basis of the fuel higher heating value (HHV) (in MW h t^{-1}) and net power output NPO (MW):

$$\eta = \frac{\mathrm{NPO}}{F_\mathrm{F} \times \mathrm{HHV}} \tag{7}$$

As shown in Fig. 7, efficiency decreases with capture rate at co-firing proportion. This is explained by the efficiency penalty imposed by both the capture system and the use of a lower quality fuel (lower HHV). It can be observed that the efficiency drop is more driven by the capture rate than by the co-firing increase: the efficiency drop is between 0.95 and 1.1% points for a 10% CO_2 capture rate increase, where it is between 0.15 and 0.40 for a 10% co-firing increase.

Similarly to the water intensity, it is interesting to see how this efficiency changes as we include biomass production energy use in the overall balance:

$$\eta_\mathrm{SC} = \frac{\mathrm{NPO}}{F_\mathrm{F}(\mathrm{HHV} + \mathrm{Cf} \times \mathrm{EE_{WM}})} \tag{8}$$

Fig. 8 displays the power plant efficiency (in grey) as well as BECCS net chain efficiency (coloured) within the uncertainty range.

The effect of including biomass supply chain is quite important, with the greatest efficiency loss (points) between 7.9% in the lower bound scenario, and 10.7% in the upper bound scenario in the case of willow, whose high supply chain embodied energy translates into a poor performance in terms of net chain efficiency. It is worth noting that if one considers BECCS as a climate mitigation technology, assuring that BECCS achieves a net negative CO_2 balance at a low water cost is the main objective. In this regard, BECCS power generation performance is not as critical as the system's carbon and water intensities in the evaluation of BECCS potential for climate mitigation. However, the system efficiency and biomass supply chain energy cost will ultimately determine the marginal cost of a BECCS power plant. If we assume that BECCS plants might be expected to operate within a liberalised electricity market, a substantial marginal cost of generation would result in a decreased capacity factor for these plants, in turn limiting

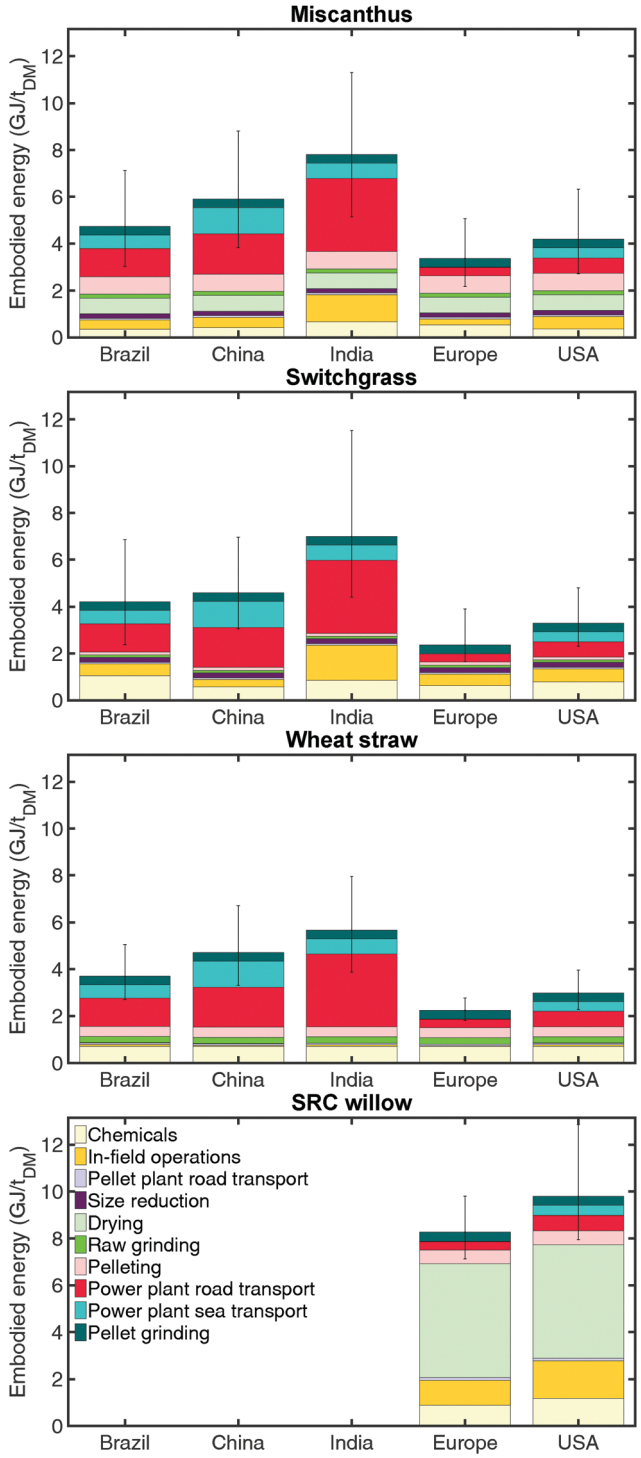

Fig. 6 Embodied energy in pellets from different regions. Road transport and industrial drying for high moisture biomass such as willow are large contributors to the biomass energy cost. Other means of transport (sea, rail) and alternative drying (natural drying, ventilated storage) should be thoroughly investigated.

the amount of CO_2 that would be removed from the atmosphere. This is something which will bear careful examination in the context of understanding how BECCS will operate in practice.

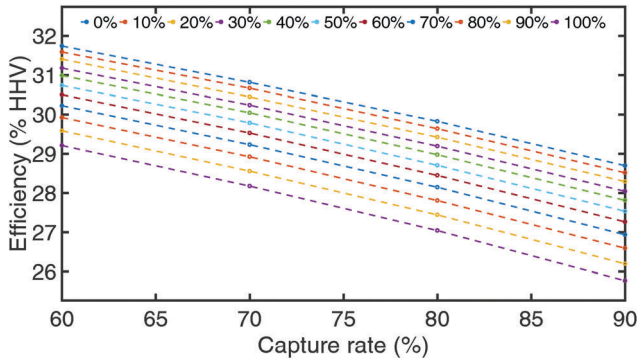

Fig. 7 500 MW supercritical coal – miscanthus pellet fired power plant efficiency (%HHV) as a function of capture and for different co-firing proportions. Efficiency decreases with capture rate, as the capture unit requires extra energy, and to a smaller extent with the increase in biomass share in the fuel.

3.3 BECCS carbon intensity

3.3.1 Biomass carbon footprint without land use changes. The carbon footprint model follows a very similar methodology to that of the embodied energy model. For input product contribution, a product embodied energy EE_k is replaced by its carbon footprint CF_k, *i.e.* the direct and indirect emissions from the product supply chain. For fuel use in processing and transport, fuel embodied energy is replaced by its carbon footprint, and heating value by its carbon emission factor. Three additional emission contributions are considered in the carbon footprint model:

- N_2O emissions due to nitrogen-based fertilizer application,
- Negative emissions through biomass combustion and carbon capture and storage (BECCS),
- Direct and indirect land use changes.

As N_2O has a global warming potential (GWP) 298 times (100 year-basis) higher than that of CO_2, N_2O emissions through nitrogen leaching and volatization from fertilizer application were also considered in the analysis. N_2O emissions were calculated using the FEAT methodology,[67] and the detailed equations are presented in Appendix A.

Biomass carbon footprint results were also compared with existing evaluations from the literature in Table 5, evaluating the model under the same conditions (transport distance, region if possible, process included, *etc.*). Again, Table 5 shows the great diversity in the results found in the literature, with carbon footprints found between 90 and 600 $kg_{CO_2}\ t_{DM}^{-1}$. With an average relative error between the model mean values and the literature results under 30%, and considering the uncertainty range of results, the model results were considered consistent with those found in the literature.

In order to evaluate biomass carbon negative potential, biomass carbon intensity in $t_{CO_2}\ t_{DM}^{-1}$ biomass was also evaluated. For a BECCS power plant operating at a given capture rate, R_{CCS}, biomass carbon intensity has the following expression:

$$CI_B = R_{CCS} \times C_B \frac{MW_{CO_2}}{MW_C} \quad (9)$$

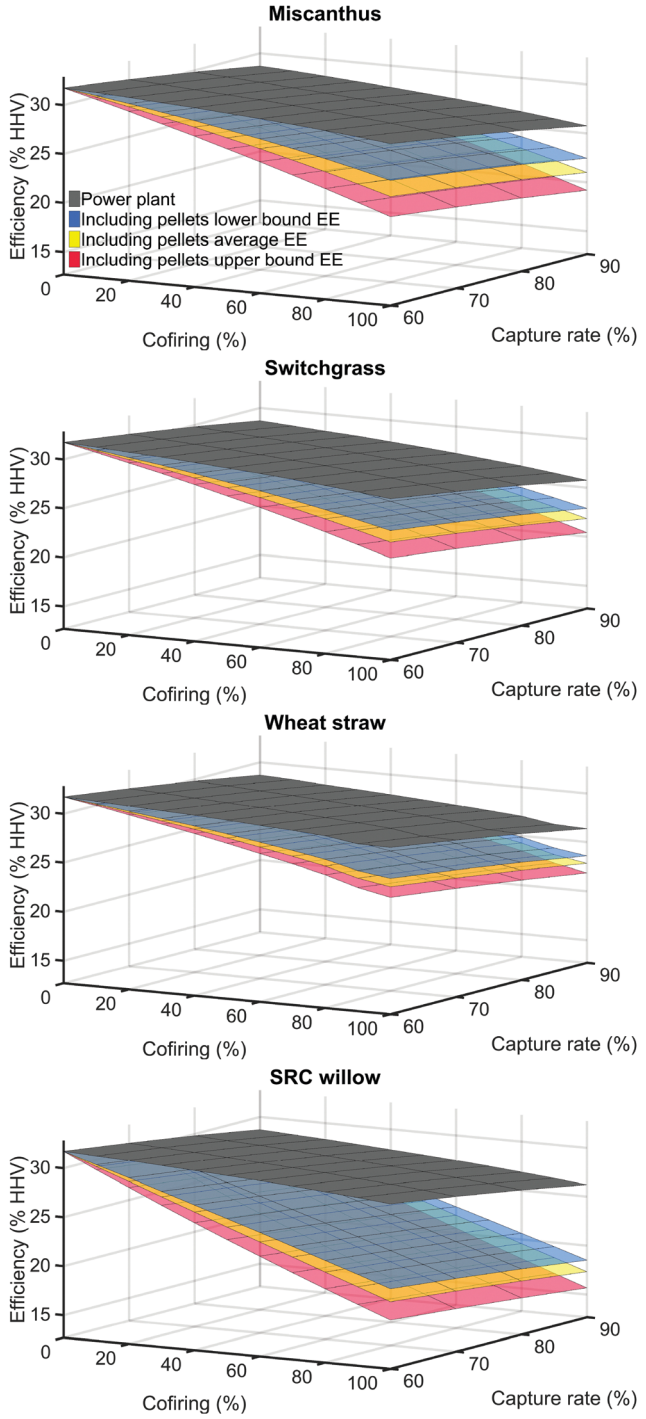

Fig. 8 500 MW supercritical coal – US biomass pellet fired power plant power generation efficiency (%HHV) as a function of capture rate and co-firing proportion with and without including a biomass supply chain (incl. sc). The efficiency drop with the biomass supply chain is up to 11% in the case of willow, which would critically increase the power plant operational cost, thus decreasing BECCS competitiveness in a global electricity market.

where MW_{CO_2} and MW_C are the molecular weights of CO_2 and carbon, respectively. C_B is biomass carbon content (dry weight basis).

Carbon footprints of different feedstock from different regions are presented in Fig. 9.

The addition of N_2O emissions, which have a large weight in the overall balance, underlines the double effect of fertilizers, both from their energy and carbon intensive production process, and from the subsequent emissions they cause after their application to the field. Biomass processing also has a higher weight in the carbon balance because of the relatively high electricity carbon intensity values chosen for this model – 470–800 $kg_{CO_2\text{-eq}}$ MW h^{-1}.[137,138] This input is highly dependent on the power source and region, and could be significantly improved in the context of a decarbonised electricity system – 50 $kg_{CO_2\text{-eq}}$ MW h^{-1}. Drying of high moisture biomass such as willow still constitutes an important contribution. Aside from management practices like natural open-field or storage drying, this cost could be reduced by substituting natural gas with biomass in rotary dryers.[94,139] These options are further investigated in Section 4.

3.3.1.1 Effect of direct and indirect land use changes. As illustrated in Fig. 10, this analysis provides an evaluation of the potential impact direct and indirect land use change effects would have on the system.

To account for direct land use changes, conversion emission factors in t_{CO_2} ha^{-1} for each land type were taken from the literature.[102,103] For indirect land use changes however, conversion factors also depend on the initial use of the land. Land types were thus classified into two categories; managed land, *i.e.*, already allocated to an activity, and unmanaged land. If converting part of a managed land – cropland or grassland – to biomass production, an ILUC conversion factor in t_{CO2} was attributed. When converting a land unallocated to any activity, ILUC was considered to be zero. ILUC conversion factors in t_{CO_2} ha^{-1} are not found as such in the literature. Indirect land use changes have been thoroughly investigated in the context of biofuels in which conversion factors are expressed in t_{CO_2} MJ^{-1}, and are a function of the biofuel energy yield MJ $(ha\ year)^{-1}$, time horizon (in years), fraction of land displaced (in $\%_{ha}$) and average emission factor resulting from the activity displaced (in t_{CO_2} ha^{-1}). Two different sources were used: an analysis by Plevin *et al.* based on corn bioethanol in the US,[103] and an analysis from Overmars *et al.* based on bioethanol production in Europe, from three different feedstocks: wheat and sugar beet grown in Europe and sugarcane imported from Brazil and Pakistan.[107] As ILUC factors are expressed in $kg_{CO_2\text{-eq}}$ MJ^{-1} of biofuels in both analysis, the data provided in the studies were used to derive land ILUC factors in $kg_{CO_2\text{-eq}}$ per hectare cultivated for bioenergy. These factors can then be used independently from biomass yield and project time horizon. When average net displacement factors (ha displaced/ha of biofuels) and emission factors ($t_{CO2\text{-eq}}$ ha^{-1}) were provided,[103] the land ILUC factor was obtained by multiplying these two parameters. When the data provided were less straightforward,[107] the land ILUC factor was obtained by multiplying the ILUC factor by the time horizon and bioenergy yield. Plevin *et al.* described two additional analyses on US bioethanol from maize[140] and corn,[108] and these results were also included in the ILUC coefficient data set to ensure the consistency of the statistical analysis. Fig. 11 provides further details on the methodology and data used.

Table 5 Carbon footprint model comparison with literature results

Crop, region[source]	Units	Results	Model
Miscanthus, Germany[76]	$kg_{CO_2}\ t_{DM}^{-1}$	111.8	97–237 (152)[a]
Miscanthus, Ireland[65]	$kg_{CO_2}\ GJ_{HHV}^{-1}$	20.6	9.8-20.9 (14.5)[b]
Switchgrass, US[87]	$kg_{CO_2}\ t_{DM}^{-1}$	191–204	92–274 (162)[c]
Switchgrass, US[79]	$kg_{CO_2}\ t_{DM}^{-1}$	144.7–146.7	72–246 (139)[d]
Switchgrass, US[67]	$kg_{CO_2}\ t_{DM}^{-1}$	172	72–246 (139)[d]
Switchgrass, US[136]	$kg_{CO_2}\ t_{DM}^{-1}$	195–198	95–284 (168)[e]
Willow, UK–US[99]	$kg_{CO_2}\ GJ_e^{-1}$	118–242	147–396[f]
Willow, average[67]	$kg_{CO_2}\ t_{DM}^{-1}$	89	87–253 (153)[d]
Wood pellets, Australia and Russia[94]	$kg_{CO_2}\ t_{DM}^{-1}$	143–594	166–603 (306)[g]
Wheat straw, UK[97]	$kg_{CO_2}\ GJ_e^{-1}$	66	26–53 (38)[h]

[a] Model lower bound–upper bound (average) results for Europe, production (bale), 100k transport, chopping and milling for combustion. [b] Model lower bound–upper bound (average) results for Europe, production (bale) no irrigation, 100k transport, drying and pelleting. [c] Model lower bound–upper bound (average) results for the US, production (bale or chopped). [d] Model lower bound–upper bound (average) results for the US, production only no irrigation. [e] Model lower bound–upper bound (average) results for US, production only no irrigation, 40k transport. [f] Model lower bound (av. grassland)–upper bound (av. forest) results for Europe, production, LUC, no irrigation, processing, 25–75k transport. [g] Model lower bound–upper bound (Europe–US) results, production, drying (50%), pelleting and transport. [h] Model lower bound–upper bound (average) results for Europe, collection (bale), 40k transport, grinding.

In this analysis net displacement and emission factors were considered the same for all managed land types (grassland or cropland), biomass types and regions. This is a first estimation to give indications as to the potential impact of including land use change. Applying this analysis to a certain case study in order to provide precise insight for a given region would require the use of region specific coefficients.

For each land type, the initial carbon debt, D_C, including both direct and indirect land use changes, was then known. In this analysis, the time horizon chosen was 50 years, as this was deemed to be sufficiently long to give a fair evaluation of every option. The carbon debt was expressed in $kg_{CO2}\ t_{DM}^{-1}$ when dividing by the overall amount of dry biomass delivered by a hectare of land over 50 years:

$$\frac{D_C}{y_{50,dry}} \tag{10}$$

In can be observed from Fig. 12 that direct and indirect land use changes have a substantial impact on the supply chain. When adding indirect land use change both the overall carbon footprint and uncertainty are up to three times higher than those in the base case. It is important to note that as conversion factors are expressed on a per hectare basis, their impact is all the more important for lower yield biomass such as willow.

3.4 BECCS net carbon intensity

Carbon intensity is defined as the power plant emissions per MW h of electricity produced. A key assumption in this analysis is that the amount of CO_2 absorbed by the biomass during its growth equates the amount of CO_2 released upon biomass combustion. Emissions resulting from biomass combustion are thus considered to be zero. As a result, carbon intensity is calculated based on the fuel carbon content, C_F, the biomass carbon content, C_B, and the co-firing proportion, Cf:

$$CI = \frac{F_F((1 - R_{CCS}) \times C_F - Cf \times C_B) \times \frac{MW_{CO_2}}{MW_C}}{NPO} \times 10^3 \tag{11}$$

where MW_{CO_2} and MW_C are the molecular weights of CO_2 and carbon, respectively.

As illustrated in Fig. 13, carbon intensity decreases as coal gets displaced by biomass and carbon capture rate decreases. To the power plant carbon intensity are added biomass supply chain CO_2 emissions:

$$CI_{SC} = \frac{F_F((1 - R_{CCS}) \times C_F - Cf \times C_B) \times \frac{MW_{CO_2}}{MW_C} \times 10^3 + Cf \times CF_{WM})}{NPO} \tag{12}$$

BECCS net carbon intensities as a function of biomass co-firing proportion and capture rate with and without land use changes are presented in Fig. 14 and 15.

As can be observed from Fig. 14 and 15, whilst the majority of scenarios result in the net removal of CO_2 from the atmosphere, no two scenarios achieve an equivalent amount of net CO_2 removal. Importantly, it can be observed that some scenarios, such as those relying upon willow in Fig. 18, appear to be net carbon positive, resulting in the net emission of up to 1200 kg_{CO_2} MW h^{-1}. For comparison, an unabated coal-fired power plant might emit between 700 and 1000 kg_{CO_2} MW h^{-1}. Thus, if the wrong choices are made throughout the supply chain, BECCS could indeed be substantially more carbon intense than an unabated coal-fired power plant. This is one of the core results of this study. At 90% co-firing, a willow-based BECCS system is, in the mean scenario, carbon negative within the 20–100% co-firing range with no land use changes, carbon negative within the 30–100% co-firing range with LUC, and always carbon positive with ILUC. In practical terms, this narrows the feasible range of power plant operability – capture rate and co-firing proportion – for the system to be carbon negative, and ultimately decreases its flexibility. However, it is important to notice that BECCS systems including ILUC can still be carbon negative in the average scenario, within the 30–100% co-firing range for a miscanthus-based system, and 40–100% for a switchgrass-based system, at 90% capture rate. Limiting the effects of indirect land use changes as well as assuring high yield

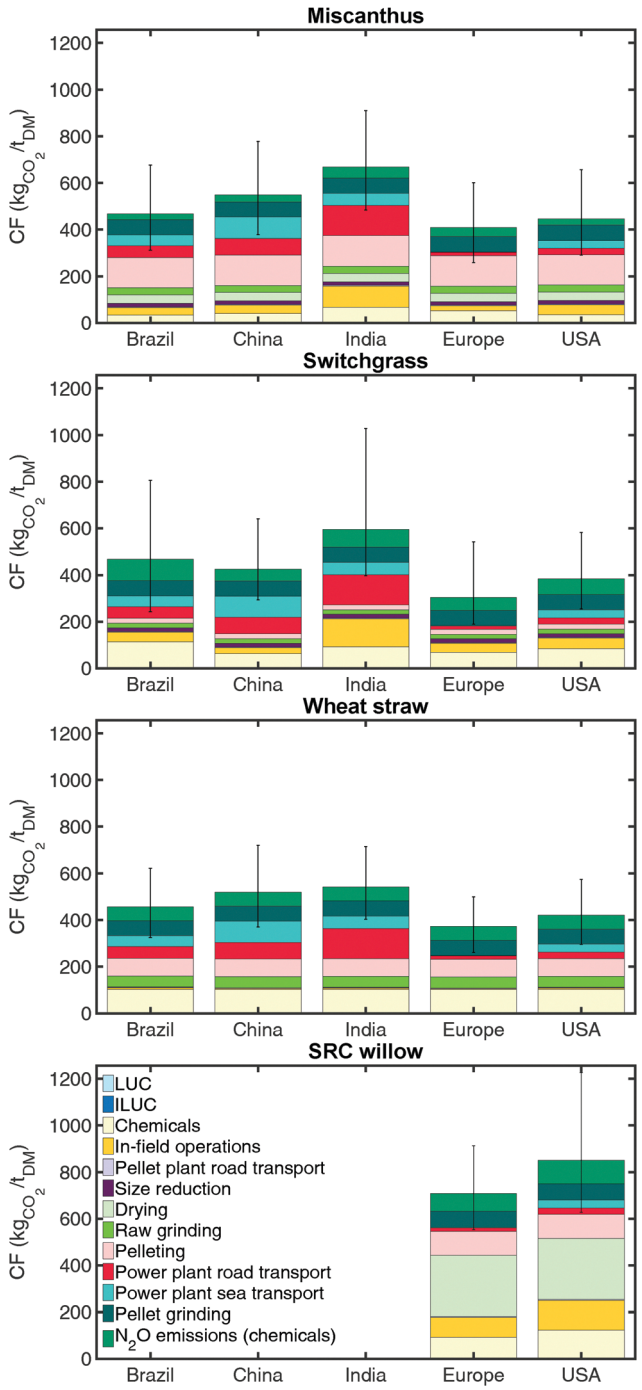

Fig. 9 Carbon footprint of pellets from different regions without accounting for land use. In addition to road transport and drying, chemical application also represents a large portion of biomass carbon footprint, with a contribution from both chemical production and resulting N_2O emissions after application.

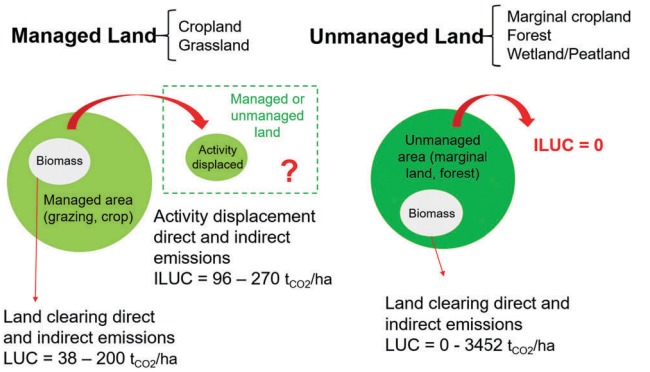

Fig. 10 Methodology of accounting for the direct and indirect land use change effects. Upon considering indirect land use change, clearing a managed land could be as bad as clearing a more dense unmanaged land such as a forest. The wide uncertainty range of indirect land use changes in turn impacts the uncertainty of the model.

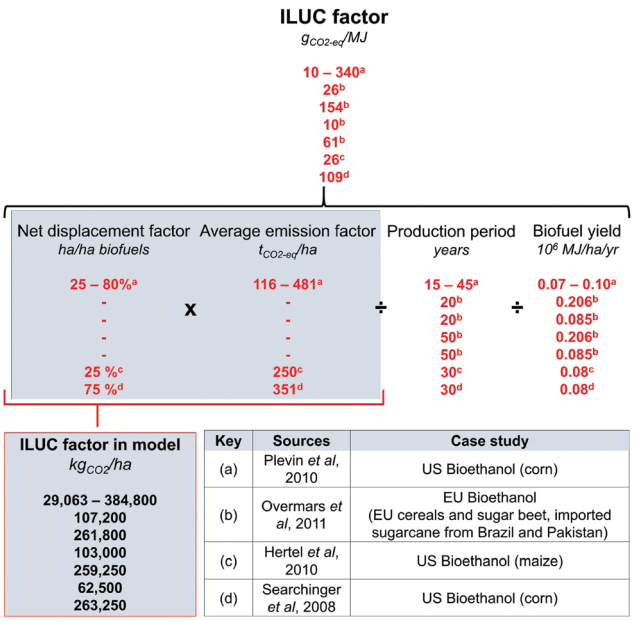

Fig. 11 Methodology for the derivation of ILUC conversion factors in $kg_{CO_2\text{-eq}}$ ha^{-1}. Values derived from Plevin *et al.*, Searchinger *et al.*, and Hertel *et al.* were obtained for bioethanol production in the US,[103,108,140] whereas the results from Overmars *et al.* are the lower and upper bounds obtained for bioethanol production in Europe, considering three different feedstocks: wheat and sugar beet grown in Europe and sugarcane imported from Brazil and Pakistan.

and low fuel, power and chemical input during biomass production will be capital for the BECCS overall balance to be negative.

3.5 BECCS net carbon efficiency

If BECCS were a perfect system, one ton of CO_2 captured biologically would equate one ton of CO_2 sequestered geologically. However, this is not the case, and GHG direct and indirect emissions throughout the BECCS value chain carbon, as well as biomass dry mass loss, must be considered as this "carbon leakage" will decrease the net amount of CO_2 removed from the atmosphere. From this perspective, carbon intensity can also be equated to carbon efficiency: how many tons of CO_2 must be sequestered biologically in order to store 1 ton of CO_2 geologically? Carbon efficiency can then be interpreted in terms of carbon negativity: systems whose carbon efficiency is over 50% are carbon negative. The carbon efficiencies of a switchgrass-based system from a marginal land and a central grassland are represented by Fig. 16.

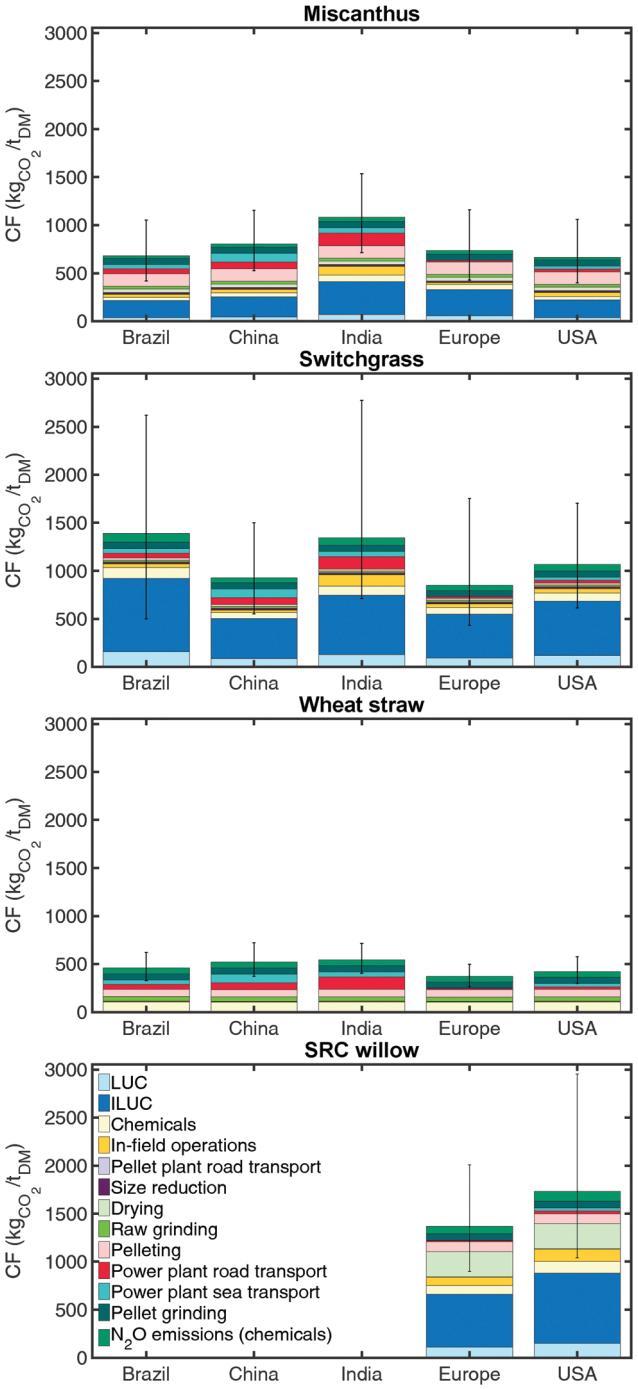

Fig. 12 Carbon footprint of pellets from different regions, including both direct and indirect land use change effects (cropland). Other contributions are minor when compared to indirect land use change effects, which increase the biomass carbon footprint value and uncertainty range by over 100%. Straw as a residue is not impacted by land use, and is represented here to emphasise the impact of land use changes.

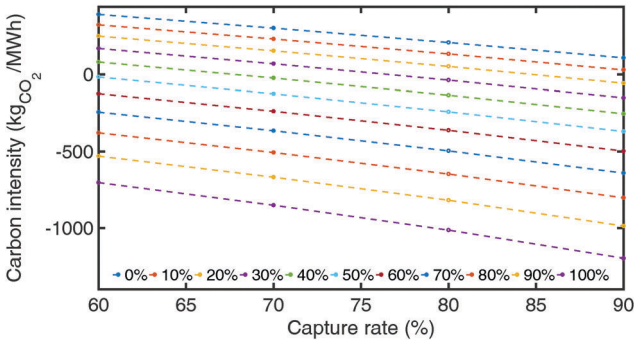

Fig. 13 500 MW supercritical coal – miscanthus pellet fired power plant carbon intensity as a function of capture rate and for different co-firing proportions. Naturally, increasing the capture rate and biomass co-firing proportion both decrease the power plant carbon intensity.

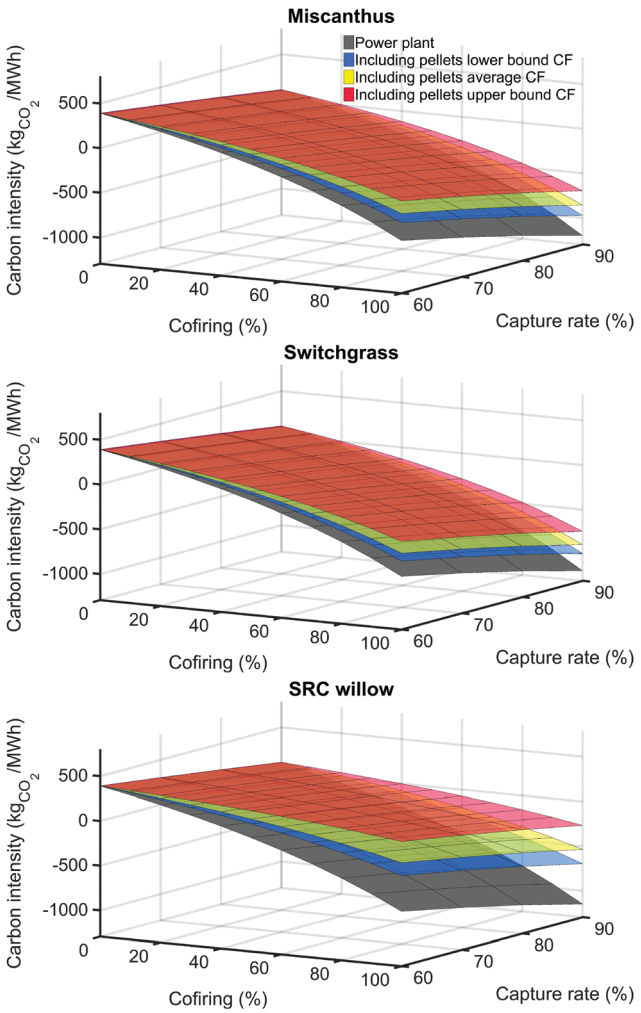

Fig. 14 500 MW supercritical coal – US biomass pellet fired power plant carbon intensity as a function of capture rate and co-firing proportion. Adding biomass supply chain emission can offset the power plant carbon negativity, which increases the minimum co-firing and capture rate values for the power plant to be carbon negative, hence decreasing its flexibility.

For the purpose of this analysis, CO_2 transport and storage was included in the BECCS value chain, assuming an energy use and subsequent GHG emissions resulting in a 6% CO_2 loss.[136]

As can be observed in Fig. 16, BECCS carbon efficiency reduces from 62% (marginal land) to 46% (grassland) when adding LUC and ILUC, with the latter accounting for over 26% of the carbon leakage. Upon adding land use changes,

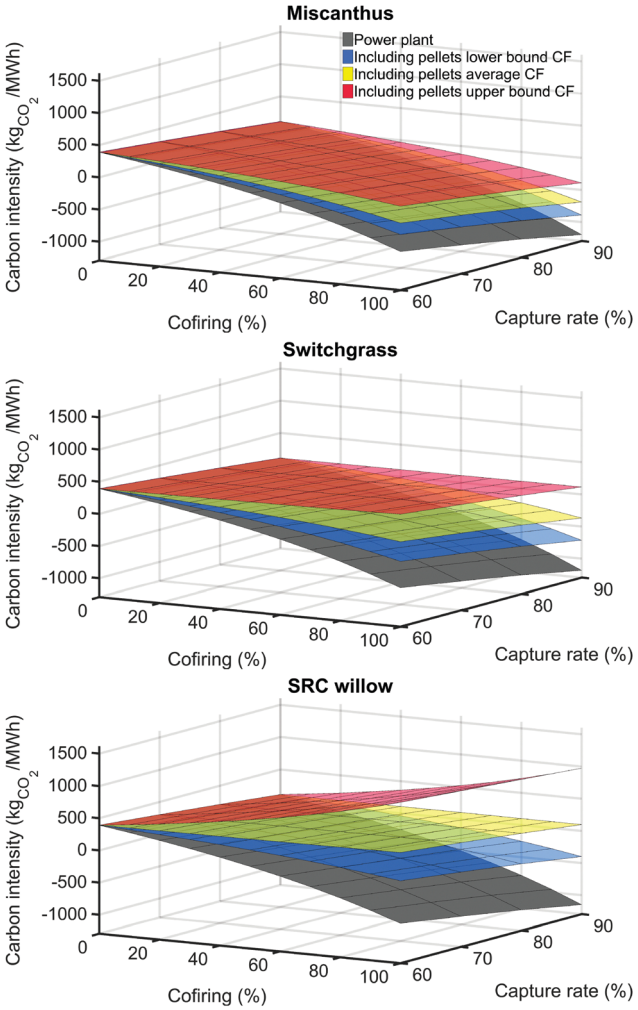

Fig. 15 500 MW supercritical coal – US biomass pellet fired power plant carbon intensity as a function of capture rate and co-firing proportion. The offset effect is exacerbated with indirect land use changes: BECCS systems do not reach carbon negativity in the upper bound scenarios.

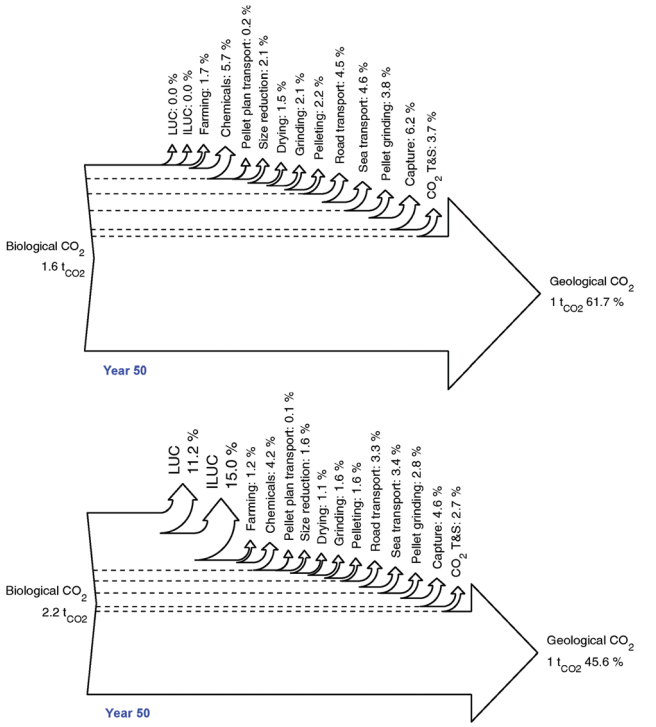

Fig. 16 Carbon efficiency diagram of the carbon flux in a US switchgrass-based BECCS system from the biological storage in the biomass to the geological storage, with (bottom) and without (top) land use changes. In this case, accounting for land use change leads to a carbon positive system (efficiency under 50%). Even with decreasing the carbon leakages resulting from the use of chemicals and biomass transport (about 11% of the losses), a substantial improvement to BECCS carbon efficiency will only be possible by limiting direct and indirect land use changes.

the facility is thus no longer carbon negative. This emphasizes the fact that though efforts throughout BECCS supply chain must be made to reduce further carbon leakages (chemicals, transport, carbon capture), a better understanding and control of land use changes will be necessary to maximise BECCS carbon efficiency.

We have demonstrated the importance of including the biomass supply chain in the evaluation of the thermo- and hydrodynamic efficiencies, and carbon intensity of the overall system. Chemicals, road transport, drying and grinding were identified as important leakages in BECCS efficiencies, though negligible when compared to land use change effects. In the next section, a dynamic accounting of the GHG emissions is performed to evaluate BECCS efficiency at removing CO_2 from a time perspective.

4 BECCS dynamic GHG emission profile

We define the number of years required for the power plant cumulative emissions to reach zero as the biomass carbon breakeven time. To assess BECCS sustainability from a plant lifetime perspective and evaluate BECCS carbon breakeven time, a dynamic carbon balance was performed on the system.

4.1 Single dynamic balance

In this model, the land is cleared and the crop established at year 1, thus generating an initial carbon debt. The crop is harvested every n years, and therefore further biomass processing, transport and capture are accounted for until the end-of-life for that crop in year $1 + N$ which is the crop end of life. As the dynamic balance is performed from the perspective of the BECCS power plant, the balance is made over 50 years, which is considered to be an upper bound of the power plant lifetime. Fig. 17 shows CO_2 cumulative emissions from a miscanthus fired BECCS power plant, from land conversion (year 1) to the power plant end of life (year 50).

Miscanthus imported from Brazil breaks even after 3, 7 and 26 years, if grown on a cropland, central grassland and forest, respectively. When grown on a Brazilian forest, miscanthus is the only crop reaching carbon break even time before year 50. When including the effects of indirect land use changes for cropland and grassland in Fig. 17, carbon

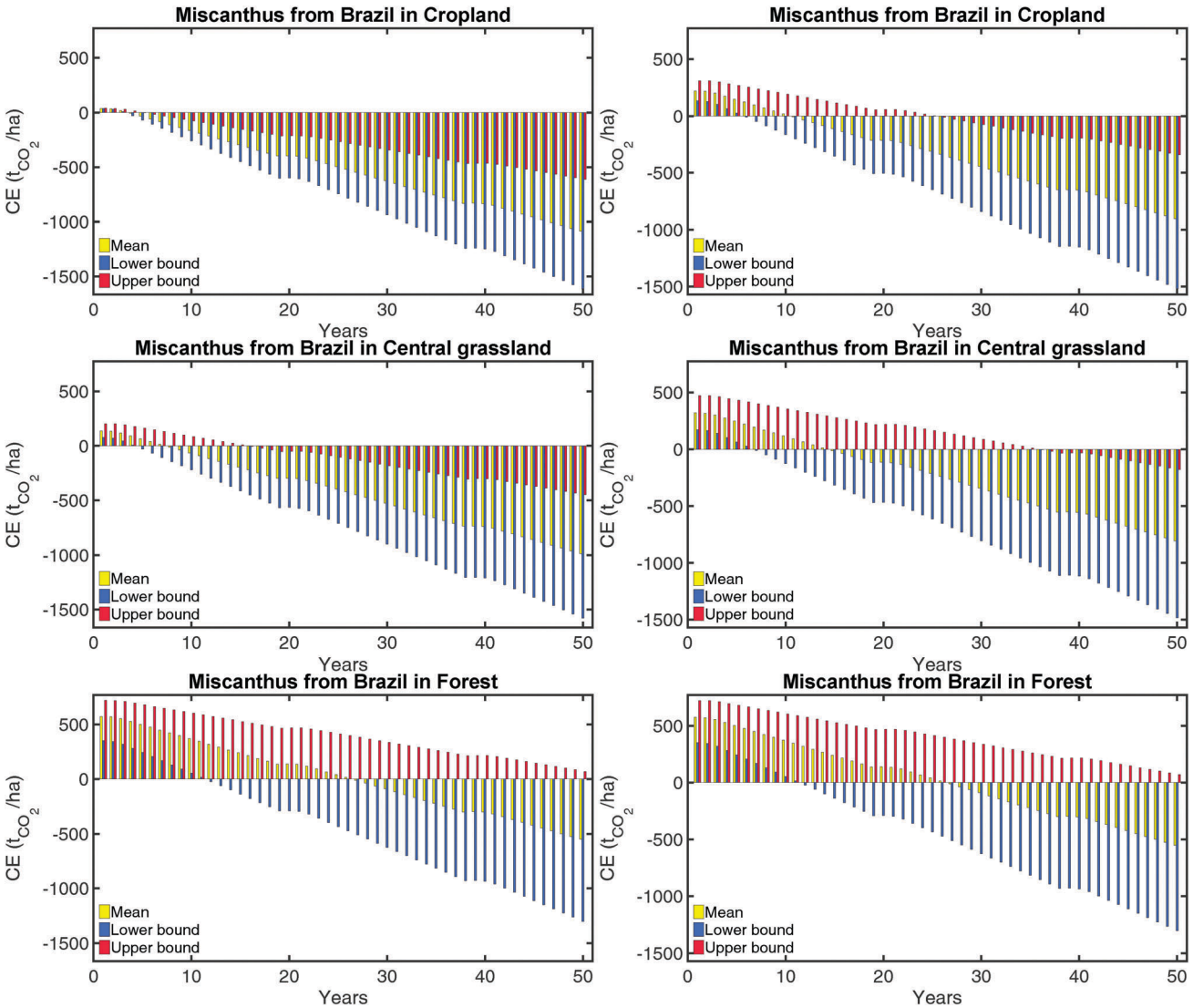

Fig. 17 Miscanthus-based BECCS cumulative emissions in t_{CO_2} ha^{-1} over 50 years for different land types including LUC (left) and ILUC (right). The system breakeven time increases from 1 to 26 years with direct land use changes. Miscanthus-based BECCS presents carbon positive scenarios before year 50 within the increased uncertainty range. Upon adding indirect land use changes, the system average breakeven time on a managed land increases by 7 years.

breakeven time increases by seven years for cropland and grassland.

4.2 Multiple dynamic balances

Rather than simply representing average, lower bound and upper bound scenarios, it is important to evaluate the whole scope of BECCS outcomes. Four case studies were selected for this analysis:

(1) Case A: miscanthus from Brazil on marginal land (no LUC and ILUC),

(2) Case B: miscanthus from Brazil on central grassland (LUC and ILUC),

(3) Case C: willow from Europe on marginal land (no LUC and ILUC),

(4) Case D: willow from Europe on central grassland (LUC and ILUC).

Fig. 18 represents the 729 outcomes when evaluating the model with the low, average and high values of biomass moisture content, carbon content, electricity carbon footprint, LUC conversion factor and ILUC conversion factors in those four case studies.

We can note from this analysis the diversity of possible outcomes, associated with a BECCS facility, as a function of the decisions made along the supply chain. In the case of miscanthus, which showed the lowest carbon footprint in the steady-state analysis, all scenarios are carbon negative over 50 years on a marginal land, with a carbon negative potential ranging from 0.7 to 1.6 kt_{CO_2} ha^{-1} captured over 50 years. When including land use effects, the number of scenarios leading to a capture potential greater than 0.5 kt ha^{-1} was reduced to 648 out of 729, but no scenario led to a dynamic carbon positive balance. For the willow case study that showed higher carbon

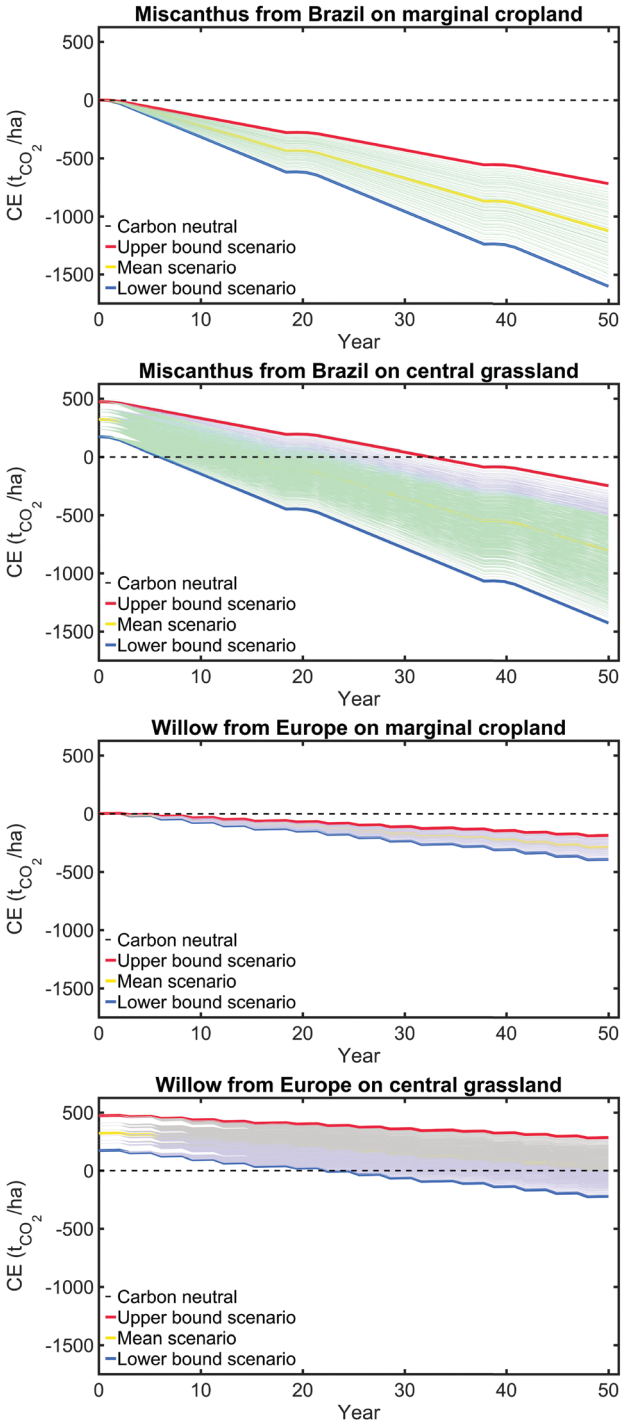

Fig. 18 BECCS cumulative emissions in t_{CO_2} ha^{-1} over 50 years for case studies A–D. Depending on the conditions, the system can be carbon positive (grey), slightly carbon negative – cumulative capture over 50 year below 0.5 kt_{CO_2} (purple), and highly carbon negative – capture over 0.5 kt_{CO_2} (green). Upon including land use changes (moving from marginal land to grassland), the spectrum of potential outcomes substantially increases.

footprints on a steady-state basis, the dynamic carbon balance was always negative on a marginal land, with a carbon capture potential ranging from 190 to 390 t ha^{-1} over 50 years. On a central grassland however, the number of carbon negative scenarios dropped to 223. In terms of carbon breakeven time, without land use effects, the time required for BECCS to be negative varied on average between 1 year for miscanthus and 3 years for willow. This became on average 15 times longer for miscanthus and willow when including land use changes. These results are presented in Table 6.

Table 6 Repartition of the results of dynamic GHG balance in case studies

Outcomes	Units	A	B	C	D
Positive scenarios		0	0	0	**460**
Negative scenarios		729	729	729	269
CO_2 removed	Mean (t ha^{-1})	−1124	−805	−288	31
	Min (t ha^{-1})	−1600	−1429	−392	−222
	Max (t ha^{-1})	−718	−248	−186	285
Breakeven time	Mean (years)	1	15	3	46
	Min (years)	1	6	3	22
	Max (years)	2	32	3	**>50**

4.3 Sensitivity analysis and alternative scenarios

A sensitivity analysis was carried out in order to rank the parameters in terms of level of impact on the GHG dynamic emission profile. The model was run with the lower, mean and upper values of 8 parameters: biomass carbon content, biomass moisture content, rate and footprint of chemicals, fuel emission factors and carbon footprint, electricity footprint, yield, LUC and ILUC conversion emission factors. Fig. 19 presents the dynamic emission profile of the 6561 scenarios simulated for a miscanthus-based BECCS facility, coloured differently depending on the corresponding parameter. For each parameter, the profiles corresponding to the lower bound scenario are coloured in blue (red for yield and carbon content), to the mean scenario in yellow, and to the upper bound scenarios, in red (in blue for yield and carbon content).

As can be observed from both figures, ILUC is the primary determining factor, followed by LUC, yield, electricity footprint, biomass carbon content and biomass moisture content. Compared to these parameters, the fuel emission factor and carbon footprints as well as chemicals rates and carbon footprints were found to have a limited impact on these results. The same analysis was performed on a willow-based system. The results are presented in Fig. 24 in Appendix D.

It is evident that LUC and ILUC conversion factors should be carefully evaluated on a case by case basis, but so should be biomass yield, composition and electricity footprint. In practice, a crop yield is a complex function of a range of parameters, including climate, biomass properties, soil type, nutrients and water availability.[141]

These results also indicate ways of improving BECCS sustainability. In order to evaluate the potential for improvements in BECCS, the following alternate scenarios were investigated:

(1) Organic chemicals (no carbon footprint),

(2) Biodiesel for in-field activities (100%) and road transport (blend 20% with conventional diesel B20),

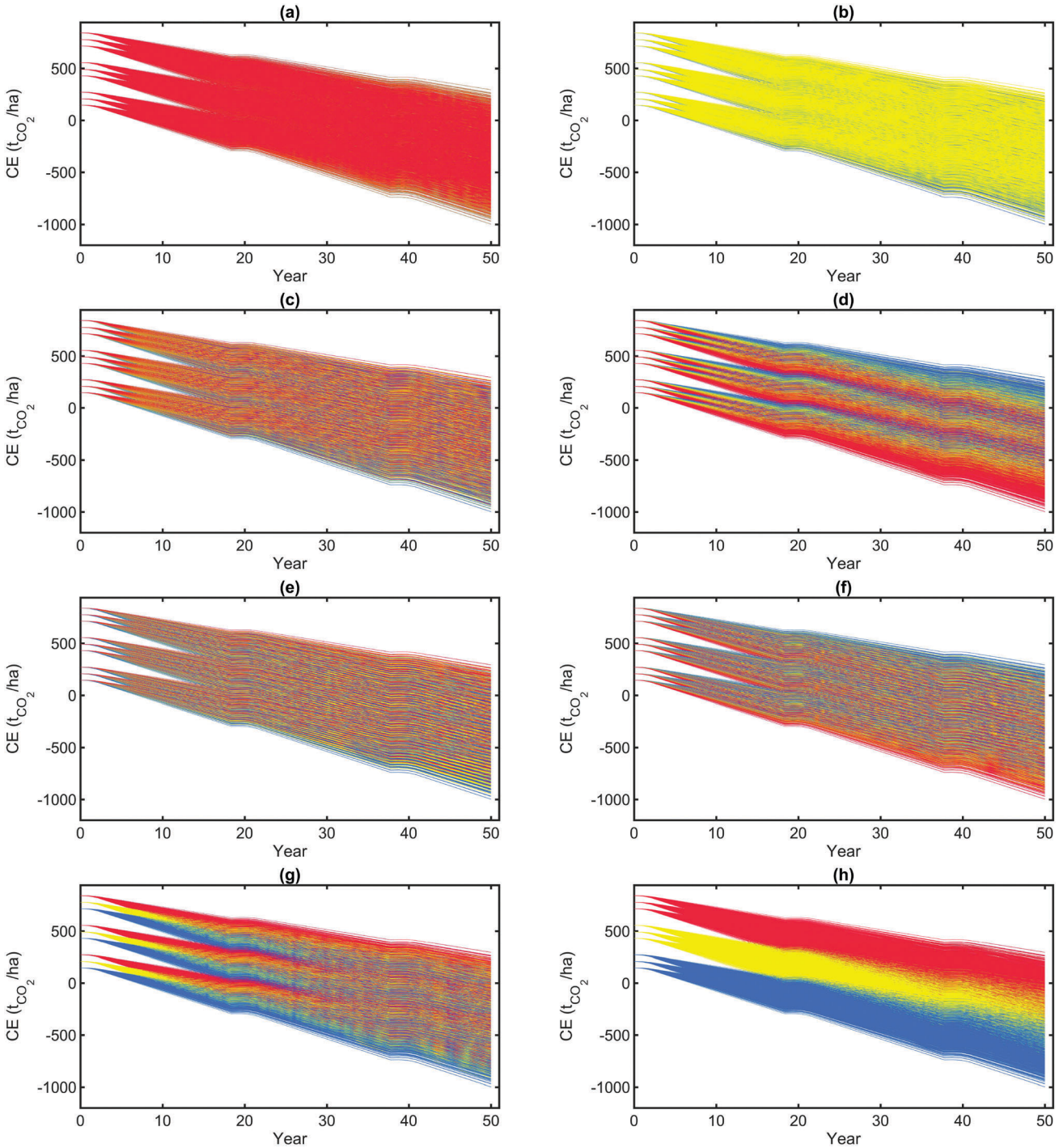

Fig. 19 Sensitivity of miscanthus based-BECCS dynamic emission profile towards eight parameters ((a) fuel footprint and efficiency, (b) chemical footprint and application, (c) moisture content, (d) yield, (e) electricity footprint, (f) biomass carbon content, (g) LUC, (h) ILUC). Emission profiles are coloured in red when the parameter is set to its upper bound (lower bound for yield and carbon content), yellow when set to its mean value, and blue when set to its lower bound (upper bound for yield and carbon content). Patterns indicate that ILUC is the determining factor, followed by LUC, yield, electricity carbon footprint and carbon content.

(3) Bioethanol with CCS for in-field activities (blend 25% with conventional gasoline E25) and road transport (blend 25% with conventional gasoline E25). We assume that bioethanol carbon footprint is -100 g_{CO_2} MJ^{-1} of fuel used.[111]

(4) Carbon neutral electricity,

(5) Drying with biomass rather than natural gas.

Ranges of uncertainty of chemical footprint and fuel emission factors were relatively small compared to other parameters,

Table 7 Effect of alternative scenarios on the BECCS carbon intensity over 50 years in t_{CO_2} ha^{-1}. Using carbon neutral power had the most important impact on BECCS cumulative emissions, followed by using bioethanol with CCS, and farming with organic chemicals. The impact of using carbon negative bioethanol could be further increased by increasing the bioethanol/fossil fuel ratio in engines, limited to 25% in our assumptions. Due to the variability in bioenergy carbon footprint, using biodiesel and drying with biomass could lead to both positive and negative impacts on BECCS cumulative emissions. This underlines the need for precise accounting of the GHG emissions associated with production and supply of bioenergy materials

Case study	Base case	Sc1	Sc2	Sc3	Sc4	Sc5
A	−1124	−1158	−1192–(−**1119**)	−1246	−1364	−1158
B	−805	−839	−873–(−**800**)	−927	−1044	−824
C	−288	−316	−313–(−306)	−345	−348	−343
D	31	3	6–13	*−26*	*−29*	**132**

which could explain their limited impact observed in the sensitivity analysis. For this reason, those parameters were included in the alternate scenarios. Table 7 summarizes the ranges of impact on BECCS cumulative capture potential over 50 years in t_{CO2} $year^{-1}$ for each alternative scenario, as compared to the base case.

Due to the uncertainty around biodiesel carbon footprint, and the proportion limit to 20% in volume for biodiesel/diesel blend in road transport, bio-diesel impact was limited and even positive in some cases. With bioethanol + CCS, in-field operations become carbon sinks rather than carbon sources, thus decreasing the overall CO_2 emissions of the value chain. The use of bioethanol + CCS in transport further decreases the overall carbon footprint of biomass, though carbon negative road transport could not be reached due to the limitation on bioethanol proportion in engines. Going towards low carbon transport or even carbon negative transport to improve BECCS sustainability will only be possible with dedicated bioethanol engines. However, increasing the use of organic fertilizers for farming and carbon neutral electricity for biomass processing could bring substantial sustainability improvements to the BECCS value chain. Similarly to biodiesel, drying with biomass was found to have both a positive and a negative impact. When land use changes are included in the case of willow, biomass carbon footprint is found to be higher than that of natural gas, hence the negative effect (decrease) on the capture potential, rather than a positive effect (increase). Most importantly, a carbon positive case study, such as willow on central grassland, could turn carbon negative by switching to carbon neutral electricity for biomass processing and carbon negative bioethanol for farming and transport. This demonstrates the importance of intelligent management – organic chemicals, carbon neutral electricity, low carbon or carbon negative fuels for transport and drying – to ensure bioenergy sustainability. This supports the assertion raised in Dale *et al.* that bioenergy can be sustainable when carefully managed.[142]

4.4 Implications for resource mobilisation

In a given case study, the outcomes of BECCS sustainability analysis were observed to be very variable. In practical terms, this means that resource mobilisation to meet a mitigation target could vary widely from project to project. In order to stay within the 2 °C scenarios, studies showed that the required level of deployment for BECCS was of the order of 3.3 Gt_C $year^{-1}$ by 2100.[42] We evaluated the biomass, land, water, energy and nutrient requirements of BECCS given this annual carbon removal target. Smith *et al.* carried out a similar meta analysis in order to compare switchgrass-based BECCS and afforestation, given a removal target of 1 Gt_C $year^{-1}$.[83] The difference from our analysis is that biomass supply chain results were obtained from various sources in the literature[136] and did not include direct and indirect land use changes. We performed the calculations on switchgrass and miscanthus from US and Brazil marginal lands (no direct and indirect land use changes), based on the same target and system boundaries in order to check the consistency of our results with the literature.[42,83] The study by Smith *et al.* was not location and biomass specific, but most of the results were obtained for miscanthus.[42] Results for switchgrass in Smith *et al.* were adapted to the 3.3 Gt_C $year^{-1}$ target.[83] BECCS scenarios resulting in very variable dynamic emission profiles translated into different resource requirements in terms of land, water and energy given a fixed mitigation target. As can be seen in Table 8, removing 3.3 Gt of carbon per year from the atmosphere using BECCS would require the annual mobilisation of 9 and 13 Gt_{DM} of processed switchgrass, 60 to 371 Mt of nutrients (N and P_2O_5), 1250 to 2490M ha of marginal land in the US, and 7800 to 15 700B m^3 of water. As a means of comparison, 17 Mt of N and P_2O_5 nutrients are used annually in the US, 721M ha of land are harvested for cereal production in the world[128] (2014), and 7980B m^3 of water is withdrawn – including green water – for the world agriculture.[143] This raises the question of water and land availability and whether marginal land will be sufficiently available and productive to enable biomass production at this scale, so as to avoid direct and indirect land use change effects. Using a higher yield crop such as miscanthus would lower the land and water requirements to 360–940M ha and 3600–9700B m^3, respectively.

Furthermore, BECCS would need to be deployed at the scale of 1.7 to 2.4 TW. For reference, at the time of writing, the total installed coal-fired thermal power capacity is 1.8 TW. Conversion of both coal and natural gas-fired power plants to dedicated biomass and biogas might well be necessary to meet these deployment targets. Furthermore, assuming a base load operation of the BECCS unit (85% load factor), this deployed capacity would represent an annual power generation of between 9700 and 14 600 TW h, or between 44% and 68% of the global power demand in 2012.[144] This result is highly dependent on the BECCS annual load factor, and while a BECCS unit should run at full capacity to remove a maximum amount of CO_2 from the atmosphere, this value could potentially be dictated by the system short run marginal cost relative to that of the other power sources within the electricity market. Policies rewarding CO_2 removal from the atmosphere will be crucial in increasing BECCS competitiveness relative to other technologies, and in turn will maximise the

Table 8 Comparison of the resource efficiency given a 3.3 Gt_C $year^{-1}$ target removal of a BECCS utility operating at 100% load factor with the literature, in two case studies: switchgrass from the US and miscanthus from Brazil. Biomass is grown on marginal lands (no direct and indirect land use changes). Achieving this target would require between 1.7 and 2.4 TW of BECCS installed capacity, 1250 and 2400M ha of marginal land, 7800 and 15700B m^3 $year^{-1}$, and 60 and 370 Gt of nutrients for a switchgrass-based system, which is in agreement with the literature. Such an installed capacity would result in a net energy output of 15 EJ $year^{-1}$ on average, but could also require 1 EJ $year^{-1}$ in the upper bound case. In the case of miscanthus, water requirement could be lowered to between 3600 and 9700, land requirement to 360 and 940M ha. However a miscanthus based system could lead to a net energy use of 37 EJ $year^{-1}$ in the upper bound scenario

Metrics	Switchgrass US	Smith *et al.* (2013)	Miscanthus Brazil	Smith *et al.* (2016)
Nb plants	3413–4852 (3887)		3323–5758 (4104)	
Biomass (Gt_{DM} $year^{-1}$)	9.2–13.1 (11.1)		9.0–15.5 (10.5)	
Water (Tm^3 $year^{-1}$)	7.8–15.7 (10.4)	5.3–24.4 (14.5)	3.6–9.7 (5.5)	**0.072**
Land (M ha)	1245–2392 (1630)	726–3270 (1910)	363–943 (538)	380–700
Energy (EJ $year^{-1}$)	−22.4 to 1.0 (−15.1)		−15.3 to 37.0 (−0.01)	**−170**
Nitrogen (Mt $year^{-1}$)	61–210 (112)		21–92 (42)	
Phosphate (Mt $year^{-1}$)	0–161 (55)		8–98 (34)	
Sources		83		42

BECCS load factor. However, the BECCS supply chain energy requirement must be subtracted from the annual power generation. Within the uncertainty range, BECCS net energy balance could be both positive and negative, which needs to be considered when talking about BECCS energy supply potential.

It can be observed from Table 8 that the model shows very good agreement with the literature for switchgrass.[83] However, though the model land requirement for miscanthus is in good agreement with the literature,[42] water requirement and energy supply are found to be very different. The difference in water requirement can be explained by the different model assumptions. In Smith *et al.*, the contribution of bioenergy production to the BECCS water footprint is evaluated at 80 m^3 t_C^{-1} $year^{-1}$, and the power plant + CCS contribution around 450 m^3 t_C^{-1} $year^{-1}$. This study assumes an evapotranspiration value for bioenergy between 1176 and 1822 m^3 t_C^{-1} $year^{-1}$.[42] For reference, this value compares well with our model for which miscanthus evapotranspiration is 1240 m^3 t_C^{-1} and the total water footprint (evapotranspiration + grey water) 1635 m^3 t_C^{-1}. The value of 80 m^3 t_C^{-1} is then obtained by subtracting the evapotranspiration of a reference grassland (the counterfactual) from bioenergy evapotranspiration.[42] However, if considered in the water balance, the counterfactual – leaving the land as is – would also need to be considered in the carbon balance, which would mean accounting for the CO_2 which would have been captured if the land had been left as is. As this was considered out of scope in this analysis, total evapotranspiration + grey water was selected as the biomass feedstock water footprint. Furthermore the model evaluates the power plant + CCS water contribution at 14 m^3 t_C^{-1}. It is assumed that the choice of a once-through cooling system – whose water consumption factor can be 30 times higher than that of a cooling tower system – as opposed to a recirculating cooling tower is the explanation behind this difference. For reference, the model would result in a power plant water requirement of 425 m^3 t_C^{-1} with a once-through system.

As for BECCS energy supply, BECCS was found to yield 170 EJ $year^{-1}$ at this deployment. However, this value does not include BECCS energy requirement which needs to be subtracted from BECCS energy supply.

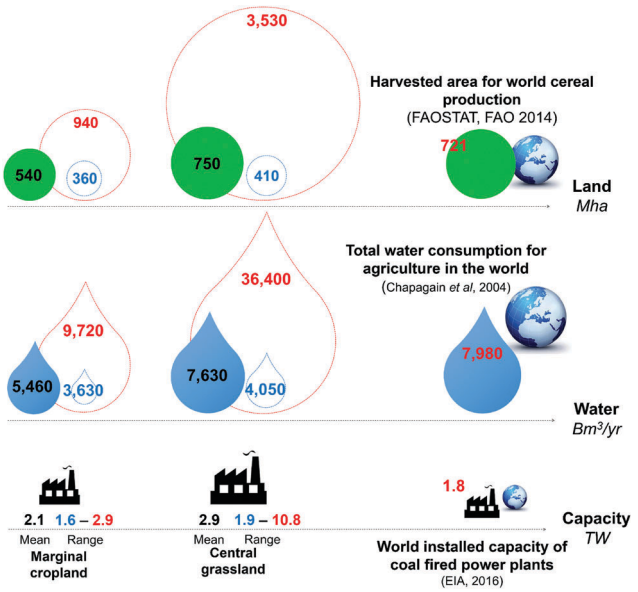

Fig. 20 Water, land and capacity annual requirements of miscanthus-based BECCS to remove 3.3 Gt_C $year^{-1}$. Land use changes (grassland as compared to marginal land) increase resource mobilisation by up to four times in the upper bound scenarios.

The same analysis was performed on grassland instead of marginal land, to account for land use changes. Fig. 20 shows the amount of land, water, and BECCS capacity in order to meet the 3.3 Gt_C annual removal target, with (central grassland) and without (marginal land) land use change. Upon including land use changes (*e.g.*, considering grassland instead of marginal land), resource mobilisation increases up to four times in the upper bound scenario.

4.5 Comparison with other negative emission technologies

The lower bound and upper bound results from the previous section were used to compare BECCS performance with other negative emission technologies, such as afforestation and

Table 9 Comparison of the performance of a BECCS facility operating at 100% load factor with afforestation and DACS given a 3.3 Gt_C $year^{-1}$ target removal. BECCS results were obtained from the lower and upper bounds of miscanthus (Brazil) and switchgrass (US) simulations. Water and land requirements for afforestation are similar to that of BECCS, though land requirement for afforestation corresponds more to the BECCS upper bound scenarios. DACS land requirement is negligible compared to that of BECCS, but naturally has a higher energy requirement. From these simulations, BECCS maximum energy use is in all cases lower than the 145 to 247 EJ $year^{-1}$ required to remove the same amount of carbon with DACS

Metrics	BECCS	Afforestation	DACS
Nb plants	3323–5758		3320
Water (Tm^3 $year^{-1}$)	3.6–15.7	5.3–11.6	
Land (M ha)	363–2392	1110–2480	0.04–3.3
Energy (EJ $year^{-1}$)	−22.4 to 37.0		81–274
Nitrogen (Mt $year^{-1}$)	21–210	0.3–2.4	
Phosphate (Mt $year^{-1}$)	0–161	0.7–2.5	
Sources		83	42 and 145–148

Direct Air Capture and Storage (DACS). For afforestation, data were directly used from Smith *et al.* (2013).[83] As land requirement was expressed in ha $year^{-1}$, the resulting afforested surface over 50 years was considered in order to compare with BECCS land requirement. Data from the literature for land and energy requirements[42,145–148] were adapted to this analysis. Table 9 summarizes these results.

Given a CO_2 annual removal target, afforestation resulted in an overall similar land and water use than that of BECCS, though its land requirement corresponded to the upper range of BECCS results. Within the uncertainty range, BECCS net energy balance could be both positive and negative, but even when positive its energy intensity was found to be lower than that of DACS. DACS land requirement was several orders of magnitude lower than that of BECCS. However, the carbon footprint of the electricity used in the process, which would have had an impact on DACS carbon efficiency, was not considered in the analysis. Using photovoltaic power could limit the carbon efficiency drop, but would on the other hand substantially increase DACS land requirement. These trade-offs will have to be considered in detail when comparing BECCS and DACS suitability for climate mitigation.

4.6 Implications for policy makers

The main conclusion of this analysis is the great variability in the possible outcomes of a BECCS project, both in terms of its cumulative net carbon removal over its lifetime, and also the time required for a given facility to start removing CO_2 from the atmosphere. Determining the sustainability or otherwise of a given BECCS project as a candidate for climate change mitigation is therefore only possible on a case-to-case basis. This has substantial implications for the regulation of those systems. The efficiency with which a BECCS project would remove CO_2 from the atmosphere is a first issue. Among carbon negative scenarios, it was observed that BECCS carbon intensity per hectare could vary greatly, which in turn means a great difference in the amount of resources (water, land, energy, power plants) used to remove a ton of CO_2 from the atmosphere. For BECCS to be a valuable asset to the system, a minimum CO_2 removal efficiency might have to be defined to differentiate inefficient from efficient systems, therefore excluding scenarios that are not worth pursuing.

In terms of time horizon, depending on the conditions and due to biomass initial carbon cost to the ecosystem, BECCS does not necessarily start being a net carbon sink from year 1. If we consider that BECCS provides a service to the market – removing CO_2 out of the atmosphere, therefore avoiding future costs associated with climate change adaptation, it is reasonable to suggest that this service could be remunerated. However, it is also reasonable to suggest that this remuneration does not start until the facility is actually removing CO_2 from the atmosphere. Given that this breakeven time could be several years, this could well serve to complicate the delivery of BECCS projects, as the incentive for investing in BECCS might be otherwise insufficient.

Finally, in the case of a global deployment of an unintegrated BECCS value chain, this carbon crediting scheme would also need to acknowledge the diversity of stakeholders – biomass production, power generation, CO_2 transport and storage, and possibly countries, involved in the BECCS value chain.

5 Conclusion

A modeling tool was developed in order to calculate the water footprint, embodied energy, and carbon footprint of a range of biomass fuels – miscanthus, switchgrass, willow, and wheat straw – grown on different land types and imported from different regions of the world. Among energy dedicated crops, herbaceous biomass (miscanthus and switchgrass) was found to be more sustainable with respect to the three metrics, mainly because of the lower yield and higher moisture content of woody biomass. Overall, the most important contributors to embodied energy were biomass transport for low moisture biomass, and transport, chemical input and processing for high moisture biomass. Drying and grinding energy costs are physically bound by biomass properties. Other biomass processing practices such as natural field drying or torrefaction for grinding will have to be investigated to reduce these inputs. As for carbon footprint, contributions were more balanced, with a significant contribution from fertilizers. The inclusion of direct and indirect land use changes however had a drastic impact, accounting for over 50% of biomass carbon footprint. It is important to note that in this analysis, representative yield values were taken from the literature. In practice yield is a complex function of various parameters including climate, soil type, nutrients and water availability and management practices. The interdependence of parameters would have to be included for more accurate results.

Supply chain results were implemented in the context of a 500 MW BECCS facility to evaluate the impact of the biomass supply chain on the overall plant carbon intensity,

water intensity and energy efficiency. The results showed a substantial impact on water and carbon intensities at high co-firing proportions, and to a smaller extent on efficiency. Including direct and indirect land use changes had a great impact on the power plant carbon intensity, narrowing the range of operability for the power plant to be carbon negative.

A dynamic carbon balance was carried out over a 50 year period to evaluate a BECCS power plant carbon negative potential over its lifetime in different biomass–region–land type scenarios. Depending on the conditions of the simulation, carbon breakeven time could vary from 1 (marginal cropland) to 35 years (central grassland) for miscanthus from Brazil, and from 6 to over 50 years for willow from Europe. Within the uncertainty bounds considered for the input data, the key factors impacting the results were identified to be the land conversion factors, electricity carbon footprint, biomass yield and moisture content. The investigation of alternative scenarios such as using carbon neutral electricity, organic chemicals and bioethanol + CCS gave indications as to BECCS potential margin of improvements. However, BECCS overall results were driven by land use conversion factors, which indicate the need for thorough evaluations of these effects. Bypassing this issue with biomass growth on marginal land could be a potential solution. Yet, marginal land availability and uncertain biomass productivity response might not make them long term candidates for BECCS large-scale deployment.

Given the variable outcomes of BECCS sustainability analysis, BECCS large scale deployment was found to have very different implications in terms of resource mobilisation. Based on the analysis on switchgrass and miscanthus, within a scenario excluding direct and indirect land use changes, removing 3.3 Gt_C $year^{-1}$ with BECCS could annually require between 360 and 2400M ha of marginal lands, 3600 and 15 700B m^3 of water, 30 to 360 Gt of nutrients, and 1.7 to 2.9 TW of installed BECCS capacity. As a means of comparison, the upper bounds of these values correspond respectively to over three times the world total harvested land for cereal production, twice the world annual water use for agriculture (including evapotranspiration), 20 times the US annual nutrient use, and 1.6 times the world total coal-fired power plant capacity. This underlines the challenges associated with the large scale deployment of BECCS, especially concerning water and nutrient consumption.

Overall it was shown that over a plant lifetime and upon choosing the right conditions, BECCS can be a reliable option for the sustainable and permanent removal of CO_2 from the atmosphere, even when including supply chain, direct and indirect land use change effects. The high variability in BECCS CO_2 removal time and space efficiencies in the model outcomes underpinned the need for case-to-case analysis when it comes to BECCS sustainability assessment, especially for the determination of land use change factors. Policy implications of this conclusion are that regulating and attributing value to these systems will have to integrate this regional specificity.

We have identified five key principles which could improve the sustainability of BECCS. The combination of a sensitivity analysis on the model combined with the investigation of alternate supply chain scenarios elucidated the following five key levers: (1) measuring and limiting the impacts of direct and indirect land use changes, (2) using carbon neutral power and organic fertilizers, (3) prioritizing sea and rail over road transport, (4) increasing the use of carbon negative fuels, and (5) exploiting alternative biomass processing options, *e.g.*, natural drying or torrefaction. This indicates that regardless of the biomass and region studied, BECCS sustainability heavily relies on intelligent management.

Appendices

A Supply chain model details

A.1 Biomass yield at power plant. Knowing the crop lifetime in terms of dry biomass $Y_{N,dry}$, moisture content at harvest MC, and each supply chain stage solid recovery SR_i in % (or dry mass loss), and moisture content loss ML_i (%), the final amount delivered $y_{N,dry}$ and moisture content mc at the power plant is calculated with the following equations:

$$y_{N,dry} = Y_{N,dry} \times \sum_i SR_i \quad (13)$$

$$mc = MC - \sum_i ML_i \quad (14)$$

$$y_{N,wet} = \frac{Y_{N,dry}}{1 - mc} \quad (15)$$

Similarly, biomass inlet and outlet of each processing unit can be calculated.

A.2 Farming input indirect energy use. Different inputs were considered in the analysis. Nitrogen based fertilizers, potassium based fertilizers, phosphate-based fertilizers, lime, herbicides, pesticides, seeds or rhizomes are used for the crop establishment and maintenance. For every crop, each product k application rate R_k is known on a kg ha^{-1} $year^{-1}$ basis. With each product is associated an embodied energy EE_k, *i.e.* the energy required for the chemical production. The embodied energy associated with those products is thus calculated:

$$\frac{\sum_k EE_k \times R_k \times N}{y_{N,dry}} \quad (16)$$

where N is the crop overall lifetime in years and $y_{N,dry}$ is the aforementioned biomass dry yield over the crop lifetime in dry biomass t_{DM} ha^{-1}.

A.3 Farming fuel use. In-field operations, such as harrowing, ploughing, seeding, packing, fertilizing, *etc.* during site preparation, or mowing, harvesting, baling, *etc.* during harvest, require fuel in the form of diesel. Knowing the fuel efficiency of each site preparation operation (SP_k) and harvest operation (H_k) in L ha^{-1}, and diesel embodied energy EE_D and energy density LHV_D, biomass embodied energy associated with farming diesel use can be calculated:

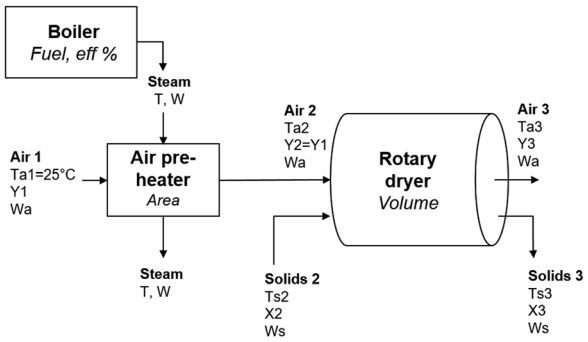

Fig. 21 Drying model.

$$\frac{\left(\sum_k \mathrm{SP}_k + \mathrm{H}_k \times n\right)(\mathrm{LHV_D} + \mathrm{EE_D})}{y_{\mathrm{N,dry}}} \quad (17)$$

where n is the number of harvests over the crop lifetime. Irrigation is also accounted for in this section, with both power and fuel requirements.

A.4 Fuel and power use in a pelleting plant. Delivering biomass in the form of pellets was the scenario investigated in this analysis. Information on the pelleting process was mainly taken from the Pellet Handbook by Obernberger and Theck.[149] In order to be condensed as a proper fuel, harvested biomass needs to have its size reduced (chopping, chipping), dried to a maximum moisture content of 15%, further milled (grinding) and go through the pelleting process (die extruder).

Processing operations require energy both in the form of fuel (drying) and electrical power (size reduction, drying, grinding, pelleting). Knowing each operation energy requirement EE_i in MJ $\mathrm{t_{MW}}^{-1}$ and biomass input $Y_{i,\mathrm{wet}}$, each processing contribution to biomass embodied energy is calculated with the following formula:

$$\frac{\mathrm{EE}_i \times Y_{i,\mathrm{wet}}}{y_{\mathrm{N,dry}}} \quad (18)$$

The energy requirement in MJ t^{-1} for biomass processing is taken from the literature (experimental and industrial data) for size reduction, grinding and pelleting.

For drying, a model was designed based on Gebreegziabher *et al.*[112] and Li *et al.*[150] Biomass drying has been covered by many studies,[113,151–153] but a precise thermodynamic and kinetic model is hard to obtain due to the lack of data on biomass properties, such as specific heat capacity, diffusivity, equilibrium moisture content, *etc.* This model uses a thermodynamic approach based on the industrial data provided by Gebreegziabher *et al.* and Li *et al.* on wood drying (Fig. 21).

Chopped or chipped biomass is dried in a rotary dryer in contact with hot air. Air is heated through a heat exchanger from room temperature to about 60 °C. Air inlet and outlet relative humidity RH_1 and RH_3 are known. Air moisture content Y_i at any stage of the process is linked with air relative humidity through psychrometric relations, involving the saturated vapor pressure P_{wsi} and vapor pressure P_{wi}:

$$P_{\mathrm{ws}_i} = \frac{\exp\left(77.345 + 0.0057(T_{\mathrm{a}_i} + 273.15) - \frac{7235}{T_{\mathrm{a}_i} + 273.15}\right)}{(T_{\mathrm{a}_i} + 273.15)^{8.2}} \quad (19)$$

$$P_{\mathrm{w}_i} = \mathrm{RH}_i \times P_{\mathrm{ws}_i} \quad (20)$$

$$Y_i = 0.62198\frac{\mathrm{Pa}}{\mathrm{Pa} - P_{\mathrm{w}_i}}, \quad i = 1,\ 3 \quad (21)$$

where Pa is air pressure, assumed constant throughout the process.

Considering a water mass balance on the pre-heater, air inlet moisture content is equal to air outlet moisture content:

$$Y_2 = Y_1 \quad (22)$$

Knowing biomass inlet MC_2 and outlet (target) MC_3 moisture content, these values can be converted into a dry basis moisture content:

$$X_i = \frac{\mathrm{MC}_i}{1 - \mathrm{MC}_i}, \quad i = 2,\ 3 \quad (23)$$

Because biomass quantity to dry W_{s} (dry basis) is also known, a water mass balance on the dryer gives the required air quantity W_{a} (dry basis):

$$W_{\mathrm{a}}(Y_3 - Y_2) = W_{\mathrm{s}}(X_2 - X_3) \quad (24)$$

Finally the pre-heater heat rate Q_{h} can be determined with an energy balance on the heat exchanger:

$$Q_{\mathrm{h}} = W_{\mathrm{a}}(H_{\mathrm{a}_2} - H_{\mathrm{a}_1}) \quad (25)$$

H_{a_i} is the enthalpy of dry air;

$$H_{\mathrm{a}_i} = C_{\mathrm{p_{da}}} \times (T_{\mathrm{a}_i} - T_{\mathrm{ref}}) + Y_i\left(C_{\mathrm{p}_{\mathrm{v}_i}} \times (T_{\mathrm{a}_i} - T_{\mathrm{ref}}) + \mathrm{LH_w}\right) \quad (26)$$

with $C_{\mathrm{p_{da}}}$, $C_{\mathrm{p}_{\mathrm{v}_i}}$ the dry air and vapor specific heat capacities, respectively, and $\mathrm{LH_w}$ the water heat of vaporization, assumed constant in this range of temperature.

Assuming the heat exchanger uses steam generated by a boiler operating with an efficiency $\mathrm{EFF_B}$, the specific boiler heat requirement is calculated:

$$q_{\mathrm{f}} = \frac{Q_{\mathrm{h}}}{\mathrm{EFF_B} \times W_{\mathrm{s}}} \quad (27)$$

This value is implemented in the embodied energy model as drying heat requirement in MJ $\mathrm{t_{DM}}^{-1}$. In this analysis, we assumed that the boiler operated with natural gas at a boiler efficiency of 90%, but other fuel/efficiency scenarios could also be investigated.

A.5 Biomass transportation. Fuel consumption for biomass transport is based on transportation mean and size. Two different transport fuel efficiencies in L (km t)$^{-1}$ are used in the analysis:

• Short and long distance diesel fueled truck for farm – pellet plant and pellet plant – power plant road transport ($\mathrm{Eff_D}$),

• Long distance heavy fuel oil (HFO) fueled bulk carriers for pellet plant – power plant sea transport (Eff_{HFO})

The transport stage contribution to biomass embodied energy is thus calculated by the following expression:

$$\frac{D_{road} \times Eff_D \times y_{N,wet} + D_{sea} \times Eff_{HFO} \times y_{N,wet}}{y_{N,dry}} \quad (28)$$

where D_{road} and D_{sea} are the road and sea travelling distances, respectively.

A.6 NO_2 emission evaluation. Nitrogen fertilizer application (in kg (ha year)$^{-1}$) is considered to cause N_2O–N direct formation, N_2O–N formation from NH_3–N and NO_x–N volatization, and N_2O–N formation from N leaching or runoff. The following expression evaluates nitrogen-based fertilizer application contribution to the biomass carbon footprint:

$$EF_{N_2O} = EF_N + EF_{NH_3\text{–}N\text{–}NO_x\text{–}N} \times EF_{N,volatalized} + EF_{N,leaching} \times LP \quad (29)$$

$$\frac{GWP_{N_2O} \times N \times R_N \times C_{N_2O\text{–}N} \times EF_{N_2O}}{y_{N,dry}} \quad (30)$$

where N is the crop lifetime in years, R_N is the nitrogen application rate in kg (ha year)$^{-1}$, $C_{N_2O\text{–}N}$ is the molecular conversion factor, EF_N is the emission factor in $kg_{N_2O\text{–}N}$ kg_N^{-1} applied, $EF_{NH_3\text{–}N\text{–}NO_x\text{–}N}$ is the emission factor in $kg_{NH_3\text{–}N\text{–}NO_x\text{–}N}$ kg_N^{-1} applied, $EF_{N,volatalized}$ is the volatization factor in $kg_{N_2O\text{–}N}$ $kg_{NH_3\text{–}N\text{–}NO_x\text{–}N}^{-1}$, $EF_{N,leaching}$ is the leaching factor in $kg_{N_2O\text{–}N}$ kg_N^{-1} leaching, and LP leaching proportion in kg_N leaching per kg_N applied.

B Overview of the water footprint and embodied energy models

Fig. 22 and 23.

C Model input data

C.1 Climate data. Tables 10–14.
C.2 Energy and GHG data. Tables 15–17.
C.3 Biomass data. Tables 18–21.

D Sensitivity analysis on willow-based BECCS dynamic GHG balance

Fig. 24.

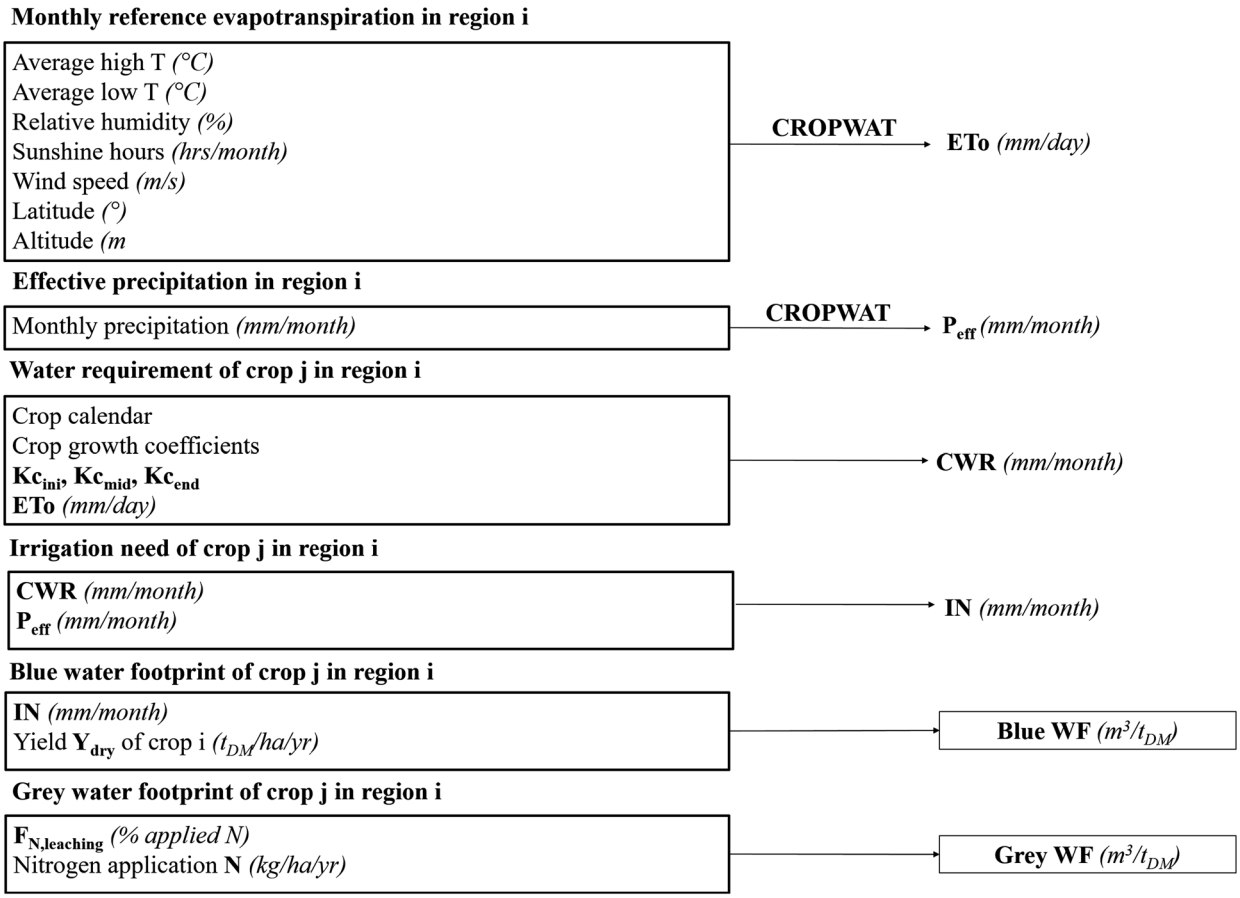

Fig. 22 Water footprint model overview. The water footprint calculation requires the calculation of four crop and region specific elements: evapotranspiration in a given climate, effective precipitation in a given climate, water requirement of a crop in a given climate, and irrigation need of a crop in a given climate. The grey water model assumed that the only source of pollution was nitrogen-based fertilizer application.

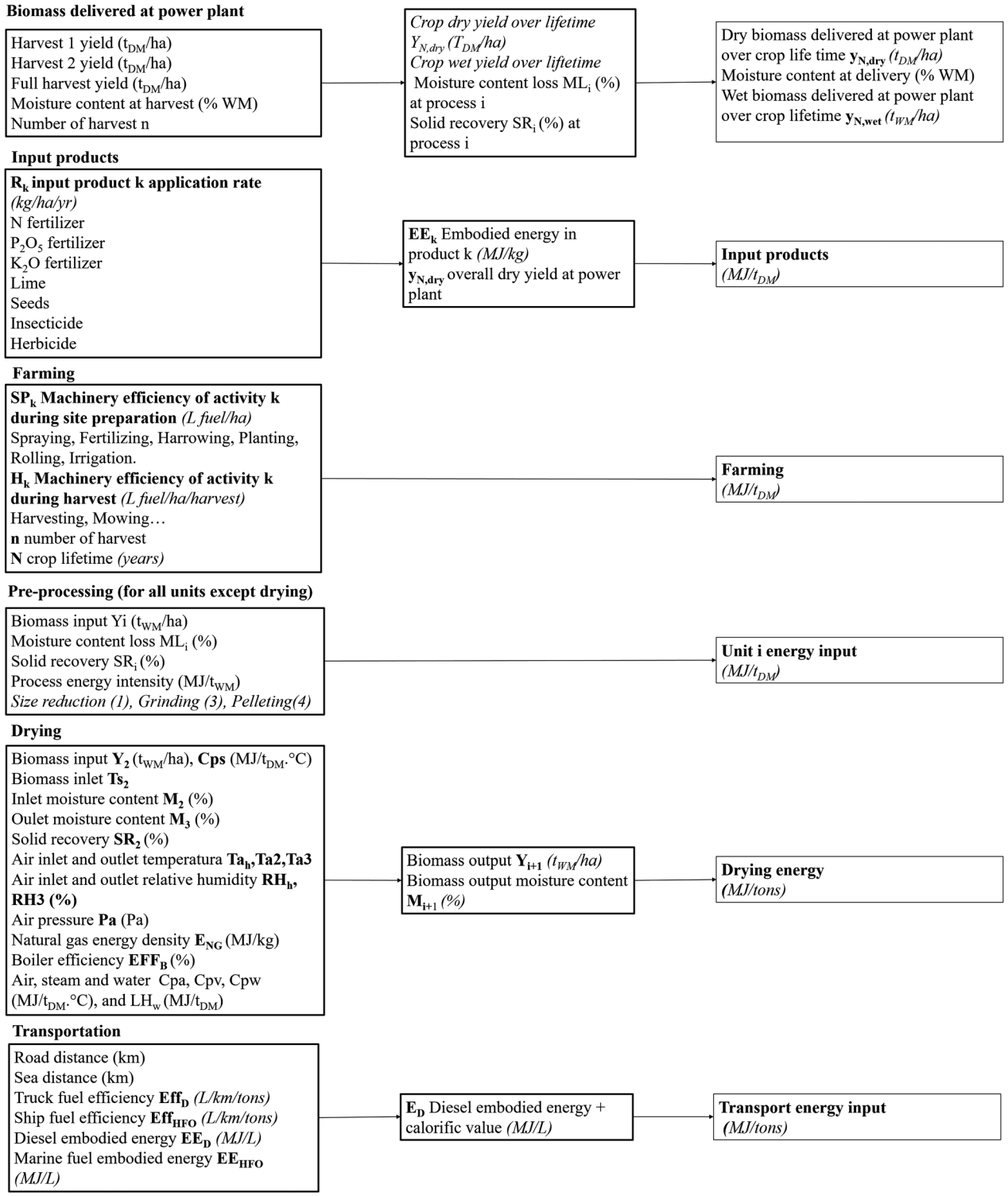

Fig. 23 Overview of the embodied energy model. Biomass embodied energy was calculated by summing the different energy contributions along the value chain following a life cycle assessment approach.

Table 10 Brazil – Sao Paulo (altitude 760 m, latitude 23°38′, 550 km road distance, 10 200 km sea distance)

Month	Average low T	Average high T	Relative humidity	Wind speed at 2 m	Sunshine hours	Average precipitation
Units	°C	°C	%	m s^{-1}	Hours	mm
January	19.4	27.5	84.0	3.0	5.0	224.7
February	19.5	28.4	84.0	3.0	4.6	149.7
March	19.7	28.4	83.0	2.9	4.9	129.3
April	18.0	26.3	83.0	2.9	5.8	44.0
May	15.0	23.3	83.0	2.7	5.5	38.5
June	14.4	23.7	82.0	2.4	5.8	24.7
July	13.4	23.3	81.0	2.4	6.0	47.9
August	14.7	25.4	79.0	2.5	6.4	25.5
September	14.9	25.0	80.0	3.5	4.5	48.9
October	16.8	26.7	82.0	3.0	3.9	110.8
November	17.2	25.9	82.0	3.5	4.7	112.1
December	18.5	27.4	83.0	3.3	5.7	164.2
Sources	123					

Table 11 China – Zhengzhou (altitude 111 m, latitude 34°46′, 780 km road distance, 20 044 km sea distance)

Month	Average low T	Average high T	Relative humidity	Wind speed at 2 m	Sunshine hours	Average precipitation
Units	°C	°C	%	m s^{-1}	Hours	mm
January	−4.5	5.3	75.1	4.8	2.6	15.6
February	−1.0	8.8	79.1	3.5	2.7	15.3
March	3.6	15.6	80.9	3.5	3.1	22.2
April	9.5	23.0	81.6	3.8	2.8	32.5
May	12.3	27.9	83.3	4.5	2.9	59.0
June	18.6	32.0	84.3	5.5	2.5	100.4
July	21.6	30.6	79.9	8.0	2.2	197.3
August	20.8	30.4	79.8	7.4	2.2	173.4
September	14.8	26.6	77.5	6.7	2.0	86.0
October	8.4	22.3	73.0	6.8	2.3	43.9
November	1.4	16.2	72.9	6.0	2.5	24.6
December	−2.0	8.5	73.1	5.7	2.8	13.7
Sources	123					

Table 12 The Netherlands (Europe) – Eindhoven (altitude 21 m, latitude 51°26′, 160 km road distance, 390 km sea distance)

Month	Average low T	Average high T	Relative humidity	Wind speed at 2 m	Sunshine hours	Average precipitation
Units	°C	°C	%	m s^{-1}	Hours	mm
January	0.5	6.6	89.0	4.8	1.8	65.1
February	0.6	7.0	88.0	3.9	2.7	69.0
March	1.8	10.1	81.0	4.4	3.6	58.9
April	5.0	16.3	75.0	3.4	5.2	45.4
May	8.8	19.7	73.0	3.9	6.6	60.2
June	11.4	22.6	74.0	3.3	5.8	45.2
July	13.8	24.3	76.0	3.5	6.3	98.8
August	12.0	21.8	78.0	3.4	6.2	63.3
September	9.3	19.7	80.0	3.3	4.4	56.1
October	7.6	16.4	85.0	3.4	3.6	57.6
November	3.8	10.4	88.0	4.0	2.2	64.8
December	1.4	6.6	90.0	4.4	1.4	69.2
Sources	123					

Table 13 India – Amritsar (altitude 232 m, latitude 31°38′, 1420 km road distance, 11 670 km sea distance)

Month	Average low T	Average high T	Relative humidity	Wind speed at 2 m	Sunshine hours	Average precipitation
Units	°C	°C	%	m s^{-1}	Hours	mm
January	2.5	18.9	74.0	1.1	9.0	35.7
February	6.6	22.2	70.0	1.4	9.0	38.0
March	10.8	27.4	64.0	1.6	11.0	19.2
April	16.2	35.9	47.0	2.0	12.0	13.7
May	21.1	40.2	38.0	1.9	13.0	24.4
June	23.7	39.6	48.0	1.8	13.0	110.1
July	24.9	35.5	72.0	1.2	11.0	135.5
August	24.6	34.8	77.0	0.9	10.0	119.0
September	22.0	34.1	70.0	1.0	11.0	54.6
October	16.6	32.7	67.0	0.8	11.0	10.9
November	10.1	27.8	73.0	0.7	10.0	5.4
December	4.4	21.1	76.0	0.9	9.0	9.4
Sources	123					

Table 14 USA – Orlando, Florida (altitude 34 m, latitude 28°32′, 300 km road distance, 7550 km sea distance)

Month	Average low T	Average high T	Relative humidity	Wind speed at 2 m	Sunshine hours	Average precipitation
Units	°C	°C	%	m s^{-1}	Hours	mm
January	10.0	24.1	71.2	3.6	7	53.8
February	9.7	24.2	69.7	3.7	7	49.6
March	12.1	26.6	67.8	3.9	8	68.6
April	14.6	29.0	66.8	4.0	10	54.3
May	18.3	31.6	66.8	3.7	10	109.0
June	21.7	32.6	75.4	3.0	11	234.0
July	23.1	33.3	76.3	2.5	10	211.3
August	23.4	34.0	77.8	2.8	9	244.4
September	22.8	32.5	78.5	3.3	9	152.3
October	19.2	29.8	75.6	3.6	8	101.4
November	12.4	25.5	73.8	3.5	8	55.7
December	13.6	25.9	73.9	3.3	7	74.3
Sources	123					

Table 15 Mean values and ranges of uncertainty of energy data implemented in the model

Parameter	Unit	Mean	Range	Sources
Nitrogen fertilizer EE	MJ kg^{-1}	55.4	49.1–61.7	67, 76, 81 and 154–162
Phosphate fertilizer EE	MJ kg^{-1}	10.5	6.9–14.1	67, 76, 81 and 154–162
Potash fertilizer EE	MJ kg^{-1}	7.3	4.6–13.6	67, 76, 81 and 154–162
Lime EE	MJ kg^{-1}	1.0	0.12–1.71	67, 81, 160 and 161
Herbicide EE	MJ kg^{-1}	292.9	243.8–342.0	67, 81, 154, 160, 161 and 163
Miscanthus rhizome EE	MJ kg^{-1}	6	4–8	76 and 97
Switchgrass seed EE	MJ kg^{-1}	14.7	6–26.1	67, 71, 81 and 164
Willow planting EE	MJ per cutting	0.101		97
Diesel EE	MJ L^{-1}	4.7	3.7–6.2	67, 96, 97 and 165
Biodiesel EE	MJ L^{-1}	14.3		97
Natural gas EE	MJ kg^{-1}	4.7		97
Diesel LHV	MJ L^{-1}	37.4	35.9–39.1	76, 97, 116, 144 and 166
Biodiesel LHV	MJ L^{-1}	34.8	33.7–37.3	97 and 167
Bioethanol LHV	MJ L^{-1}	21.2		168
Natural gas LHV	MJ kg^{-1}	47.0	46.9–47.1	169 and 170
Transport of supplies (diesel)	MJ kg^{-1}	0.52	0.44–0.64	69 and 158
Road transport diesel efficiency	L (km t_{MW})$^{-1}$	0.044	0.028–0.06	65, 92, 97, 116, 170 and 171
Road transport bioethanol E25 efficiency	L ethanol per L diesel	1.12		Own calculations
Sea transport HFO efficiency	MJ (km t_{MW})$^{-1}$	0.049	0.0302–0.0882	Adapted from ref. 97 and 172
Irrigation	MJ mm^{-1}	15.8	1.1–26.4	Adapted from ref. 76, 114 and 139

Table 16 Mean values and ranges of uncertainty of GHG data implemented in the model

Parameter	Unit	Mean	Range	Sources
Nitrogen fertilizer CF	$kg_{CO_2\text{-eq}}\ kg^{-1}$	3.6	2.9–4.4	67, 76, 88, 158, 161, 173 and 174
Phosphate fertilizer CF	$kg_{CO_2\text{-eq}}\ kg^{-1}$	1.1	0.6–1.6	67, 76, 158, 161 and 174
Potash fertilizer CF	$kg_{CO_2\text{-eq}}\ kg^{-1}$	0.64	0.44–0.86	67, 76, 158, 161 and 174
Lime CF	$kg_{CO_2\text{-eq}}\ kg^{-1}$	1.1	0.6–1.6	67, 158, 159, 161 and 174
Herbicide CF	$kg_{CO_2\text{-eq}}\ kg^{-1}$	20.3	17.2–25	67, 158, 161 and 174
Miscanthus rhizome CF	$kg_{CO_2\text{-eq}}\ kg^{-1}$	0.01		67 and 76
Switchgrass seed CF	$kg_{CO_2\text{-eq}}\ kg^{-1}$	14.7	6–26.1	67 and 71
Willow planting CF	$kg_{CO_2\text{-eq}}\ kg^{-1}$	0.01		97
Electricity CF	$kg_{CO_2\text{-eq}}\ MJ^{-1}$	4.7	3.7–6.2	67, 76, 137, 138, 158, 161, 162 and 175
Diesel EF	$kg_{CO_2\text{-eq}}\ L^{-1}$	3.4	3.2–3.5	67, 76, 89, 97, 109, 111, 158, 161, 174 and 176
Biodiesel EF	$kg_{CO_2\text{-eq}}\ L^{-1}$	3.4	3.2–3.5	89, 97 and 106
Bioethanol + CCS EF	$kg_{CO_2\text{-eq}}\ L^{-1}$	−2.12		Adapted from ref. 111
Natural gas EF	$kg_{CO_2\text{-eq}}\ L^{-1}$	3.4	3.2–3.5	97
Transport of supplies (diesel) EF	$kg_{CO_2\text{-eq}}\ (km\ t_{MW})^{-1}$	0.05		67 and 158
Road transport diesel EF	$kg_{CO_2\text{-eq}}\ (km\ t_{MW})^{-1}$	0.077	0.073–0.08	97 and 177
Road transport biodiesel 20% (B20) EF	$kg_{CO_2\text{-eq}}\ (km\ t_{MW})^{-1}$	0.065	0.062–0.068	169
Road transport bioethanol 25% (E25) EF	$kg_{CO_2\text{-eq}}\ (km\ t_{MW})^{-1}$	0.034	0.028–0.040	Own calculations
Sea transport HFO efficiency	$kg_{CO_2\text{-eq}}\ (km\ t_{MW})^{-1}$	0.004	0.00247–0.00722	172
ILUC	$kg_{CO_2\text{-eq}}\ ha^{-1}$	183 025	95 700–270 350	Adapted from ref. 103, 107, 108 and 140
LUC grassland	$kg_{CO_2\text{-eq}}\ ha^{-1}$	136 300	75 000–200 000	102 and 103
LUC cropland	$kg_{CO_2\text{-eq}}\ ha^{-1}$	37 500		102
LUC marginal land	$kg_{CO_2\text{-eq}}\ ha^{-1}$	25	0–69	102
LUC forest	$kg_{CO_2\text{-eq}}\ ha^{-1}$	573 200	350 000–719 500	102 and 103
LUC wetland	$kg_{CO_2\text{-eq}}\ ha^{-1}$	2 186 500	1 000 000–3 452 000	102 and 103
EF for N addition	$kg_{N_2O\text{–}N}\ kg_N^{-1}$	0.01		67 and 178
EF for N volatization	$kg_{N_2O\text{–}N}\ kg_{NH_3\text{–}N+NO_x\text{–}N^{-1}}$	0.01		67 and 178
EF for $NH_3 - N + NO_x - N$	$kg_{NH_3\text{–}N+NO_x\text{–}N}\ kg_N^{-1}$	0.1		67 and 178
EF for N leaching	$kg_{N_2O\text{–}N}\ kg_N^{-1}$	0.04	0.0075–0.075	65, 67 and 178

Table 17 Mean values and ranges of uncertainty of supplementary data implemented in the model

Parameter	Unit	Mean	Range	Sources
N_2O–N to N_2O conversion		1.57		67 and 178
P to P_2O_5 conversion		2.18		56
K to K_2O conversion		1.21		56
C to CO_2 conversion		3.67		166
CCS plant area	ha	15		
DAC plant area for 10 000 $t_{CO_2}\ day^{-1}$	ha	13		
DAC energy requirement	$MW\ h\ t_{CO2}^{-1}$	4.64	3.33–6.3	Adapted from ref. 146 and 147
Chopping solid recovery	$\%_{DM}$	98		
Drying solid recovery	$\%_{DM}$	98		
Drying target moisture	$\%_{DM}$	15		
Drying energy requirement	$MJ\ t_{H_2O\ evaporated}^{-1}$	3734		Own calculations
Boiler efficiency with natural gas for drying	%	90		
Boiler efficiency with biomass for drying	%	75		
Grinding solid recovery	$\%_{DM}$	98		
Grinding moisture loss	%	5		
Pelleting solid recovery	$\%_{DM}$	98		
Pelleting moisture loss	%	5		
Road transport solid recovery	$\%_{DM}$	95		
Sea transport solid recovery	$\%_{DM}$	95		

Table 18 Mean values and ranges of uncertainty of wheat straw data implemented in the model

Parameter	Unit	Mean	Range	Sources
HHV	MJ kg_{DM}^{-1}	19.2	17.3–21.2	28 and 31
Cp	MJ $(kg_{DM}\ K)^{-1}$	1.3		179
C%	$\%_{DM}$	48.4	44.4–52.3	28, 31, 33 and 56
H%	$\%_{DM}$	5.5	5.0–6.1	28, 31, 33 and 56
O%	$\%_{DM}$	39.1	34.0–43.3	28, 31, 33 and 56
N%	$\%_{DM}$	0.61	0.45–0.78	28, 31, 33 and 56
P%	$\%_{DM}$	0.09		56
K%	$\%_{DM}$	1.5		56
S%	$\%_{DM}$	0.10	0.02–0.31	28, 31, 33 and 56
Cl%	$\%_{DM}$	0.32	0.01–0.73	28, 31, 33 and 56
Ash%	$\%_{DM}$	4.5	1.6–7.3	28, 31 and 33
Moisture content at harvest%	$\%_{WM}$	10.9	5.2–16.0	31, 33, 56, 180 and 181
Straw/grain ratio	$\%_{DM}$	1.3	0.64–2.03	180
Brazil harvest grain yield	$t_{DM}\ ha^{-1}\ year^{-1}$	2.49	2.08–2.83	2009–2013[128]
China harvest grain yield	$t_{DM}\ ha^{-1}\ year^{-1}$	4.87	4.74–5.05	2009–2013[128]
Europe harvest grain yield	$t_{DM}\ ha^{-1}\ year^{-1}$	8.66	7.78–9.29	2009–2013[128]
India harvest grain yield	$t_{DM}\ ha^{-1}\ year^{-1}$	3.13	2.84–4.02	2009–2013[128]
US harvest grain yield	$t_{DM}\ ha^{-1}\ year^{-1}$	3.07	2.94–3.17	2009–2013[128]
Lifetime	Years	1		
Rotation of harvests	Years	1		
Growing cycle length	Days	180 (Brazil, China, India); 335 (Europe); 120 (US)		143
Growing cycle starting month		11 (Brazil); 12 (China); 10 (Europe, India); 5 (US)		143
Growing cycle starting day		15 (Brazil, Europe, India, US); 1 (China)		143
Initial stage t_1		20 (Brazil, China, India); 160 (Europe); 15 (US)		143
Development stage t_2		80 (Brazil, China, India); 235 (Europe); 40 (US)		143
Mid-season stage t_3		150 (Brazil, China, India); 310 (Europe); 90 (US)		143
$K_{c,ini}$		0.7		143
$K_{c,mid}$		1.15		143
$K_{c,end}$		0.3		143
Nitrogen rate	kg $ha^{-1}\ year^{-1}$	52.3 (Brazil); 185.5 (China); 53.6 (Europe); 139.6 (India); 80.4 (US)		2010[127,128]
% N available in straw	$\%_N$	30		56
% P available in straw	$\%_P$	100		56
% K available in straw	$\%_N$	100		56
Collection (bales)	L per ha per harvest	4.4		56
Chopping (diesel)	MJ t_{MW}^{-1}	7.4		56
Grinding (power)	MJ t_{MW}^{-1}	100–323		57, 182 and 183
Pelleting (power)	MJ t_{MW}^{-1}	300–409		57 and 183
Pellet grinding (power)	MJ t_{MW}^{-1}	345		34

Table 19 Mean values and ranges of uncertainty of miscanthus data implemented in the model

Parameter	Unit	Mean	Range	Sources
HHV	MJ kg_{DM}^{-1}	18.4	17.7–19.1	28, 31, 32, 76 and 184
Cp	MJ $(kg_{DM}\ K)^{-1}$	1.4		179
C%	$\%_{DM}$	47.8	45.1–50.4	28 and 31–33
H%	$\%_{DM}$	5.5	4.9–6.1	28 and 31–33
O%	$\%_{DM}$	42.3	40.2–44.3	28 and 31–33
N%	$\%_{DM}$	0.56	0.21–0.92	28 and 31–33
S%	$\%_{DM}$	0.22	0.04–0.37	28 and 31–33
Cl%	$\%_{DM}$	0.26	0.10–0.42	28 and 31–33
Ash%	$\%_{DM}$	3.9	2.5–5.4	28 and 31–33
Moisture content at harvest%	$\%_{WM}$	23	15–31	31–33, 69, 76 and 185
1st harvest yield proportion	%	21		69
2nd harvest yield proportion	%	64		69
Brazil full harvest yield	$t_{DM}\ ha^{-1}\ year^{-1}$	28.9	23.2–34.7	61, 70 and 73
China full harvest yield	$t_{DM}\ ha^{-1}\ year^{-1}$	24.3	23.1–25.4	73
Europe full harvest yield	$t_{DM}\ ha^{-1}\ year^{-1}$	18.8	15.6–22.1	64, 70, 75–78, 97 and 184–188
India full harvest yield	$t_{DM}\ ha^{-1}\ year^{-1}$	15.0	12.8–17.3	73
US full harvest yield	$t_{DM}\ ha^{-1}\ year^{-1}$	28.0	21.2–34.4	61, 70 and 90
Lifetime	Years	18	16–21	65, 69 and 97
Rotation of harvests	Years	1		69
Growing cycle length	Days	209	203–215	62
Growing cycle starting month		7 (N); 9 (S)	4–9 (N)	62

Table 19 (*continued*)

Parameter	Unit	Mean	Range	Sources
Growing cycle starting day		1		62
Initial stage t_1		45	42–48	62
Development stage t_2		67	64–70	62
Mid-season stage t_3		163	152–174	62
$K_{c,ini}$		0.4		143
$K_{c,mid}$		0.95		143
$K_{c,end}$		0.4		143
Nitrogen rate	kg ha^{-1} $year^{-1}$	78	50–100	63, 67, 71, 76 and 185
Phosphate rate	kg ha^{-1} $year^{-1}$	63	50–100	63, 67, 71, 76 and 186
Potash rate	kg ha^{-1} $year^{-1}$	124	60–200	63, 67, 71, 76 and 186
Lime rate	kg ha^{-1} $year^{-1}$	643		67 and 189
Rhizome rate	kg ha^{-1} $year^{-1}$	52.6		97
Herbicide rate	kg ha^{-1} $year^{-1}$	0.88	0.105–2.81	65, 67 and 71
Land preparation (diesel)	L ha^{-1}	75.1		69
Maintenance – harvest (bales)	L per ha per harvest	51.6		69
Chopping (diesel)	MJ t_{MW}^{-1}	108		76
Grinding (power)	MJ t_{MW}^{-1}	124	68–182	76
Pelleting (power)	MJ t_{MW}^{-1}	579	232–925	76
Pellet grinding (power)	MJ t_{MW}^{-1}	345		34

Table 20 Mean values and ranges of uncertainty of switchgrass data implemented in the model

Parameter	Unit	Mean	Range	Sources
HHV	MJ kg_{DM}^{-1}	18.4	17.3–19.4	32 and 86
Cp	MJ $(kg_{DM}\ K)^{-1}$	1.3		179
C%	$\%_{DM}$	47.1	46.5–47.8	30 and 136
H%	$\%_{DM}$	5.9	5.4–6.3	30,136
O%	$\%_{DM}$	41.4	40.3–42.5	30 and 136
N%	$\%_{DM}$	0.8	0.51–1.1	30 and 136
S%	$\%_{DM}$	0.11	0.08–0.20	30 and 136
Cl%	$\%_{DM}$	0.13	0–0.16	30 and 136
Ash%	$\%_{DM}$	5.7	5.2–6.1	30 and 136
Moisture content at harvest%	$\%_{WM}$	12	11–14	67, 79, 87, 136 and 190
1st harvest yield proportion	%	21	11–30	87 and 191
2nd harvest yield proportion	%	69	67–70	87 and 191
Brazil full harvest yield	t_{DM} ha^{-1}	28.9	23.2–34.7	67, 84 and 122
China full harvest yield	t_{DM} ha^{-1} $year^{-1}$	13.0	10.6–15.3	67 and 192
Europe full harvest yield	t_{DM} ha^{-1} $year^{-1}$	11.9	7.5–16.3	82 and 191
India full harvest yield	t_{DM} ha^{-1} $year^{-1}$	8.7	5.2–12.6	67, 135 and 192
US full harvest yield	t_{DM} ha^{-1} $year^{-1}$	9.5	28.1–10.9	67, 79, 87, 122, 135, 192 and 193
Lifetime	Years	12	10–15	79 and 86
Rotation of harvests	Years	1		79 and 86
Growing cycle length	Days	128	90–160	86 and 143
Growing cycle starting month		5 (N); 9 (S)		143
Growing cycle starting day		1		143
Initial stage t_1		10		143
Development stage t_2		25		143
Mid-season stage t_3		100		143
$K_{c,ini}$		0.5		47
$K_{c,mid}$		1.03	0.9–1.15	47
$K_{c,end}$		0.98	0.85–1.1	47
Nitrogen rate	kg ha^{-1} $year^{-1}$	68.5	49.5–98.8	67, 79, 86, 87 and 193
Phosphate rate	kg ha^{-1} $year^{-1}$	34	0–67	67, 86 and 193
Potash rate	kg ha^{-1} $year^{-1}$	34	0–67	67, 86 and 193 63, 67, 71, 76 and 186
Lime rate	kg ha^{-1} $year^{-1}$	569	494–643	67, 136 and 189
Seed rate	kg ha^{-1} $year^{-1}$	0.8	0.4–1.1	67, 71, 81, 87, 97, 164 and 194
Herbicide rate	kg ha^{-1} $year^{-1}$	0.48	0.42–0.54	67, 87 and 158
Land preparation (diesel)	L ha^{-1}	15.7		87
Maintenance – harvest (bales)	L per ha per harvest	32.6		87
Chopping (diesel)	MJ t_{MW}^{-1}	135		76
Grinding (power)	MJ t_{MW}^{-1}	124	72–90	92
Pelleting (power)	MJ t_{MW}^{-1}	46		92
Pellet grinding (power)	MJ t_{MW}^{-1}	345		34

Table 21 Mean values and ranges of uncertainty of short rotation coppice willow data implemented in the model

Parameter	Unit	Mean	Range	Sources
HHV	MJ kg_{DM}^{-1}	19.1	18.4–19.8	28, 29, 67, 92, 96 and 97
Cp	MJ $(kg_{DM}\ K)^{-1}$	1.5		179
C%	$\%_{DM}$	48.1	46–49.2	28 and 29
H%	$\%_{DM}$	5.9	5.3–6.4	28 and 29
O%	$\%_{DM}$	42.3	40.0–43.0	28
N%	$\%_{DM}$	0.5	0.2–0.8	28 and 29
S%	$\%_{DM}$	0.05	0.02–0.1	28 and 29
Cl%	$\%_{DM}$	0.03	0.01–0.05	28 and 29
Ash%	$\%_{DM}$	2.0	1.1–4.0	28, 29 and 92
Moisture content at harvest%	$\%_{WM}$	52	50–53	27, 67 and 69
1st harvest yield proportion	%	72		69
2nd harvest yield proportion	%	100		69
Europe full harvest yield	$t_{DM}\ ha^{-1}\ year^{-1}$	9.7	8.1–11.2	67, 69, 80, 96, 97, 100, 120, 131, 132, 175, 188 and 195–198
US full harvest yield	$t_{DM}\ ha^{-1}\ year^{-1}$	7.2	4.7–11.0	122 and 183
Lifetime	Years	16		69 and 96
Rotation of harvests	Years	3	2–4	69, 92 and 96
Growing cycle length	Days	150		199
Growing cycle starting month		5 (N); 9 (S)		199
Growing cycle starting day		15		199
Initial stage t_1		40		199
Development stage t_2		100		199
Mid-season stage t_3		130		199
$K_{c,ini}$		0.65		199
$K_{c,mid}$		1.6		199
$K_{c,end}$		0.90.93		199
Nitrogen rate	$kg\ ha^{-1}\ year^{-1}$	80	50–100	67, 80, 131, 175, 196 and 198
Phosphate rate	$kg\ ha^{-1}\ year^{-1}$	15	11–30	67, 80, 131, 175 and 198
Potash rate	$kg\ ha^{-1}\ year^{-1}$	40	0–67	67, 80, 131, 175 and 198
Lime rate	$kg\ ha^{-1}\ year^{-1}$	643		67 and 189
Cuttings rate	$kg\ ha^{-1}\ year^{-1}$	608	284–875	67, 97, 175 and 200
Herbicide rate	$kg\ ha^{-1}\ year^{-1}$	0.43	0.11–1.08	67, 80, 131, 175 and 198
Land preparation (diesel)	$L\ ha^{-1}$	82.8		69
Maintenance – harvest (chips)	L per ha per harvest	164.2		69
Grinding-pelleting (power)	MJ t_{MW}^{-1}	461		94
Pellet grinding (power)	MJ t_{MW}^{-1}	367		34

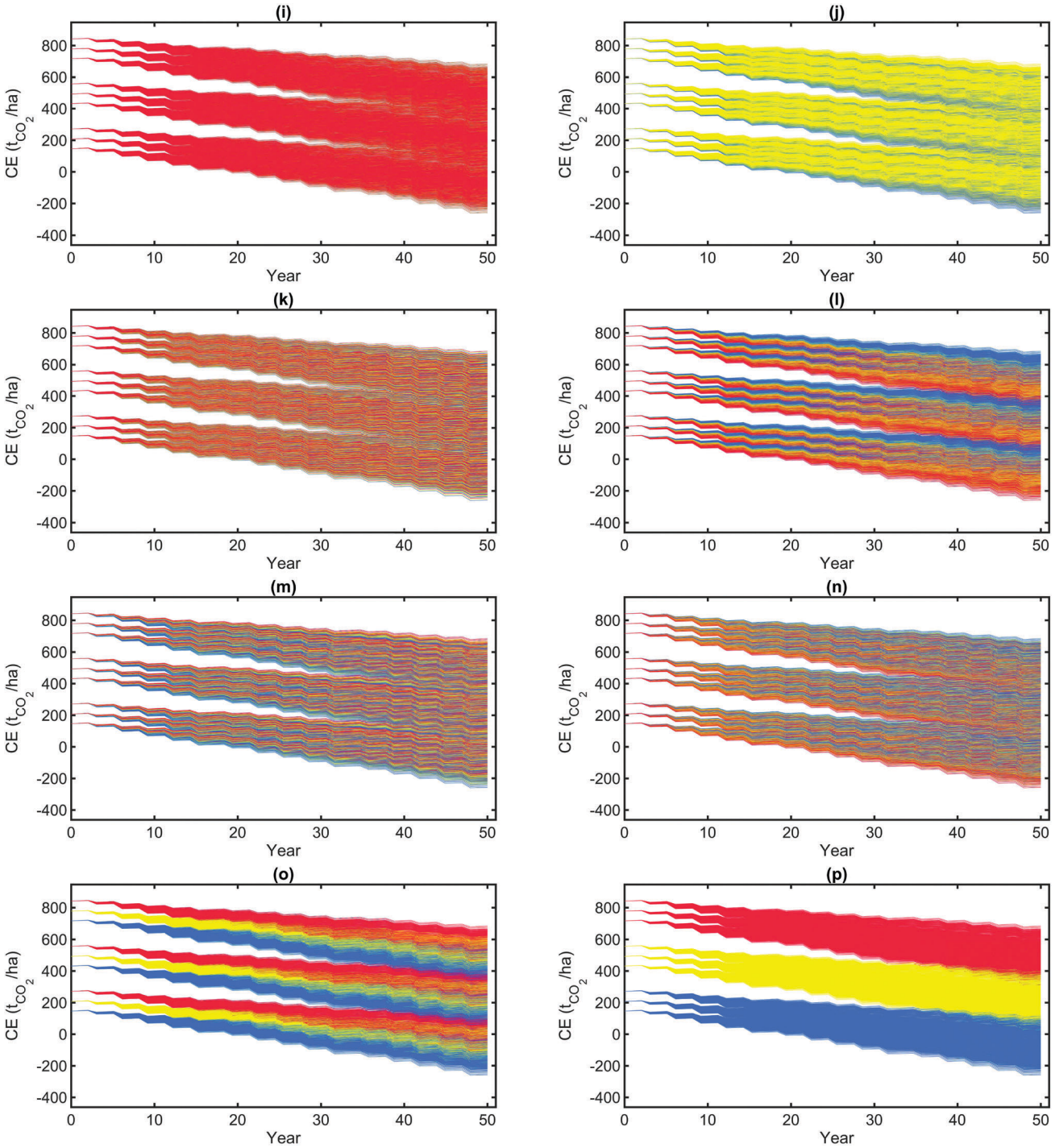

Fig. 24 Sensitivity of willow based-BECCS dynamic emission profile towards eight parameters ((i) fuel footprint and efficiency, (j) chemical footprint and application, (k) moisture content, (l) yield, (m) electricity footprint, (n) biomass carbon content, (o) LUC, (p) ILUC). Emission profiles are coloured in red when the parameter is set to its upper bound (lower bound for yield and carbon content), yellow when set to its mean value, and blue when set to its lower bound (upper bound for yield and carbon content). Patterns indicate that ILUC is the determining factor, followed by LUC, yield, electricity carbon footprint and carbon content.

Acknowledgements

We thank Imperial College London for the funding of a President's PhD Scholarship, as well as the "Multi-scale Energy Systems Modelling Encompassing Renewable, Intermittent, Stored Energy and Carbon Capture and Storage" (MESMERISE-CCS) grant, funded by the Engineering and Physical Sciences Research Council (EPSRC) under grant EP/M001369/1.

References

1 C. Marchetti, *Clim. Change*, 1977, **1**, 59–68.
2 N. Mac Dowell, N. Florin, A. Buchard, J. Hallett, A. Galindo, G. Jackson, C. S. Adjiman, C. K. Williams, N. Shah and P. Fennell, *Energy Environ. Sci.*, 2010, **3**, 1645.
3 M. E. Boot-Handford, J. C. Abanades, E. J. Anthony, M. J. Blunt, S. Brandani, N. Mac Dowell, J. R. Fernandez, M.-C. Ferrari, R. Gross, J. P. Hallett, R. S. Haszeldine, P. Heptonstall, A. Lyngfelt, Z. Makuch, E. Mangano, R. T. J. Porter, M. Pourkashanian, G. T. Rochelle, N. Shah, J. G. Yaoa and P. S. Fennell, *Energy Environ. Sci.*, 2014, **7**(1), 130–189.
4 R. H. Williams, *Fuel Decarbonization for Fuel Cell Applications and Sequestration of the Separated CO_2*, Center for Energy and Environmental Studies, Princeton University Technical Report, 1996.
5 H. J. Herzog and E. M. Drake, *Annu. Rev. Energy*, 1996, **21**, 145–166.
6 F. Kraxner, S. Nilsson and M. Obersteiner, *Biomass Bioenergy*, 2003, **24**, 285–296.
7 IEA, Combining Bioenergy with CCS, 2011.
8 P. Read and J. Lermit, *Energy*, 2005, **30**, 2654–2671.
9 A. L. Robinson, J. S. Rhodes and D. W. Keith, *Environ. Sci. Technol.*, 2003, **37**, 5081–5089.
10 S. Selosse and O. Ricci, *Energy*, 2014, **76**, 967–975.
11 *Biomass with CO_2 Capture and Storage (Bio-CCS) The way forward for Europe*, Zero Emission Platform (ZEP) technical report, 2013.
12 J. S. Rhodes and D. W. Keith, *Biomass Bioenergy*, 2005, **29**, 440–450.
13 K. Mollersten, J. Yan and J. R. Moreira, *Biomass Bioenergy*, 2003, **25**, 273–285.
14 C. Gough and P. Upham, *Biomass energy with carbon capture and storage (BECCS): a review*, 2010.
15 O. Akgul, N. Mac Dowell, L. G. Papageorgiou and N. Shah, *Int. J. Greenhouse Gas Control*, 2014, **28**, 189–202.
16 IPCC, *Climate Change 2014, Mitigation of Climate Change. Contribution of Working Group III to the Fifth Assessment Report of the Intergovernmental Panel on Climate Change*, 2014.
17 S. Fuss, J. G. Canadell, G. P. Peters, M. Tavoni, R. M. Andrew, P. Ciais, R. B. Jackson, C. D. Jones, F. Kraxner, N. Nakicenovic, C. Le Quéré, M. R. Raupach, A. Sharifi, P. Smith and Y. Yamagata, *Nat. Clim. Change*, 2014, **4**, 850–853.
18 T. W. R. Powell and T. M. Lenton, *Energy Environ. Sci.*, 2012, **5**, 8116.
19 J. M. DeCicco, D. Y. Liu, J. Heo, R. Krishnan, A. Kurthen and L. Wang, *Clim. Change*, 2016, **138**, 667–680.
20 J. Rogelj, M. den Elzen, N. Höhne, T. Fransen, H. Fekete, H. Winkler, R. Schaeffer, F. Sha, K. Riahi and M. Meinshausen, *Nature*, 2016, **534**, 631–639.
21 IEAGHG, *CO_2 Capture at Coal Based Power and Hydrogen Plants*, May, 2014.
22 A. Singh and K. Stéphenne, *Energy Procedia*, 2014, **63**, 1678–1685.
23 M. Campbell, *Energy Procedia*, 2014, **63**, 801–807.
24 Y. Zhang, B. Freeman, P. Hao and G. Rochelle, *Faraday Discuss.*, 2016, **192**, 459–477.
25 M. Bui, M. Fajardy and N. Mac Dowell, *Appl. Energy*, 2017, **195**, 289–302.
26 M. B. Berkenpas, J. J. Fry, K. Kietzke and E. S. Rubin, *Integrated Environmental Control Model Getting Started*, Center for Energy and Evironmental Studies, Carnagie mellon University Technical Report.
27 P. J. Tharakan, T. A. Volk, L. P. Abrahamson and E. H. White, *Biomass Bioenergy*, 2003, **25**, 571–580.
28 ISO, *Solid biofuels: Fuel specifications and classes. Part 1: General requirements*, 2014.
29 M. J. Stolarski, M. Krzyzaniak, S. Szczukowski and J. Tworkowski, *J. Res. Appl. Agric. Eng.*, 2013, **58**, 168–171.
30 A. Monti, *Switchgrass: A Valuable Biomass Crop for Energy*, Springer edn, 2012, p. 210.
31 H. Spliethoff and K. R. G. Hein, *Fuel Process. Technol.*, 1998, **54**, 189–205.
32 P. McKendry, *Bioresour. Technol.*, 2002, **83**, 37–46.
33 T. Heinzel, V. Siegle, H. Spliethoff and K. R. G. Hein, *Fuel Process. Technol.*, 1998, **54**, 109–125.
34 O. Williams, C. Eastwick, S. Kingman, D. Giddings, S. Lormor and E. Lester, *Fuel*, 2015, **158**, 379–387.
35 K. Savolainen, *Appl. Energy*, 2003, **74**, 369–381.
36 DRAX plc, Drax annual report and accounts, 2015.
37 Y. Shao, J. Wang, F. Preto, J. Zhu and C. Xu, *Energies*, 2012, **5**, 5171–5189.
38 M. Pronobis, *Fuel*, 2006, **85**, 474–480.
39 N. Mac Dowell and M. Fajardy, *Environ. Res. Lett.*, 2017, DOI: 10.1088/1748-9326/aa67a5.
40 UN Water, *Waterlines*, 2005, **24**, 28–29.
41 IEA, *Water for Energy: Is energy becoming a thirstier resource?*, 2012.
42 P. Smith, S. J. Davis, F. Creutzig, S. Fuss, J. Minx, B. Gabrielle, E. Kato, R. B. Jackson, A. Cowie, E. Kriegler, D. P. van Vuuren, J. Rogelj, P. Ciais, J. Milne, J. G. Canadell, D. McCollum, G. Peters, R. Andrew, V. Krey, G. Shrestha, P. Friedlingstein, T. Gasser, A. Grubler, W. K. Heidug, M. Jonas, C. D. Jones, F. Kraxner, E. Littleton, J. Lowe, J. R. Moreira, N. Nakicenovic, M. Obersteiner, A. Patwardhan, M. Rogner, E. Rubin, A. Sharifi, A. Torvanger, Y. Yamagata, J. Edmonds and C. Yongsung, *Nat. Clim. Change*, 2016, **6**, 42–50.
43 G. Fisher, H. T. van Velthuizen, M. M. Shah and F. O. Nachtergaele, *Global agro-ecological assessment for agriculture in the twenty-first century: Methodology and Results*, International Institute for Applied Systems Analysis Technical Report March, 2002.
44 L. Zhuo, M. M. Mekonnen, A. Hoekstra and Y. Wada, *Adv. Water Resour.*, 2016, **87**, 29–41.
45 Y. Wada, L. P. H. Van Beek, D. Viviroli, H. H. Drr, R. Weingartner and M. F. P. Bierkens, *Water Resour. Res.*, 2011, **47**, 1–17.
46 A. Hoekstra, A. K. Chapagain, M. M. Aldaya and M. M. Mekonnen, *Water Footprint Manual State of the Art*, November, 2009.

47 R. G. Allen, L. Pereira, D. Raes and M. Smith, *Crop evapotranspiration – Guidelines for computing crop water requirements*, 1998.
48 M. M. Mekonnen and A. Y. Hoekstra, *Environ. Sci. Technol.*, 2015, **49**, 12860–12868.
49 M. M. Mekonnen and A. Y. Hoekstra, *The green, blue and grey water footprint of crops and derived crop products*, UNESCO-IHE Technical Report 47, 2010.
50 M. M. Mekonnen and A. Y. Hoekstra, *The green, blue and grey water footprint of crops and derived crop products. Volume 2: Appendices*, UNESCO-IHE Technical Report 47, 2010.
51 P. W. Gerbens-Leenes, A. Y. Hoekstra and T. van der Meer, *Ecological Economics*, 2009, **68**, 1052–1060.
52 M. Wu, M. Mintz, M. Wang and S. Arora, *Environ. Manage.*, 2009, **44**, 981–997.
53 P. W. Gerbens-Leenes, A. Y. Hoekstra and T. H. van der Meer, *Proc. Natl. Acad. Sci. U. S. A.*, 2009, **106**, 10219–10223.
54 M. Wu and M. J. Peng, *Developing a Tool to Estimate Water Use in Electric Power Generation in the US*, 2011.
55 J. Macknick, R. Newmark, G. Heath and K. C. Hallett, *Environ. Res. Lett.*, 2012, **7**, 045802.
56 R. Parajuli, M. T. Knudsen, J. H. Schmidt and T. Dalgaard, *Biomass Bioenergy*, 2014, **68**, 115–134.
57 H. Shahrukh, A. O. Oyedun, A. Kumar, B. Ghiasi, L. Kumar and S. Sokhansanj, *Biomass Bioenergy*, 2016, **90**, 50–59.
58 W. Schakel, H. Meerman, A. Talaei, A. Ramirez and A. Faaij, *Appl. Energy*, 2014, **131**, 441–467.
59 T. L. T. Nguyen, J. E. Hermansen and L. Mogensen, *Appl. Energy*, 2013, **104**, 633–641.
60 W. Liu, J. Mi, Z. Song, J. Yan, J. Li and T. Sang, *Biomass Bioenergy*, 2014, **62**, 47–57.
61 I. E. Palmer, R. J. Gehl, T. G. Ranney, D. Touchell and N. George, *Biomass Bioenergy*, 2014, **63**, 218–228.
62 F. Triana, N. Nassi o Di Nasso, G. Ragaglini, N. Roncucci and E. Bonari, *GCB Bioenergy*, 2014, 811–819.
63 M. B. Jones and M. Walsh, *Miscanthus for energy and fibre*, James & James (Science Publishers) Ltd, 2001, p. 192.
64 L. Price, M. Bullard, H. Lyons, S. Anthony and P. Nixon, *Biomass Bioenergy*, 2004, **26**, 3–13.
65 F. Murphy, G. Devlin and K. McDonnell, *Renewable Sustainable Energy Rev.*, 2013, **23**, 412–420.
66 B. Gabrielle, L. Bamière, N. Caldes, S. De Cara, G. Decocq, F. Ferchaud, C. Loyce, E. Pelzer, Y. Perez, J. Wohlfahrt and G. Richard, *Renewable Sustainable Energy Rev.*, 2014, **33**, 11–25.
67 G. G. T. Camargo, M. R. Ryan and T. L. Richard, *BioScience*, 2013, **63**, 263–273.
68 M. A. Mehmood, M. Ibrahim, U. Rashid, M. Nawaz, S. Ali, A. Hussain and M. Gull, *Sustainable Production and Consumption*, 2016, 1–19.
69 A. Grzybek, *Modelling of biomass utilisation for energy purpose*, 2010.
70 E. A. Heaton, J. Clifton-Brown, T. B. Voigt, M. B. Jones and S. P. Long, *Mitigation and Adaptation Strategies for Global Change*, 2004, **9**, 433–451.
71 M. Bullard and P. Metcalfe, *Estimating the energy requirements and CO_2 emissions from production of the perennial grasses miscanthus, switchgrass and reed canary grass*, Energy Technology Support Unit Technical Report, 2001.
72 D. G. Christian, A. B. Riche and N. E. Yates, *Ind. Crops Prod.*, 2008, **28**, 320–327.
73 S. Xue, I. Lewandowski, X. Wang and Z. Yi, *Renewable Sustainable Energy Rev.*, 2016, **54**, 932–943.
74 C. Bohmen, PhD thesis, University of Hohenheim2007.
75 I. Lewandowski, J. C. Clifton-Brown, J. M. O. Scurlock and W. Huisman, *Biomass Bioenergy*, 2000, **19**, 209–227.
76 I. Lewandowski, A. Kicherer and P. Vonier, *Biomass Bioenergy*, 1995, **8**, 81–90.
77 J. Hillier, C. Whittaker, G. Dailey, M. Aylott, E. Casella, G. M. Richter, A. Riche, R. Murphy, G. Taylor and P. Smith, *GCB Bioenergy*, 2009, **1**, 267–281.
78 J. C. Clifton-brown, J. Breuer and M. B. Jones, *Global Change Biology*, 2007, **13**, 2296–2307.
79 X. Lu, M. R. Withers, N. Seifkar, R. P. Field, S. R. H. Barrett and H. J. Herzog, *Bioresour. Technol.*, 2015, **183**, 1–9.
80 S. Lettens, B. Muys, R. Ceulemans, E. Moons, J. Garcia and P. Coppin, *Biomass Bioenergy*, 2003, **24**, 179–197.
81 D. Pimentel and T. Patzek, *Nat. Resour. Res.*, 2005, **14**, 65–76.
82 N. Nassi o Di Nasso, M. V. Lasorella, N. Roncucci and E. Bonari, *Ind. Crops Prod.*, 2015, **65**, 21–26.
83 L. J. Smith and M. S. Torn, *Clim. Change*, 2013, 89–103.
84 J. van Dam, A. P. C. Faaij, J. Hilbert, H. Petruzzi and W. C. Turkenburg, *Renewable Sustainable Energy Rev.*, 2009, **13**, 1710–1733.
85 J. S. Tumuluru, *Front. Energy Res.*, 2015, **3**, 1–11.
86 R. Samson, *Switchgrass Production in Ontario: A Management Guide*, Resource Efficient Agricultural Production (REAP) Canada Technical Report, 2007.
87 B. Kalita, PhD thesis, University of Guelph2012.
88 C. S. Snyder, T. W. Bruulsema, T. L. Jensen and P. E. Fixen, *Agric., Ecosyst. Environ.*, 2009, **133**, 247–266.
89 J. Daystar, C. Reeb, R. Gonzalez, R. Venditti and S. S. Kelley, *Fuel Process. Technol.*, 2015, **138**, 164–174.
90 M. Wu and Y.-W. Chiu, *Developping County-Level Water Footprints of Biofuel Produced from Switchgrass and Miscanthus in the US*, Argonne National Laboratory Technical Report, 2014.
91 A. J. Ashworth, A. M. Taylor, D. L. Reed, F. L. Allen, P. D. Keyser and D. D. Tyler, *J. Cleaner Prod.*, 2015, **87**, 227–234.
92 R. Samson and P. Duxbury, *Assessment of pelletized biofuels*, 2000.
93 M. Mobini, T. Sowlati and S. Sokhansanj, *Appl. Energy*, 2013, **111**, 1239–1249.
94 R. Ehrig, PhD thesis, Technical University (TU) Berlin2014.
95 P. Thornley, P. Gilbert, S. Shackley and J. Hammond, *Biomass Bioenergy*, 2015, **81**, 35–43.
96 R. W. Matthews, *Biomass Bioenergy*, 2001, **21**, 1–19.
97 M. Elsayed, R. Matthews and N. Mortimer, *Carbon and energy balances for a range of biofuels options*, Resources

Research Unit, Sheffield Hallam University Technical Report, 2003.
98 J. Wickham, B. Rice, J. Finnan and R. McConnon, *A review of past and current research on short rotation coppice in Ireland and abroad*, COFORD and Sustainable Energy Authority of Ireland Technical Report, 2010.
99 A. L. Stephenson and D. J. MacKay, *Life Cycle Impacts of Biomass Electricity in 2020*, Department of Energy and Climate Change Technical Report July, 2014.
100 L. Gustavsson, P. Borjesson, B. Johansson and P. Svenningsson, *Energy*, 1995, **20**, 1097–1113.
101 DECC, *UK Bioenergy Strategy*, DECC Technical Report April, 2012.
102 J. Fargione, J. Hill, D. Tilman, S. Polasky and P. Hawthorne, *Science*, 2008, **319**, 1235–1237.
103 R. J. Plevin, M. O'Hare, A. D. Jones, M. S. Torn and H. K. Gibbs, *Environ. Sci. Technol.*, 2010, **44**, 8015–8021.
104 T. Searchinger, *Sound principles and an important inconsistency in the 2012 UK bioenergy strategy*, Woodrow Wilson School of Public and International Affairs Technical Report, 2012.
105 H. Haberl, D. Sprinz, M. Bonazountas, P. Cocco, Y. Desaubies, M. Henze, O. Hertel, R. K. Johnson, U. Kastrup, P. Laconte, E. Lange, P. Novak, J. Paavola, A. Reenberg, S. van den Hove, T. Vermeire, P. Wadhams and T. Searchinger, *Energy Policy*, 2012, **45**, 18–23.
106 European Commission, *Impact Assessment*, 2012.
107 K. P. Overmars, E. Stehfest, J. P. M. Ros and A. G. Prins, *Environ. Sci. Policy*, 2011, **14**, 248–257.
108 T. Searchinger, R. Heimlich, R. A. Houghton, F. Dong, A. Elobeid, J. Fabiosa, S. Tokgoz, D. Hayes and T. Yu, *Science*, 2008, **423**, 1238–1241.
109 M. R. Withers, R. Malina and S. R. H. Barrett, *Ecological Economics*, 2015, **112**, 45–52.
110 F. Cherubini, G. P. Peters, T. Berntsen, A. H. Strømman and E. Hertwich, *GCB Bioenergy*, 2011, **3**, 413–426.
111 X. Lu and H. Herzog, *Biomass to Liquid Fuels Pathways: A Techno-Economic Environmental Evaluation*, 2015.
112 T. Gebreegziabher, A. O. Oyedun and C. W. Hui, *Energy*, 2013, **53**, 67–73.
113 C. J. Roos, *Biomass Drying and Dewatering for Clean Heat & Power*, US Department of Energy – CHP Technical Assistance Partnerships Technical Report September, 2008.
114 T. Pacetti, L. Lombardi and G. Federici, *J. Cleaner Prod.*, 2015, **101**, 1–14.
115 A. L. Borrion, M. C. McManus and G. P. Hammond, *Biomass Bioenergy*, 2012, **47**, 9–19.
116 T. Ramjeawon, *J. Cleaner Prod.*, 2008, **16**, 1727–1734.
117 M. C. Rulli, D. Bellomi, A. Cazzoli, G. De Carolis and P. D'Odorico, *Sci. Rep.*, 2016, **6**, 22521.
118 J. Khan and T. Powell, *Office for National Statistics*, London, UK, 2011, p. 5.
119 T. Skevas, S. M. Swinton and N. J. Hayden, *Biomass Bioenergy*, 2014, **67**, 252–259.
120 M. J. Aylott, E. Casella, I. Tubby, N. R. Street, P. Smith and G. Taylor, *New Phytol.*, 2008, **178**, 358–370.
121 M. R. Schmer, K. P. Vogel, R. B. Mitchell and R. K. Perrin, *Proc. Natl. Acad. Sci. U. S. A.*, 2008, **105**, 464–469.
122 R. L. Graham, L. J. Allison and D. A. Becker, *ORECCL – Summary of a National database on energy crop landbase, yields, and costs*, 1997.
123 FAO, *FAOClim-NET*, http://geonetwork3.fao.org/climpag/agroclimdb_ en.php.
124 FAO, *CROPWAT 8.0*, http://www.fao.org/nr/water/infores_databases_cropwat.html.
125 I. Dimitriou, PhD thesis, Swedish University of Agricultural Sciences, 2005.
126 L. Sevel, T. Nord-Larsen, M. Ingerslev, U. Jørgensen and K. Raulund-Rasmussen, *BioEnergy Res.*, 2014, **7**, 319–328.
127 P. Heffer, *Assessment of Fertilizer Use by Crop at the Global Level*, International Fertilizer Industry Association (IFA) Technical Report August, 2013.
128 FAO, *FAOSTAT*, http://www.fao.org/faostat/en/#homex.
129 Y. Yimam, T. E. Ochsner and V. G. Kakani, *Agricultural Water Management*, 2015, **155**, 40–47.
130 IEAGHG, *Water Intensity of Power Generation*, 2013.
131 P. Börjesson, *Biomass Bioenergy*, 1996, **11**, 305–318.
132 S. Njakou Djomo, O. El Kasmioui, T. De Groote, L. S. Broeckx, M. S. Verlinden, G. Berhongaray, R. Fichot, D. Zona, S. Y. Dillen, J. S. King, I. A. Janssens and R. Ceulemans, *Appl. Energy*, 2013, **111**, 862–870.
133 V. Forgie and R. Andrew, *Life Cycle Assessment of Using Straw to Produce Industrial Energy in New Zealand*, Landcare Research and New Zealand Centre for Ecological Economics Technical Report May, 2008.
134 J. E. King, Reducing Bioenergy Cost by Monetizing Environmental Benefits of Reservoir Water Quality Improvements from Switchgrass Production, Coriolis Technical Report, 1999.
135 L. Wang, Y. Qian, J. E. Brummer, J. Zheng, S. Wilhelm and W. J. Parton, *Biomass Bioenergy*, 2015, **75**, 254–266.
136 X. Qin, T. Mohan, M. El-Halwagi, G. Cornforth and B. A. McCarl, *Clean Technol. Environ. Policy*, 2006, **8**, 233–249.
137 Atlantic Consulting, LPG's Carbon Footprint Relative to Other Fuels – A Scientific Review, 2009.
138 S. Hinchliffe, R. V. Diemen, C. Heuberger and N. Mac Dowell, *Transitions in Electricity Systems Towards 2030*, The Energy Centre of the Institution of Chemical Engineers (IChemE) Technical Report October, 2015.
139 VERSA, personal communication, 2016.
140 T. W. Hertel, A. A. Golub, A. D. Jones, M. O'Hare, R. J. Plevin and D. M. Kammen, *BioScience*, 2010, **60**, 223–231.
141 C. Folberth, R. Skalský, E. Moltchanova, J. Balkovič, L. B. Azevedo, M. Obersteiner and M. van der Velde, *Nat. Commun.*, 2016, **7**, 11872.
142 B. E. Dale, J. E. Anderson, R. C. Brown, S. Csonka, V. H. Dale, G. Herwick, R. D. Jackson, N. Jordan, S. Ka, K. L. Kline, L. R. Lynd, C. Malmstrom, R. G. Ong, T. L. Richard, C. Taylor and M. Q. Wang, *Environ. Sci. Technol.*, 2014, **48**, 7200–7203.
143 A. K. Chapagain and A. Y. Hoekstra, *Water footprint of nations. Volume 1: Main report*, UNESCO-IHE Technical Report, 2004.

144 EIA, *Annual Energy Outlook 2016*, 2015.
145 J. Wilcox, *CCS Leaders Forum*, London, 2016.
146 M. Ranjan and H. J. Herzog, *Energy Procedia*, 2011, **4**, 2869–2876.
147 R. Baciocchi, G. Storti and M. Mazzotti, *Chem. Eng. Process.*, 2006, **45**, 1047–1058.
148 Carbon Engineering, http://carbonengineering.com/our-technology/.
149 I. Obernberger and G. Thek, *The Pellet Hanbook, the production and thermal utilisation of biomass pellets*, 2010, p. 600.
150 H. Li, Q. Chen, X. Zhang, K. N. Finney, V. N. Sharifi and J. Swithenbank, *Appl. Therm. Eng.*, 2012, **35**, 71–80.
151 Q. X. Xu and S. S. Pang, *Drying Technol.*, 2008, **26**, 1344–1350.
152 M. N. Haque, *Drying Technol.*, 2007, **25**, 547–555.
153 J. Selivanovs, D. Blumberga, J. Ziemele, A. Blumberga and A. Barisa, *Environ. Clim. Technol.*, 2012, **10**, 46–50.
154 D. A. Lewis and J. A. Tatchell, *J. Sci. Food Agric.*, 1979, **30**, 449–457.
155 B. S. Panesar and A. P. Bhatnagar, Indian Society of Agricultural Engineers National Conference, 1981.
156 R. E. Muller, in *Energy in World Agriculture*, ed. R. M. Peart and R. C. Brook, Elsevier, Amsterdam, vol. 5, 1992.
157 G. Kongshaug, IFA Technical Conference, Marrakech, 1998.
158 M. Q. Wang, *Development and Use of GREET 1.6 Fuel-Cycle Model for Transportation Fuels and Vehicle Technologies*, 2001.
159 N. Mortimer, P. Cormack, M. A. Elsayed and R. E. Horne, *Evaluation of the comparative energy, global warming and socio-economic costs and benefits of biodiesel*, Sheffield Hallam University Technical Report, 2003.
160 M. S. Graboski, *National Corn Growers Association*, 2002.
161 T. O. West and G. Marland, *Agric., Ecosyst. Environ.*, 2002, **91**, 217–232.
162 H. Shapouri, *The 2001 net energy balance of corn ethanol*, U.S. Department of Agriculture (USDA) Technical Report, 2001.
163 T. Nemecek and S. Erzinger, *Special LCA Forum*, Lausanne, 2003.
164 M. E.Walsh and D.Becker, BIOENERGY '96 - The Seventh National Bionergy Conference: Partnerships to Develop and Apply Biomass Technologies, Nashville, 1996.
165 *Energy Use and the U.S. Economy*, Office of Technology Assessment, U.S. Congress, Technical Report June, 1990.
166 Direct energy use in agriculture: opportunities for reducing fossil fuel inputs, DEFRA Technical Report May, 2007.
167 P. S. Mehta and K. Anand, *Energy Fuels*, 2009, **23**, 3893–3898.
168 L. Luo, E. van der Voet and G. Huppes, *Renewable Sustainable Energy Rev.*, 2009, **13**, 2003–2011.
169 *Vehicle Technologies Program*, Energy Efficiency and Renewable Energy, U.S. Department of Energy (DOE) Technical Report, 2011.
170 M. Q. Wang, *The Greenhouse Gases, Regulated Emissions, and Energy Use in Transportation (GREET) Model Version 1.5*, 1999.
171 J. E. A. Seabra, I. C. Macedo, H. L. Chum, C. E. Faroni and C. A. Sarto, *Biofuels, Bioprod. Biorefin.*, 2011, **5**, 519–532.
172 C. Walsh and A. Bows, *Appl. Energy*, 2012, **98**, 128–137.
173 G. P. Robertson, E. A. Paul, R. R. Harwood, L. E. Drinkwater, P. Wagoner, M. Sarrantonio, A. R. Mosier, D. Schimel, D. Valetine, K. Bronson, W. Parton, W. H. Schlesinger, A. R. Mosier, P. A. Matson, R. Naylor, I. Ortiz-Monasterio, R. A. Houghton, J. L. Hackler and K. T. Lawrence, *Science*, 2000, **289**, 1922–1925.
174 R. Lal, *Environ. Int.*, 2004, **30**, 981–990.
175 M. C. Heller, G. A. Keoleian, M. K. Mann and T. A. Volk, *Renewable Energy*, 2004, **29**, 1023–1042.
176 J. Sheehan, A. Aden, K. Paustian, J. Brenner, M. Walsh and R. Nelson, *J. Ind. Ecol.*, 2004, **7**, 117–146.
177 *Shipping, World Trade and the Reduction of $C0_2$*, International Chamber of Shipping (ICS) Technical Report, 2013.
178 C. De Klein, R. Novoa, S. Ogle, K. Smith, P. Rochette, T. Wirth, B. McConkey, A. Mosier and K. Rypdal, *Lignes directrices 2006 du GIEC pour les inventaires nationnaux de gaz à effet de serre. Volume 4: Agriculture, foresterie et autres affectations des terres*, 2006, pp. 1–60.
179 C. Dupont, R. Chiriac, G. Gauthier and F. Toche, *Fuel*, 2014, **115**, 644–651.
180 J. Dai, B. Bean, B. Brown, W. Bruening, J. Edwards, M. Flowers, R. Karow, C. Lee, G. Morgan, M. Ottman, J. Ransom and J. Wiersma, *Biomass Bioenergy*, 2016, **85**, 223–227.
181 Y. Zhang, A. E. Ghaly and B. Li, *Am. J. Eng. Appl. Sci.*, 2012, **5**, 98–106.
182 S. Sokhansanj, A. Kumar and A. F. Turhollow, *Biomass Bioenergy*, 2006, **30**, 838–847.
183 R. Samson, P. Girouard and Y. Chen, Evaluation of switchgrass and short-rotation forestry willow in Eastern Canada as bio-energy and agri-fibre feedstocks, Resource Efficient Agricultural Production (REAP) Canada Technical Report, 1997.
184 R. Michel, N. Mischler, B. Azambre, G. Finqueneisel, J. Machnikowski, P. Rutkowski, T. Zimny and J. V. Weber, *Environ. Chem. Lett.*, 2006, **4**, 185–189.
185 N. G. Danalatos, S. V. Archontoulis and I. Mitsios, *Biomass Bioenergy*, 2007, **31**, 145–152.
186 D. G. Christian, P. R. Poulton, A. B. Riche and N. E. Yates, *Biomass Bioenergy*, 1997, **12**, 21–24.
187 J. Copeland and D. Turley, *National and regional supply/demand balance for agricultural straw in Great Britain*, 2008.
188 A. Hastings, M. J. Tallis, E. Casella, R. W. Matthews, P. A. Henshall, S. Milner, P. Smith and G. Taylor, *GCB Bioenergy*, 2014, **6**, 108–122.
189 *Summary report soils test results and recommendations*, Agricultural Analytical Services Laboratory, Penn State University Technical Report, 2014.
190 S. B. McLaughlin, R. Samson, D. Bransby and A. Wiselogel, *Evaluating physical, chemical, and energetic properties of perennial grasses as biofuels*, 1996.
191 H. W. Elbersen, *Switchgrass (Panicum virgatum L.) as an alternative energy crop in Europe - Initiation of a productivity network*, Agrotechnological Research Institute (ATO-DLO) Technical Report, 2001.

192 J. E. King, J. M. Hannifan and R. Nelson, *An Assessment of the Feasibility of Electric Power Derived from Biomass and Waste Feedstocks*, 1998.
193 M. Hall, *Warm season grasses, Agronomy facts 29*, Department of Crop and Soil Sciences, Penn State University Technical Report, 2010.
194 A. Teel and S. Barnhart, *Switchgrass Seeding Recommendation for the Production of Biomass Fuel in Southern Iowa*, Iowa State University Technical Report, 2003.
195 D. Styles and M. B. Jones, *Environ. Sci. Policy*, 2008, **11**, 294–306.
196 L. van Bussel, *The potential contribution of a short- rotation willow plantation to mitigate climate change*, Wageningen University Technical Report, 2006.
197 U. R. Boman and J. H. Turnbull, *Biomass Bioenergy*, 1997, **13**, 333–343.
198 K. A. Thyö and H. Wenzel, *Life Cycle Assessment of Biogas from Maize silage and from Manure*, 2007.
199 W. Guidi, E. Piccioni and E. Bonari, *Bioresour. Technol.*, 2008, **99**, 4832–4840.
200 M. Manzone, G. Airoldi and P. Balsari, *Biomass Bioenergy*, 2009, **33**, 1258–1264.

